Analysis of Short-Term Variations in Beach Morphology (and Concurrent Dynamic Processes) for Summer and Winter Periods, 1971-72, Plum Island, Massachusetts

by

Ralph Warren Abele, Jr.

MISCELLANEOUS REPORT NO. 77-5
MARCH 1977

Prepared for

U.S. ARMY, CORPS OF ENGINEERS
COASTAL ENGINEERING
RESEARCH CENTER

Kingman Building
Fort Belvoir, Va. 22060

REPORT DOCUMENTATION PAGE		READ INSTRUCTIONS BEFORE COMPLETING FORM
1. REPORT NUMBER MR 77-5	2. GOVT ACCESSION NO.	3. RECIPIENT'S CATALOG NUMBER
4. TITLE (and Subtitle) ANALYSIS OF SHORT-TERM VARIATIONS IN BEACH MORPHOLOGY (AND CONCURRENT DYNAMIC PROCESSES) FOR SUMMER AND WINTER PERIODS, 1971-72, PLUM ISLAND, MASSACHUSETTS		5. TYPE OF REPORT & PERIOD COVERED Miscellaneous Report
		6. PERFORMING ORG. REPORT NUMBER
7. AUTHOR(s) Ralph Warren Abele, Jr.		8. CONTRACT OR GRANT NUMBER(s) DACW72-71-C-0023
9. PERFORMING ORGANIZATION NAME AND ADDRESS Coastal Research Center University of Massachusetts Amherst, Massachusetts 01002		10. PROGRAM ELEMENT, PROJECT, TASK AREA & WORK UNIT NUMBERS V04130
11. CONTROLLING OFFICE NAME AND ADDRESS Department of the Army Coastal Engineering Research Center (CEREN-GE) Kingman Building, Fort Belvoir, Virginia 22060		12. REPORT DATE March 1977
		13. NUMBER OF PAGES 101
14. MONITORING AGENCY NAME & ADDRESS(If different from Controlling Office)		15. SECURITY CLASS. (of this report) UNCLASSIFIED
		15a. DECLASSIFICATION/DOWNGRADING SCHEDULE

16. DISTRIBUTION STATEMENT (of this Report)

Approved for public release, distribution unlimited.

17. DISTRIBUTION STATEMENT (of the abstract entered in Block 20, if different from Report)

18. SUPPLEMENTARY NOTES

19. KEY WORDS (Continue on reverse side if necessary and identify by block number)

Beach morphology	Currents	Plum Island, Massachusetts
Beach profiles	Meteorological variables	Waves
Breakers		

20. ABSTRACT (Continue on reverse side if necessary and identify by block number)

An analysis of the relationship between wave and meteorological variables and beach morphology was undertaken during summer and winter periods, 1971-72, on Plum Island, Massachusetts. Variables were measured or computed bihourly, 24 hours per day, throughout both study periods. The variables were wave period, wave height, breaker type, breaker angle, longshore current velocity, wave steepness, breaker power, windspeed and direction, barometric pressure, air and water temperature, and ground water elevation. Daily topographic maps of the intertidal zone were constructed for 12 beach profiles spaced at 60-meter intervals. (continued)

DD FORM 1 JAN 73 1473 EDITION OF 1 NOV 65 IS OBSOLETE

Variations in beach process variables, during both the summer and winter periods, were directly related to the passage of high- and low-pressure systems and to the proximity of the system to Plum Island. With an increase in breaker power and breaker steepness, the high tide beach-face gradient increased. Increases in breaker power also resulted in a rise in the level of the ground water surface. Although most process variables were similar for the summer and winter periods, strong offshore winds and extreme low temperatures that accompany polar high-pressure systems are unique to the winter period.

Differences in beach morphology within a small area appear to reflect the state of recovery of the beach profiles after a storm. Adjacent profiles at different stages of maturity are controlled by the proximity of the nearshore bar. The closer the bar is to shore, the faster the sediment is returned to the beach zone.

PREFACE

This report is published to provide coastal engineers with an analysis of the relationship between wave and meteorological variables and beach morphology during summer and winter periods, 1971-72, at Plum Island, Massachusetts. The work was carried out under the coastal processes program of the U.S. Army Coastal Engineering Research Center (CERC).
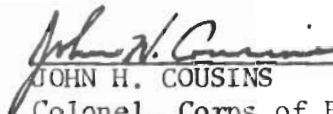
The report was prepared by Ralph Warren Abele, Jr., while with the Coastal Research Center (CRC), Department of Geology, University of Massachusetts, Amherst, Massachusetts, under CERC Contract No. DACW72-71-C-0023. M.O. Hayes of CRC supervised the research project. R. Gonter and J. Hill were responsible for modifying and writing computer programs from research grants provided by the University of Massachusetts Research Computing Center. W.T. Fox, Williams College, Williamstown, Massachusetts, also wrote several computer programs and assisted in the field techniques and data analysis.

M.J. Girard, D.K. Hubbard, W.L. Kiendzior, and R.G. Piepul gave considerable effort to the field study. The author is grateful to the various members of CRC who helped run beach profiles after the February 1972 "northeaster," especially to F.J. Raffaldi who assisted in most of the photographic work. Appreciation is extended to J.M. Colonell and J.F. Hubert for critically reviewing the manuscript.

S.J. Williams, CERC, provided technical and liaison support for the report, under the general supervision of Dr. David Duane, former Chief, Geology Branch (now Geotechnical Engineering Branch), Engineering Development Division.

Comments on this publication are invited.

Approved for publication in accordance with Public Law 166, 79th Congress, approved 31 July 1945, as supplemented by Public Law 172, 88th Congress, approved 7 November 1963.

JOHN H. COUSINS
Colonel, Corps of Engineers
Commander and Director

3

CONTENTS

CONTENTS--Continued

FIGURES

CONTENTS

FIGURES--Continued

CONTENTS

FIGURES--Continued

CONTENTS

FIGURES--Continued

CONVERSION FACTORS, U.S. CUSTOMARY TO METRIC (SI)
UNITS OF MEASUREMENT

U.S. customary units of measurement used in this report can be converted to metric (SI) units as follows:

Multiply	by	To obtain
inches	25.4	millimeters
	2.54	centimeters
square inches	6.452	square centimeters
cubic inches	16.39	cubic centimeters
feet	30.39	centimeters
	0.3048	meters
square feet	0.0929	square meters
cubic feet	0.0283	cubic meters
yards	0.9144	meters
square yards	0.836	square meters
cubic yards	0.7646	cubic meters
miles	1.6093	kilometers
square miles	259.0	hectares
knots	1.8532	kilometers per hour
acres	0.4047	hectares
foot-pounds	1.3558	newton meters
millibars	1.0197×10^{-3}	kilograms per square centimeter
ounces	28.35	grams
pounds	453.6	grams
	0.4536	kilograms
ton, long	1.0160	metric tons
ton, short	0.9072	metric tons
degrees (angle)	0.1745	radians
Fahrenheit degrees	5/9	Celsius degrees or Kelvins[1]

[1]To obtain Celsius (C) temperature readings from Farenheit (F) readings, use formula: $C = (5/9) (F - 32)$.

To obtain Kelvin (K) readings, use formula: $K = (5/9) (F - 32) + 273.15$.

ANALYSIS OF SHORT-TERM VARIATIONS IN
BEACH MORPHOLOGY (AND CONCURRENT DYNAMIC PROCESSES)
FOR SUMMER AND WINTER PERIODS, 1971-72,
PLUM ISLAND, MASSACHUSETTS

by
Ralph Warren Abele, Jr.

I. INTRODUCTION

Continuous bihourly measurement of beach processes variables was
carried out on Plum Island, Massachusetts (Fig. 1) during a 6-week
period in July and August 1971, and a 4-week period in January 1972.
These measurements included meteorological variables, i.e., barometric
pressure, windspeed and direction; and wave parameters such as breaker
height, breaker depth, breaker angle, breaker type, and wave period.
Wave steepness and breaker power were calculated for each set of wave
measurements. In addition, longshore current velocity, and, in July and
August, ground water elevation were measured.

A series of 12 profile lines, spaced at 60-meter intervals and extend-
ing from a base stake on the foredune ridge to a point seaward of spring
low water, was surveyed daily for 42 days in July and August 1971 and 24
days in January 1972. Also, 12 daily profiles were run for an 8-day
period following the "northeaster" of 19 February 1972. The southern-
most profile, PL-0 (Fig. 1), was located near the position of an original
Plum Island profile (PLB) that was measured at biweekly intervals between
September 1965 and July 1971 (Coastal Research Group, 1969). The other
11 profile locations (PL-1 to PL-11) extended in a northerly direction
from PL-0. Bimonthly aerial photos of the study area and offshore pro-
files (linked to beach profiles) augmented data gathered during the study
period.

A computer program developed by W.T. Fox (Davis and Fox, 1971) was
used to process and plot the large numbers of beach profiles measured.
Vertical changes were measured every 3 meters on each profile; the pro-
gram converted these data to elevations with respect to mean low water
(MLW) and made a linear interpolation of elevation changes every 50 cen-
timeters between data points. These interpolated data were plotted at
2-meter horizontal intervals. Linear interpolation was also calculated
between each of the profile lines at 1-meter intervals. A 2 to 1 exag-
geration normal to the shoreline was shown on computer printouts (Davis
and Fox, 1971). From these two-dimensional data, erosion-deposition maps
were constructed by comparing individual profile lines at any specified
interval of days. The results obtained from these maps, contoured at
10-centimeter intervals, may be used to delineate zones of erosion and
deposition through time.

Beach process measurements were analyzed by using CALCOMP plots of
the observed data and visually comparing trends evident between different
process variables.

11
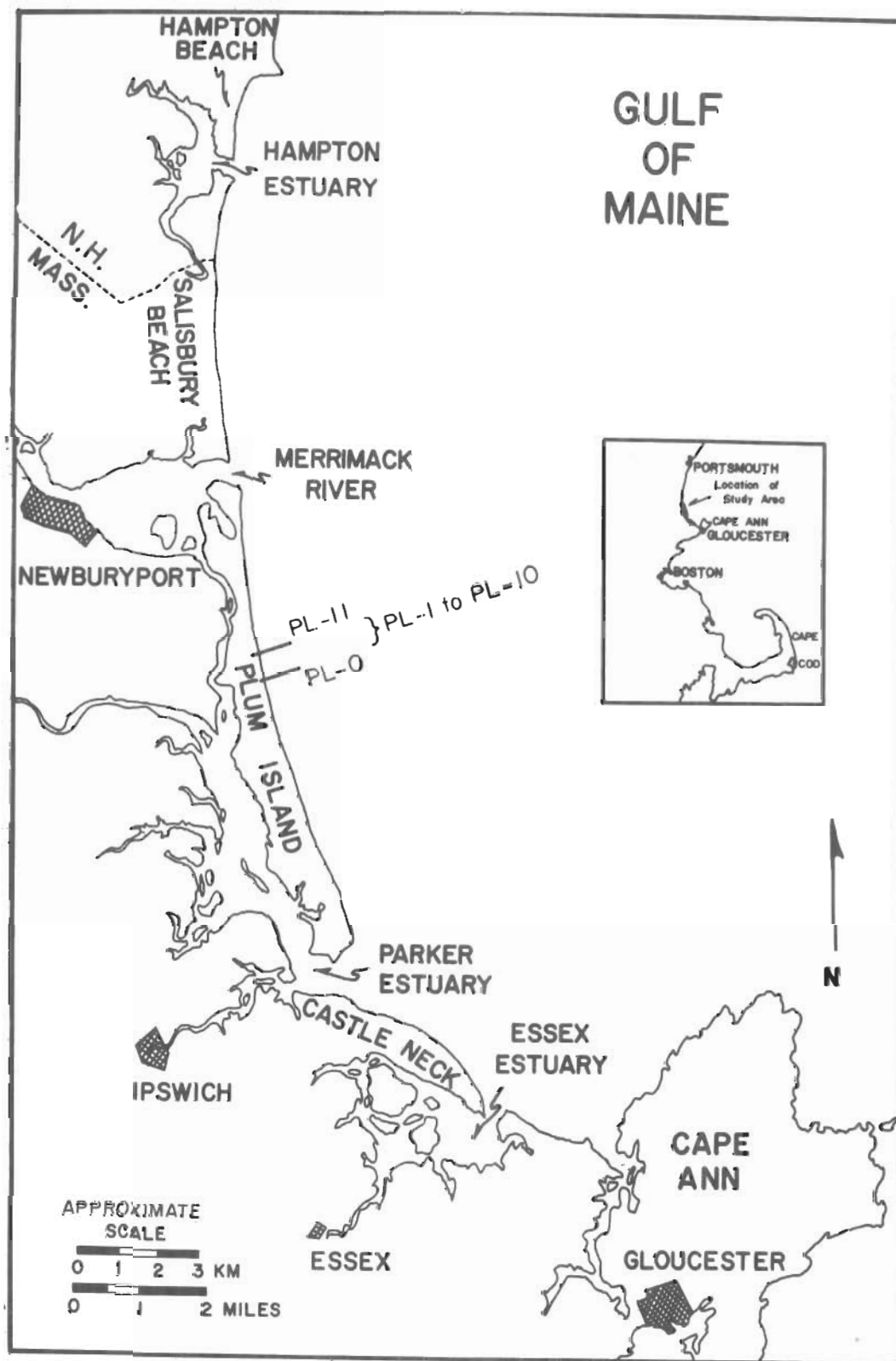
Figure 1. Location map of study area.

Many techniques used during this study are outgrowths of studies conducted on Lake Michigan during 1969 and 1970 by Fox and Davis (1970). Earlier work on time-series studies or detailed beach process studies was carried out by Harrison and Krumbein (1964), Sonu and Russell (1966), Sonu, McCloy, and McArthur (1966), Dolan, Ferm, and McArthur (1968), and Harrison, et al. (1968). The techniques and methods of data analysis reported in these earlier studies proved valuable in the development of this program.

Coastal processes of Plum Island and adjacent estuaries have been discussed in detail by several members of the Coastal Research Division, University of South Carolina (formerly the Coastal Research Group, University of Massachusetts), including McCormick (1968), DaBoll (1969), Coastal Research Group (1969), Hartwell (1970), and Anan (1971).

II. FIELD METHODS

Wave conditions, longshore currents, ground water elevations, meteorological parameters, and tidal elevations were measured bihourly for 6 weeks in July and August 1971 (summer period) and for 4 weeks in January 1972 (winter period). Meteorological parameters measured included barometric pressure, air and water temperature, windspeed and direction, sky conditions, and precipitation. Tide readings were taken hourly using a series of 250-centimeter stakes located about 20 meters apart and extending from the base of the dune scarp seaward to a point beyond the seaward edge of the low tide terrace. Ground water elevation was measured by a 1.5-inch pipe driven 5 meters into the incipient berm. Wave height and breaker depth were measured at the point of the breaking waves. Longshore currents were measured immediately landward of the breaker zone.

1. Wave Conditions.

Wave data collected consisted of bihourly measurements of breaker height, breaker depth, wave period, breaker type, and breaker angle. Values for wave steepness and breaker power were calculated from measured wave parameters.

The mean breaker power, expressed in kilograms per square second per meter of crest width, was calculated from:

$$\bar{P_b} \, \bar{n} \sim \frac{8}{3\sqrt{3}} \frac{pg \, H^{3/2} \, h^{3/2}}{T} \, ,$$

where

$\bar{P_b}$ = the mean breaker power;
pg = the specific weight of saltwater;
H = the mean breaker height;
h = the breaker depth; and
T = the mean wave period.

This estimate of breaker power is for a solitary wave and is a summation of the potential and kinetic energies of the wave (Ippen, 1966).

a. Breaker Height. Breaker height was measured during the summer period by a swimmer using a 3-meter rod graduated in 2-centimeter intervals. Measurements were taken at the location of the breaking waves. During the winter period breaker height was measured by 250-centimeter-long fenceposts, extending seaward from the beach face, and marked with fluorescent paint at 5-centimeter intervals. Every 2 hours, about 5 to 10 successive wave crests were measured and the average value was recorded. The mean breaker height for the summer period was 51.8 centimeters, with a minimum of 0 centimeter recorded on several occasions and a maximum of 183 centimeters measured during the passage of an offshore low-pressure system. A mean breaker height of 52.4 centimeters was recorded during the winter period, with extremes of 0 and 152 centimeters. Only during extreme storm conditions were waves observed to break on the offshore bar located about 450 meters seaward of the low tide terrace.

Wave steepness was calculated from the equations $\overline{Hb}/\overline{Tb}\sqrt{gh}$, where Hb is mean breaker height, Tb is the mean wave period, and h is the breaker depth.

b. Breaker Depth. Breaker depth is defined in this study as the distance from the bottom to a line midway between the trough and crest of the wave in the breaker zone. Breaker depths were measured for 5 to 10 waves every 2 hours during the study periods. The graduated 3-meter rod was used for measurements during the summer (and the winter period when practical). Measurements during adverse winter conditions were made with the 250-centimeter-long fenceposts used in the breaker height measurements. In the summer period the mean breaker depth was 45.5 centimeters, with a maximum of 130 centimeters and a minimum of 0 centimeter. Breaker depth was measured frequently during surging wave conditions at high tide. The winter mean breaker depth was 51.4 centimeters, with a maximum of 180 centimeters and a minimum of 0 centimeter.

c. Wave Period. Wave period was measured as the time in seconds necessary for two successive wave crests to pass a stationary point. In the summer a swimmer with a staff was used as the stationary point; in the winter, poles in the surf were used as reference points. The period was computed five times every 2 hours for 11 successive wave crests. On several occasions, two distinct wave families with different periods were observed during a shift in wind direction. Periods for both sets of waves were measured; however, only the wave period most influential on longshore drift and sediment transport was used in the final data analyses. Summer minimum and maximum wave periods were 4.7 and 12 seconds, with a mean of 8.9 seconds. A winter mean of 8.8 seconds was recorded; extreme values were 2.8 and 13.5 seconds.

d. Breaker Types. The following classification of breaker types is based on definitions used by the Coastal Engineering Research Center (CERC) in their Littoral Environment Observation (LEO) program. Detailed definitions are given in Allen (1972).

(1) *Spilling*. Spilling occurs when the wave crest becomes unstable and flows down the front face of the wave producing an irregular, foamy surface.

(2) *Plunging*. Plunging occurs when the wave crest curls over the front face of the wave and falls into the base of the wave producing a high splash and much foam.

(3) *Surging*. Surging occurs when the wave crest remains unbroken while the base of the front face of the wave advances shoreward to break on the shore.

A scale of 1 to 6 was set up to record different individual and mixed waves: (a) Type 1, spilling waves; (b) type 2, spilling and plunging; (c) type 3, plunging; (d) type 4, surging; (e) type 5, surging and plunging; and (f) type 6, surging and spilling. Spilling, plunging, and spilling-plunging waves are prevalent at low and high tide conditions. Surging waves (types 4, 5, and 6) are common at approximately 1 hour on either side of high tide.

e. Breaker Angle. Breaker angle was measured by a Brunton compass to determine the azimuth of the wave crests as they approached the breaker zone. The shoreline orientation of the study area was 350°; therefore, breaker azimuths between 80° and 170° represent wave crests approaching from the south and southeast and azimuths between 350° and 80° represent waves approaching from the north and northeast. Azimuth readings were converted to plus and minus acute angles to make breaker-angle readings compatible with longshore current readings. Plus readings indicated waves approaching from the north or northeast (azimuths between 350° and 80°); minus breaker angles indicated waves approaching from the south or southeast (azimuths between 80° and 170°) (Fig. 2). Azimuths of 170° or 350° indicate wave crests parallel to the shoreline (breaker angle = 0). Breaker angles for the summer period varied between -40° and $+10^\circ$ with a mean of -3.8°. In the winter period, breaker angles ranged from -8° to $+25^\circ$ with a mean of $+0.4^\circ$. Since ridges located on the low tide terrace may cause wave refraction between low and midtide, breaker-angle measurements may not reflect the actual breaker angle prevalent along the rest of the study area. Under such conditions, it is necessary to use the breaker angle of areas unaffected by local topography.

2. Longshore Currents.

Longshore current velocities were measured bihourly in the area immediately landward of the breaker zone. Measurement of littoral transport in this zone is known as *beach drift* (U.S. Army, Corps of Engineers, Coastal Engineering Research Center, 1966). Current velocities were measured in centimeters per second and given a sign value to indicate longshore transport direction (- = north; + = south). A series of stakes perpendicular to and extending seaward from the berm crest was used as the starting point for the measurements. A plastic "whiffle ball" was
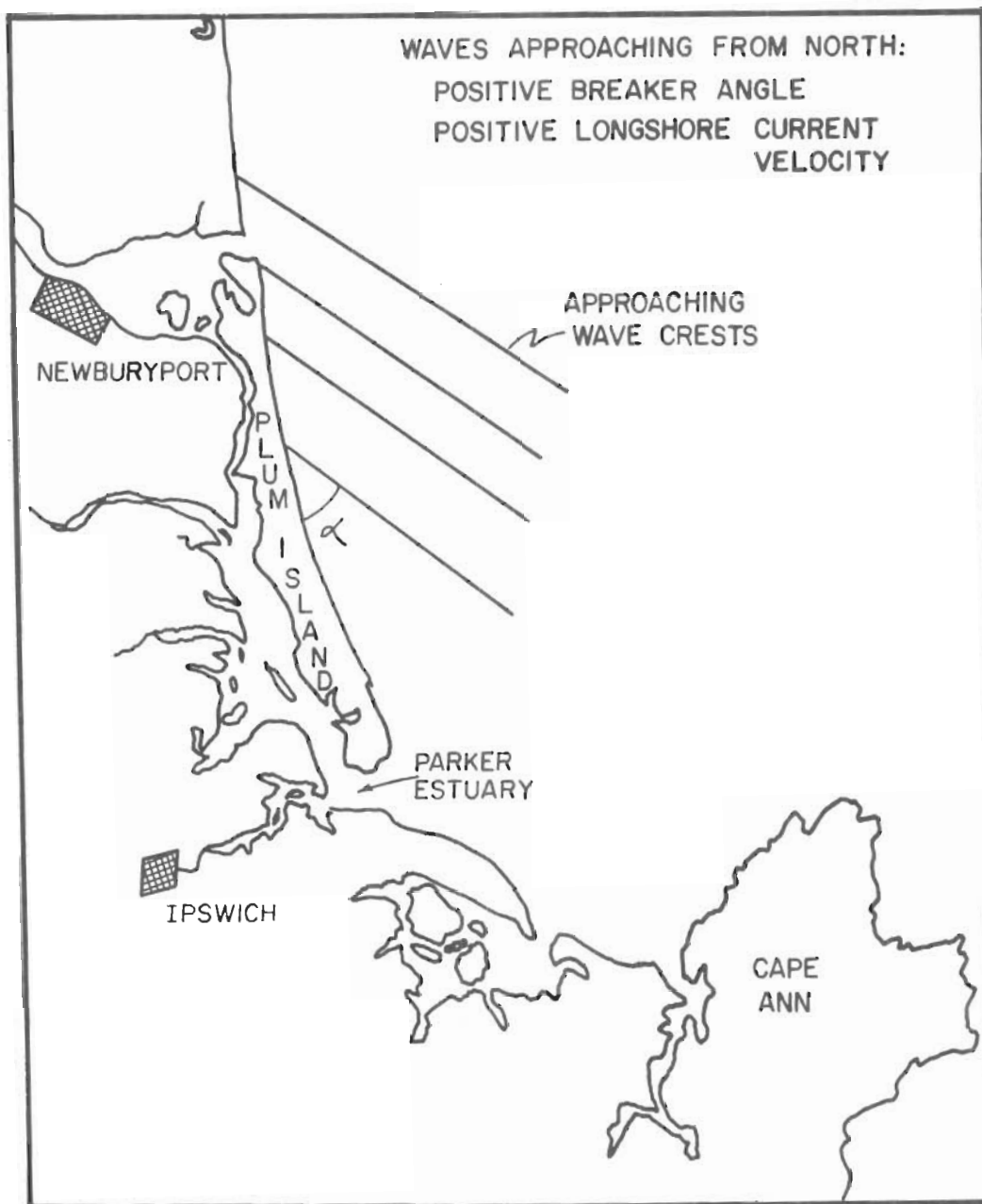
Figure 2. Schematic showing relationship between the direction of wave approach, breaker angle, and longshore current velocity. Alpha (α) is a positive breaker angle of approximately 45° (azimuth 35° or 215°). The linear wave crests shown are for illustration only and not intended to show a lack of wave refraction.

cast into the water immediately landward of the breaker zone in line with two or more of the marker stakes. The distance traveled by the ball in a 50-second period was measured. This process was repeated about 5 to 10 times. In the summer period, winds were sufficiently weak so that the ball's travel was unaffected by the wind. In the winter period, winds were of sufficient velocity frequently enough to require a different technique and the ball was replaced by a balloon filled with freshwater.

The presence of rip currents and runnel currents may cause problems in measurement as these currents often flow in a different direction than the dominant drift pattern or they may represent extremely localized energy conditions; therefore, they may not accurately reflect the dominant longshore currents operating over a large area.

The sum of longshore current velocity measurements for the summer period was -13.8 centimeters per second with extremes of -84.2 and +33 centimeters per second. In the winter period, extremes of -93.7 and +64 centimeters per second were recorded; the sum of the winter readings was +1.2 centimeters per second.

3. Ground Water Elevation.

The elevation of the ground water surface above MLW was measured hourly during the summer period. Subfreezing winter temperatures prevented measurement during the winter study. A 5-meter section of 1.5-inch pipe with a well point attached to one end was driven into the incipient berm to a depth of about 4.5 meters using a sling and hammer-type drilling rig. The elevation of the top of the pipe was tied in to MLW. Measurements were made from the top of the pipe to the water surface by using an aluminum dipstick streaked with carpenter's chalk. Readings ranged from 242 to 348 centimeters above MLW depending upon the amount of precipitation and the tidal stage.

4. Meteorological Parameters.

a. Windspeed and Direction. Windspeed and direction were measured with a Taylor Windscope three-cup anemometer and wind-direction indicator. The instruments were mounted on a 15-foot pole placed at the crest of the foredune ridge adjacent to the instrument shelter. Windspeed and wind-direction measurements were taken every 2 hours by recording eight readings, spaced 10 to 15 seconds apart. A sealed potentiometer, coupled with a weather vane mounted opposite to the anemometer, gave wind-direction readings over a 360° range.

By using the sine of the wind direction, measured as an azimuth, it is possible to determine onshore and offshore components of the wind data (Fox and Davis, 1971). The shoreline of the study area trends 350°, so that wind azimuths between 350° and 170° are classified as onshore winds and wind azimuths between 170° and 350° as offshore winds.

The onshore-offshore components are computed by taking the sine of the wind azimuth, with a 10° correction for the shoreline orientations, multiplied by the wind velocity. Winds blowing onshore, or between 350° and 170°, will result in positive sine values, while offshore winds between 170° and 350° will result in negative components. Ideally, where wind velocity is constant, the highest positive or onshore value would be for a wind azimuth of 80° (sine = 1), whereas the highest offshore or negative value would be for an azimuth of 260° (sine = -1).

Alongshore wind components may be determined by taking the cosine of the wind direction multiplied by the wind velocity. Wind-direction measurements between 260° and 80° will have a positive sign or a northerly alongshore component, whereas winds between 80° and 260° will have a negative or southerly component. The maximum southerly alongshore component will occur, with wind velocity held constant, at 170° (cosine = -1), whereas the maximum northerly alongshore component will occur at 350° (cosine = +1). The cosine function was chosen so that the signs for alongshore wind components are consistent with those for breaker angle and longshore current velocity.

The percentage of the time different windspeeds were measured (in 5-mile per hour classes) is shown in the Table. The greater percentage of winds in excess of 10 miles per hour recorded during the winter study period is directly related to the frequent passage of polar high-pressure systems during that period. Wind-direction readings averaged 218° for the summer period and 223° for the winter period.

Table. Summary of windspeed measurements, 1971-72.

Wind velocity (mi/h)	Pct measured
Summer	
0	2.1
0.1 to 5.0	33.0
5.1 to 10.0	44.1
10.1 to 20.0	20.1
>20.0	0.7
Mean velocity: 6.7 mi/h. Maximum recorded: 21.5 mi/h.	
Winter	
0	3.9
0.1 to 5.0	36.4
5.1 to 10.0	19.2
10.1 to 20.0	31.8
>20.0	8.7
Mean velocity: 8.7 mi/h. Maximum recorded: 39.4 mi/h (gusts in excess of 55 mi/h).	

b. Barometric Pressure. Barometric pressure was measured with a Danforth Marine Barometer. Periodic checks were made with the National Ocean Survey (NOS) Merrimack River Station to maintain the instrument calibration. Mean barometric pressure readings for the summer and winter periods were 29.75 and 29.88 inches. Maximum and minimum readings for both periods reflect the passage of high- and low-pressure systems.

c. Air and Water Temperature. Measurements of air and water temperature were taken bihourly throughout both study periods. Air temperatures were taken from thermometers mounted adjacent to the instrument shelters. The thermometers were placed to shield them from direct sunlight and wind. Mean temperatures were 72.5° and 28.2° Fahrenheit for the summer and winter periods. Water temperatures were measured by attaching a swimming pool thermometer on a line to the waist of a swimmer as breaker height and depth were measured. Summer water temperature readings varied between 47° and 68° Fahrenheit with a mean of 57.3° Fahrenheit. Minimum and maximum water temperature readings during the winter period were 28° and 45° Fahrenheit, with a mean of 37° Fahrenheit.

5. Beach Profile Techniques.

Beach profiles were run daily at low tide for each of the 12 profile locations (PL-0 to PL-11).

The profiling technique used was modified after the technique of K.O. Emery (1961) which required the use of two 300-centimeter profile rods and a 200-centimeter spacing rod. The observer sights the horizon with the top of the seawardmost post and determines where the two levels line up on the landwardmost post. This difference in elevation is recorded as a decrease in centimeters per "standard interval" (300 centimeters). Where profiles cross significant breaks in slope, smaller surveying intervals are used. Traverses across ridges located on the low tide terrace require lining up the landwardmost post with the horizon and sighting off of the seawardmost post. These measurements are recorded as a certain rise in centimeters per 3-meter interval.

During periods of reduced visibility, an Abney Level was attached to the horizontal spacing rod and elevation changes were determined by leveling the spacing rod between the two upright posts and recording the elevation difference.

Initially, each of the 12 base stakes, including the backup stakes, was surveyed in relation to profile PL-0 by using a Theodolite and stadia rod. A series of 8-foot metal fenceposts was placed along the PL-0 profile line for tide-measuring stakes. Tide measurements for the study period were used to calculate MLW. This datum was then related to the elevation at stake PL-0 and thence to PL-1 to PL-11.

III. SUMMER BEACH PROCESS VARIABLES

1. Introduction.

Throughout the summer study, few periods of high-wave energy condi-
tions were encountered with the result that changes in beach morphology
during this time were related mostly to uninterrupted accretion. Changes
in beach process variables were caused primarily by the passage of high-
and low-pressure systems through the study area.

2. Meteorological Variables.

Continuous measurement of barometric pressure showed the passage of
five high-pressure systems and three low-pressure systems over Plum Island
during the study period. The effects of these pressure systems on beach
process variables were multifold. As a result of the cyclonic flow asso-
ciated with low-pressure systems and the anticyclonic flow common to high-
pressure systems, the dominant wind direction varied in relation to these
two factors. Also important was the path of the air mass in the study
area. Low-pressure systems such as the one on 14 July resulted in wind
directions between 240° and 270°. As the low-pressure system moved past
Plum Island, the winds shifted from dominantly southwest to between 270°
and 340° or dominantly northwest. Minor fluctuations in the relationship
between wind direction and barometric pressure were due to the path of
the pressure system over Plum Island.

Barometric pressure measurements and alongshore wind components are
shown in Figure 3. Alongshore winds with a negative component commonly
preceded low-pressure systems as they moved into the area. As a high-
pressure system moved in, the winds shifted to a westerly or north-
westerly direction and changed from a negative to a positive alongshore
wind component.

Windspeed and onshore-offshore wind components are compared in
Figure 4. Wind data were recorded in this form by applying techniques
discussed in Section II,4. The results were plotted in a CALCOMP plotter.
Qualitative correlations were made by visually analyzing data printouts.
The highest wind velocities recorded during the summer period, which
exceeded 20 miles per hour on several occasions (e.g., 25 and 31 July),
were associated with offshore winds. Onshore winds rarely exceeded 10
miles per hour. During the summer period the resultant of the onshore-
offshore wind components was -3.52 miles per hour with a maximum onshore
reading of 9.8 miles per hour and a maximum offshore reading of -21.03
miles per hour. The resultant of the alongshore wind component readings
was -1.03 miles per hour with a northerly maximum of 9.03 miles per hour
and a southerly maximum of -14.359 miles per hour.

The relationships between air temperature and surface water tempera-
ture are shown in Figure 5. Air temperature readings had a 51° range of
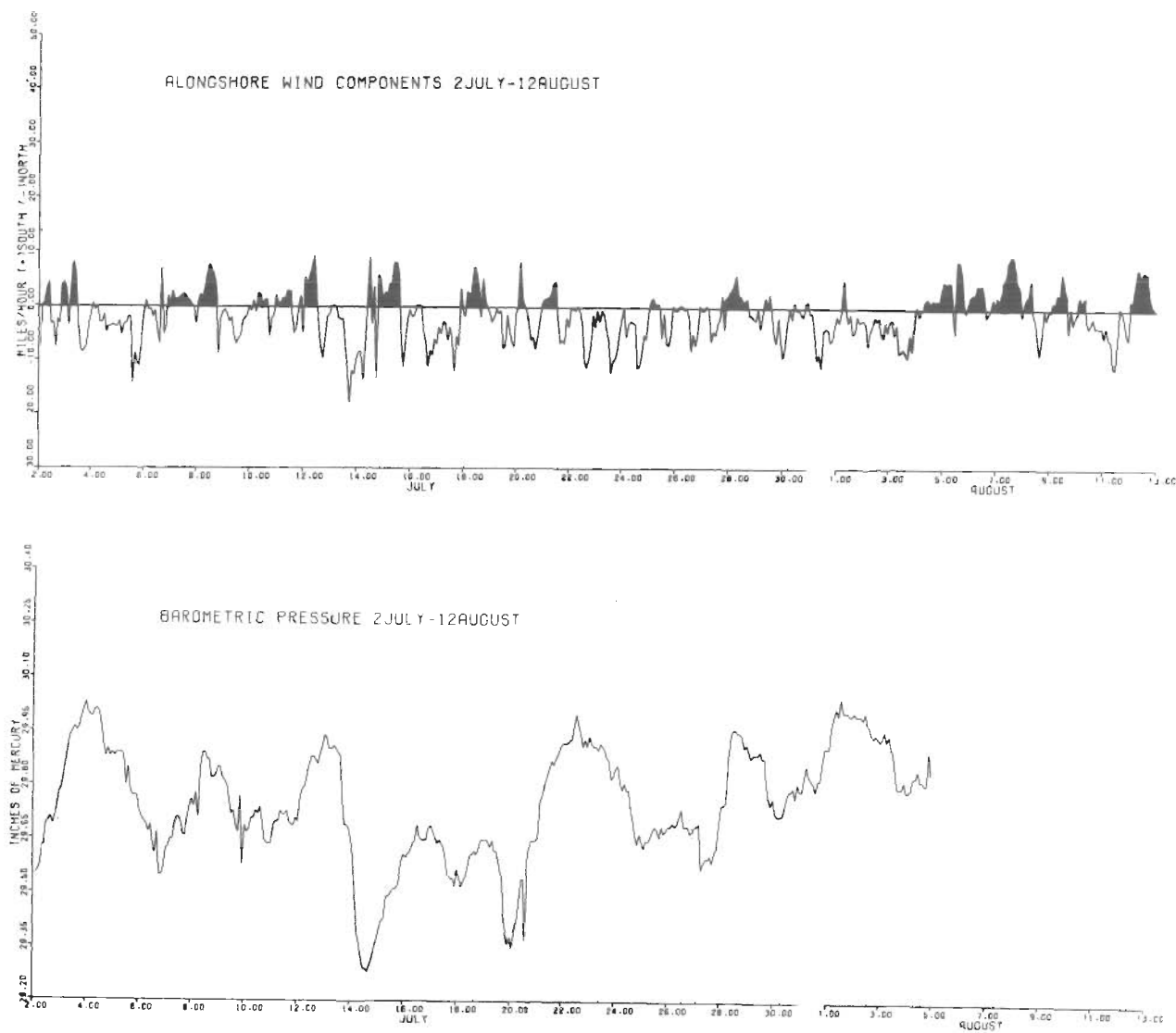48° to 99° Fahrenheit; surface water temperature had a 21° range of 47°

20

ALONGSHORE WIND COMPONENTS 2JULY-12AUGUST

BAROMETRIC PRESSURE 2JULY-12AUGUST

Figure 3.   Comparison of alongshore wind components with barometric pressure, July-August 1971.

ONSHORE-OFFSHORE WIND COMPONENTS   2 July - 12 August
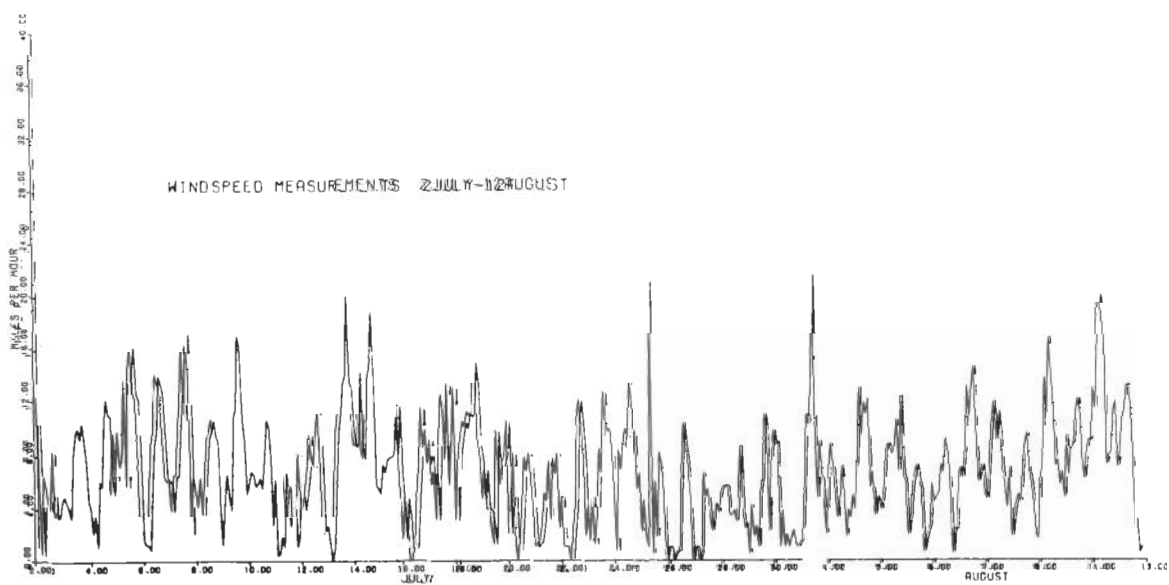
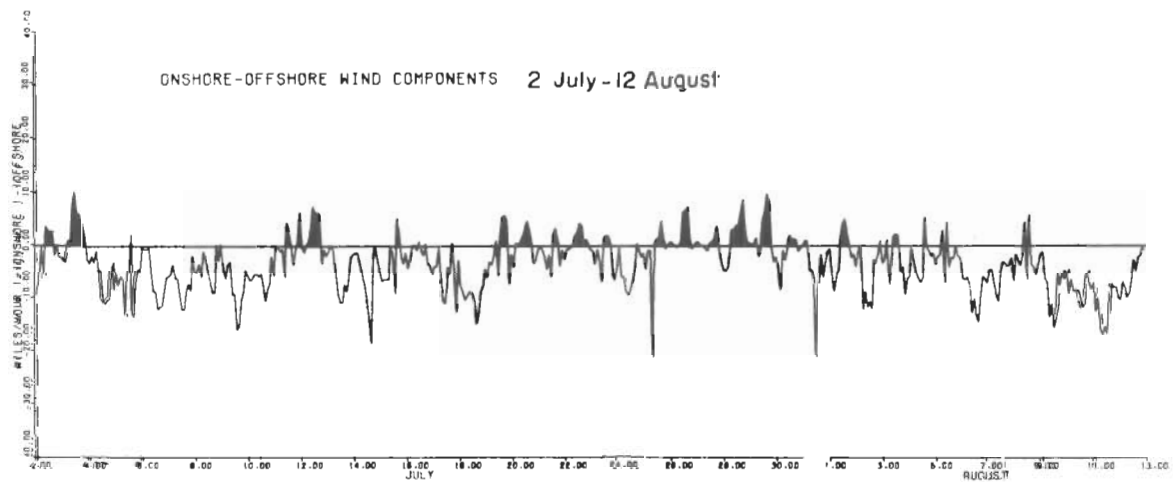WINDSPEED MEASUREMENTS   2 July - 12 August

Figure 4.   Relationship between onshore-offshore wind components and
windspeed for the summer period. Shaded areas above 0 (+)
are onshore components of wind; negative values (-) are
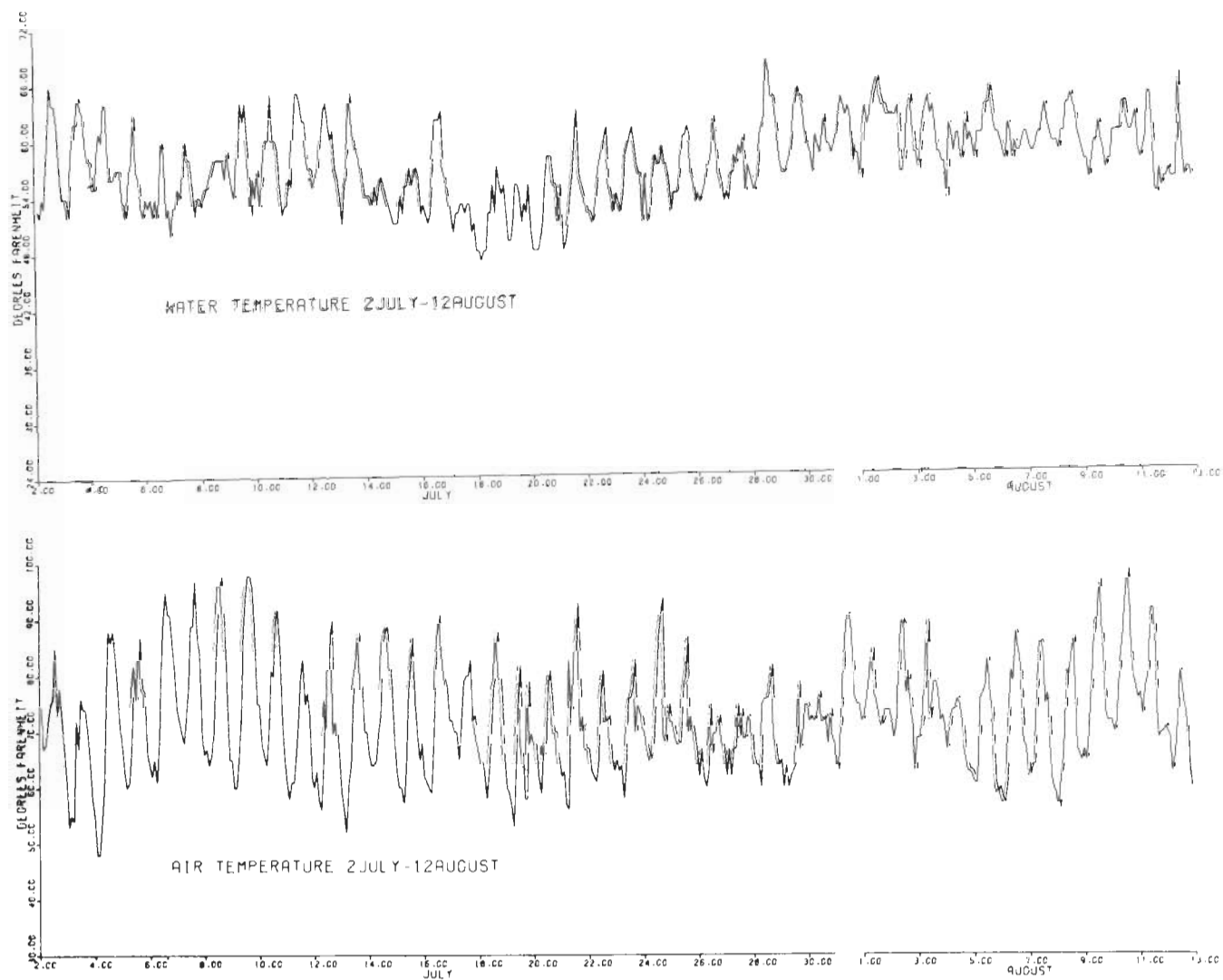offshore components.

Figure 5.   Water and air temperature measurements, July-August 1971.

to 60° Fahrenheit. As low-pressure systems passed through the area, the daily temperature range was reduced from an average range of 20° to 25° to 10° to 15°. With the passage of a low (e.g., 6 and 14 July) out of the area, the air temperature range increased, usually within 1 day. However, water temperature required 2 to 4 days to return to previous conditions. From the middle of July until the end of the study period, the mean water temperature increased as the surface waters were gradually heated by higher summer temperatures.

3. Wave Measurements.

The relationships between barometric pressure, breaker height, and breaker power are shown in Figure 6. With the passage of low-pressure systems over Plum Island (6 and 14 July), breaker height and breaker power tended to increase. The increase in breaker height on 15 July was due to long-period swells generated by a low-pressure system which passed through the area on 14 July. The effect of changes in breaker power is discussed later.

Wave steepness data and breaker height measurements are given in Figure 7. A comparison of wave period and barometric pressure for the summer period reveals no consistent correlation between local pressure systems and wave period. Local shifts in wind direction may cause short-period waves to form and coexist with longer period waves generated far-ther offshore. Late afternoon southeasterly winds were usually responsi-ble for these short, 5- to 6-second waves, but as the wind velocity decreased after several hours, only longer period waves persisted.

The daily fluctuations in breaker height and wave steepness were due to surging-type waves occurring at high tide. The surging waves averaged less than 30 centimeters in height and were less steep than spilling and plunging waves.

Breaker-angle measurements are affected by changes in wind conditions more rapidly than most other wave parameters. The relationships between alongshore wind components, those components which are locally responsible for the direction of wave approach, and breaker angle are presented in Figure 8. The lack of northerly or northeasterly winds resulted in few positive alongshore wind components and hence few positive breaker angles. Increases in the magnitude of alongshore wind components often result in a corresponding increase in breaker angle. However, high breaker-angle measurements were never accompanied by high-energy wave conditions suffi-cient to cause marked beach erosion.

4. Ground Water Measurements.

Hourly ground water readings revealed close relationships between ground water elevation above MLW and tides, precipitation, and breaker height (Fig. 9). Ground water elevations before 10 July were not recorded because of instrument problems. Changes in ground water elevation lag approximately 3 hours behind changes in the tide. The effect of spring and neap tides for parts of the ground water elevation curve is shown in
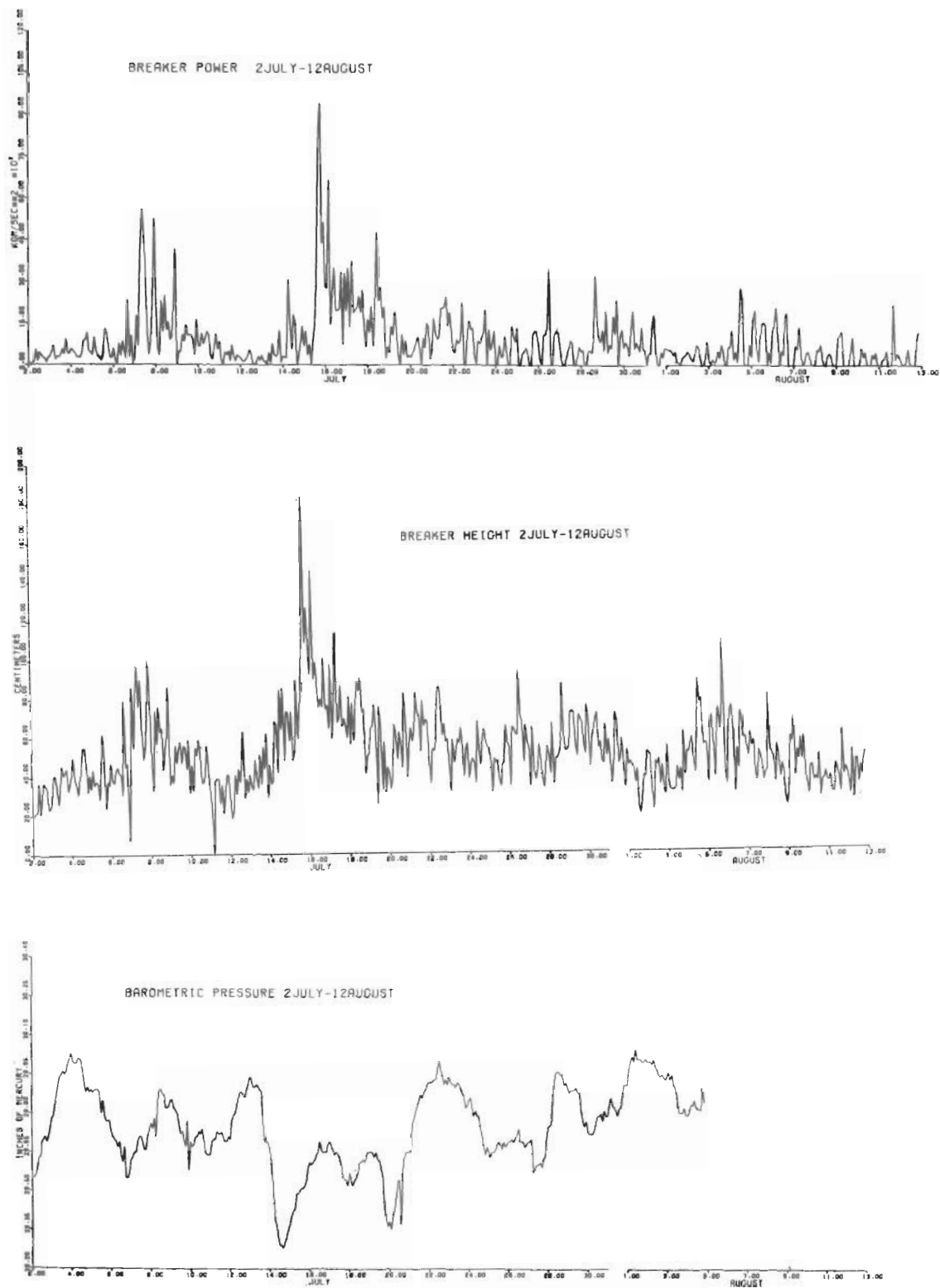
Figure 6. Relationship between breaker power, breaker height, and barometric pressure for the summer period.
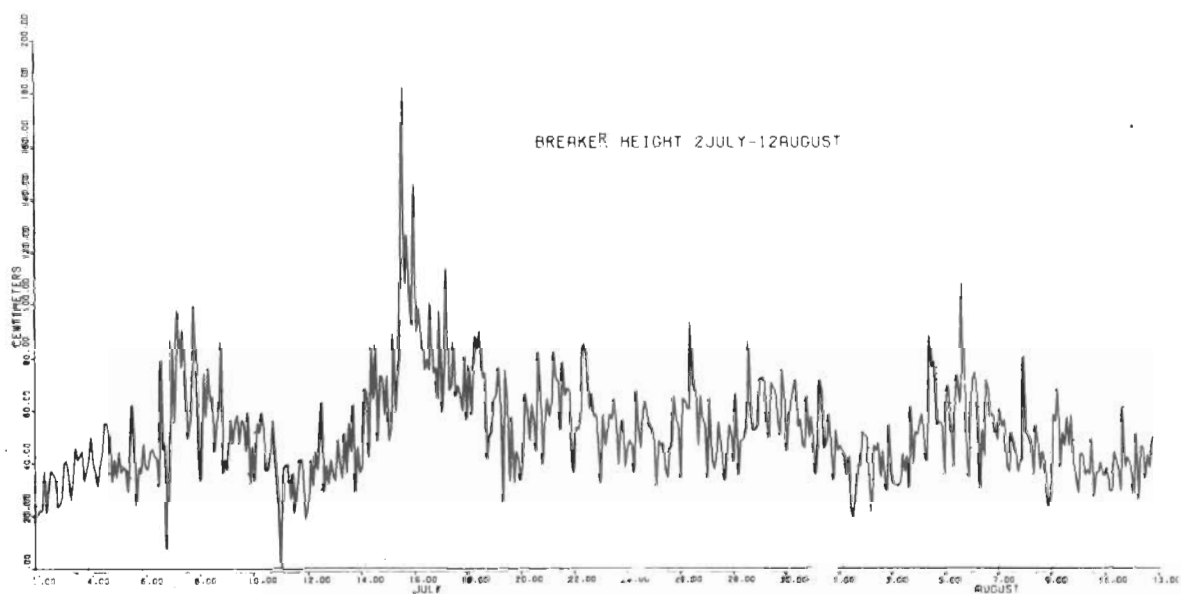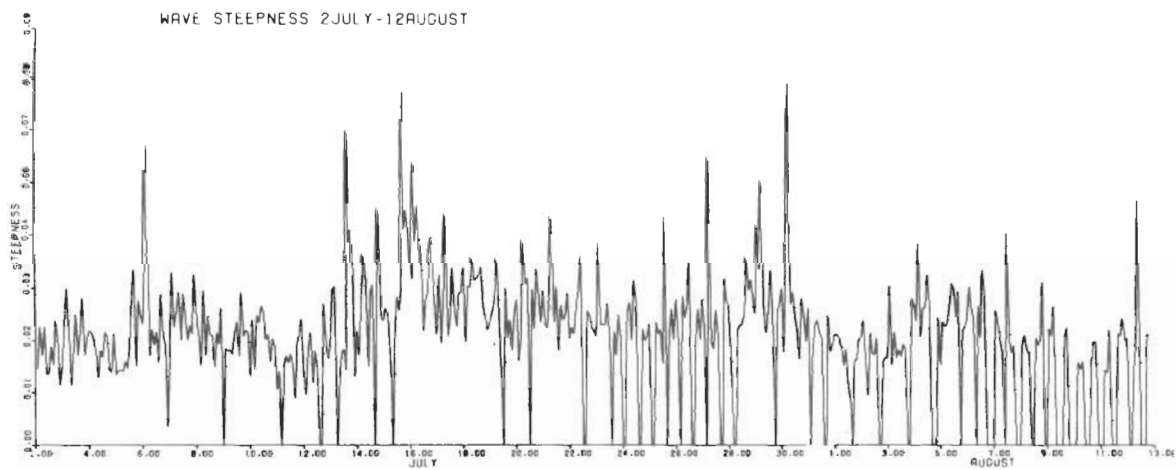
25

Figure 7. Relationship between wave steepness and breaker height,
July-August 1971. Wave steepness values of zero are obtained
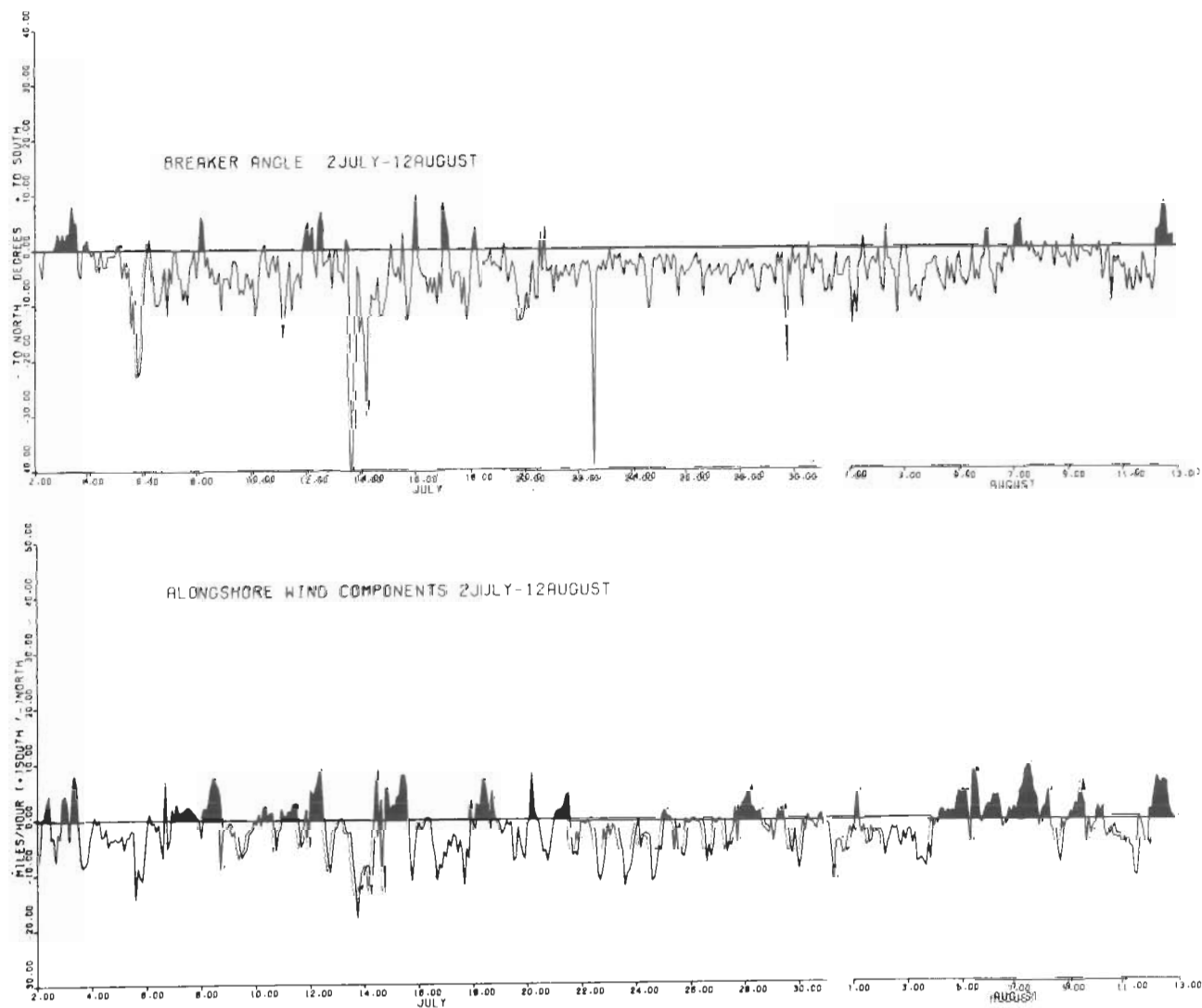for surging waves which commonly occur near high tide.

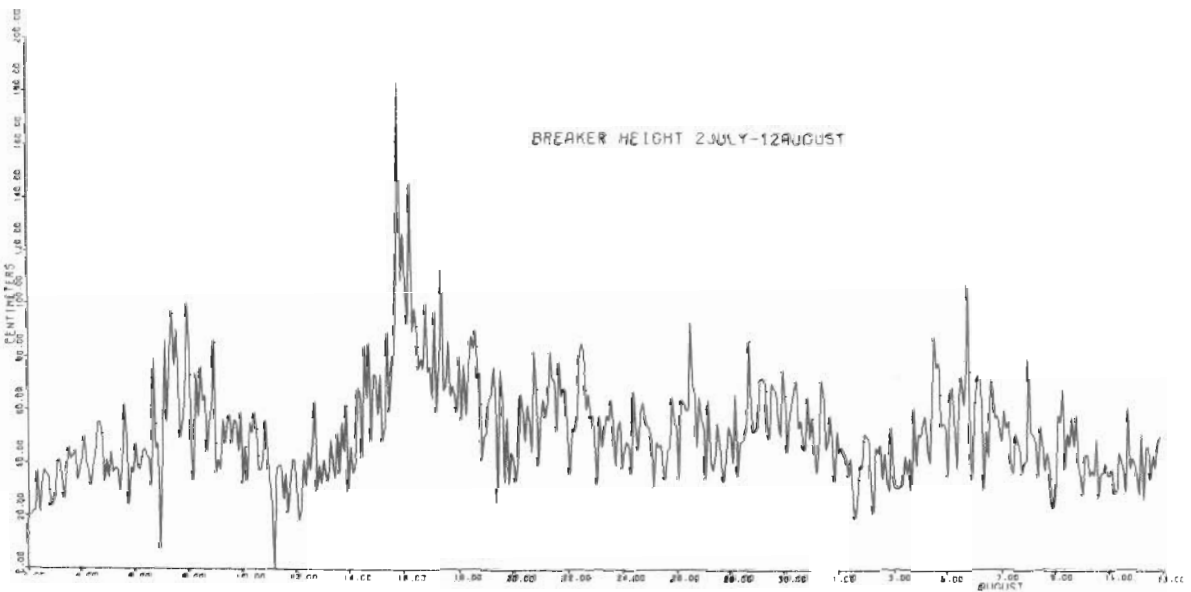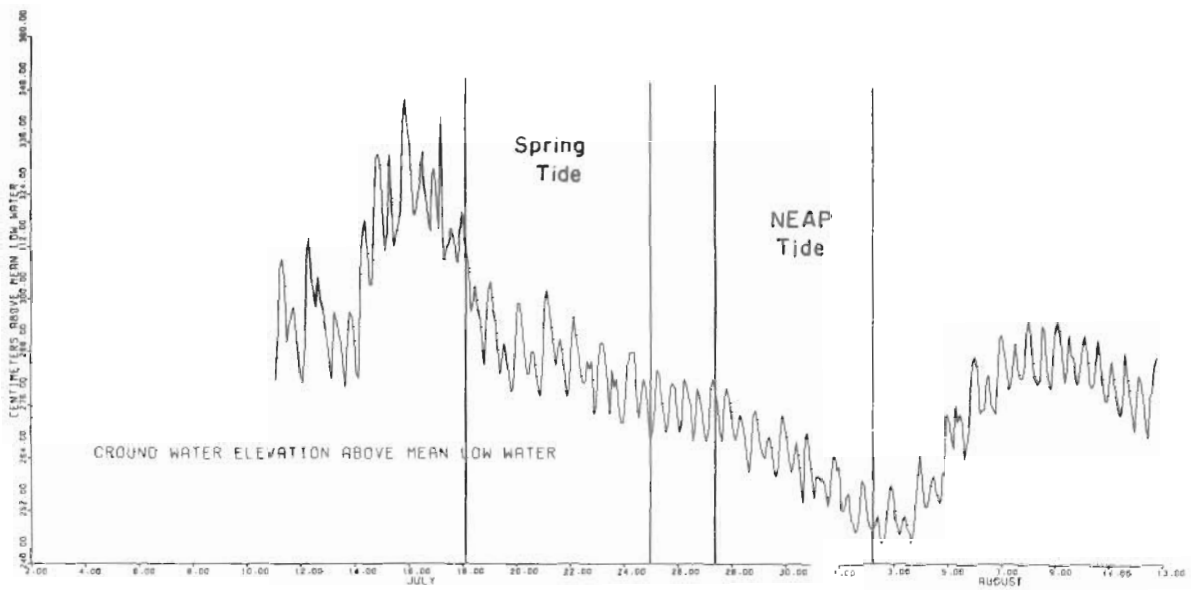Figure 8. Breaker angle and alongshore wind components, July-August 1971.

Figure 9. Ground water elevation and breaker height measurements, July-August 1971.

Figure 9. Spring tides occurred between 18 and 25 July while neap tides occurred between 27 July and 2 August. Figure 9 shows the effect of breaker height on the water table. Precipitation on 14 July raised the water table nearly 30 centimeters. This, along with the large breakers of 15 July, resulted in an even higher ground water level. Analogous conditions occurred on 4 and 5 August, when precipitation and an increase in breaker height resulted in a rise of the ground water surface level. The rapid rise of the ground water level with the onset of storm conditions would seem to increase the erosion associated with a storm.

Duncan (1964) found that the position of the water table with respect to the beach surface was important in controlling erosion and deposition:

> "Swash water, upon transgressing over and above the inter-section of the water table with the foreshore surface, rapidly percolates into the sand. This reduction of water volume is accompanied by a decrease in velocity as well as deposition of sediment transported in that portion of swash which vanished into the interstices of the beach sands. Hence, a dry beach (low water table) facilitates deposition in the upper reaches of the foreshore until slope equilibrium is gradually reached and backwash velocities prevent further net accretion."

5. Longshore Current Measurements.

One of the initial problems in measuring longshore drift is defining longshore drift or littoral drift velocity. There are three basic modes of littoral transport (U.S. Army, Corps of Engineers, Coastal Engineering Research Center, 1966) (Fig. 10). Beach drift is "material which is moved
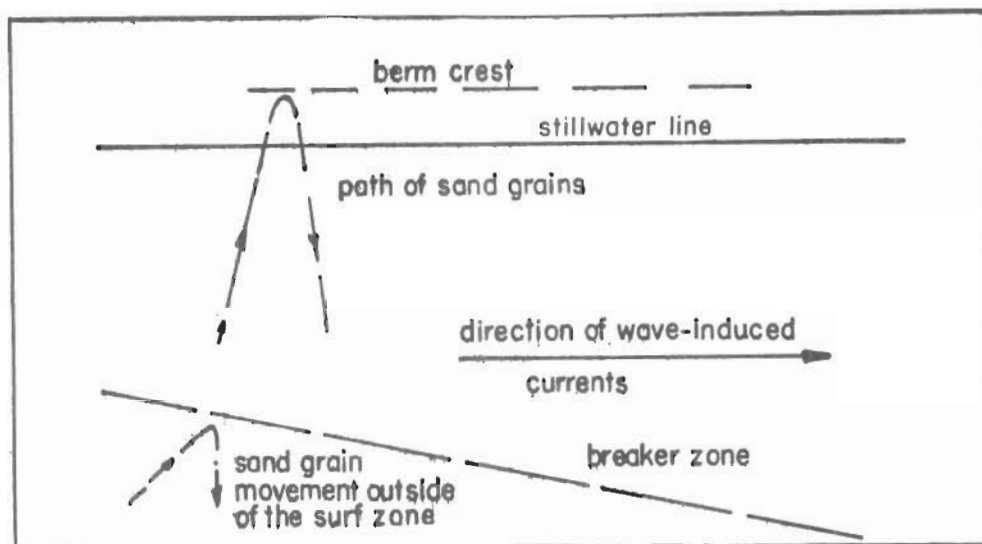

Figure 10. Longshore or lateral movement of littoral drift (U.S. Army, Corps of Engineers, Coastal Engineering Research Center, 1966).

29

along the foreshore in a saw-toothed or zigzag path due to upwash and backwash of obliquely approaching waves." Material is also moved in suspension in the surf zone by longshore currents and the energy associated with breaking waves. A third mechanism is bedload transport which is sediment moved close to the sediment-water interface by sliding, rolling, and bed form migration. The longshore current measurements taken during the study period (according to U.S. Army, Corps of Engineers, Coastal Engineering Research Center, 1966) would be considered a combination of beach face velocity and wave-induced currents in the surf zone.

Computations were carried out for theoretical conditions on a mature beach profile in which all of the parameters used in the Eagleson formula for longshore drift were held constant except for slope angle of the beach. Beach-face gradients taken from beach profile data were inserted to approximate velocity conditions as the tide rises (2^O to 3° slope of the low tide terrace) and begins to flood the beach face (7° to 10° slope). As the tide rises, assuming constancy of other variables (i.e., breaker height, breaker depth, and breaker angle), the current velocity on the high tide beach face was greater than twice that of the low tide terrace. This points out that the longer that waves can act on the high tide beach face, as during spring tides or storm surges, the greater the longshore transport of sediment and the greater the net erosion.

There is a direct relationship between breaker angle and longshore drift velocities for breaker angles less than 45°. However, as breaker angles become greater than 45°, a decrease in longshore current velocities occurs (Vollbrecht, 1966).

The strength of longshore currents necessary to produce littoral transport can be qualitatively estimated from Figure 11. The range of
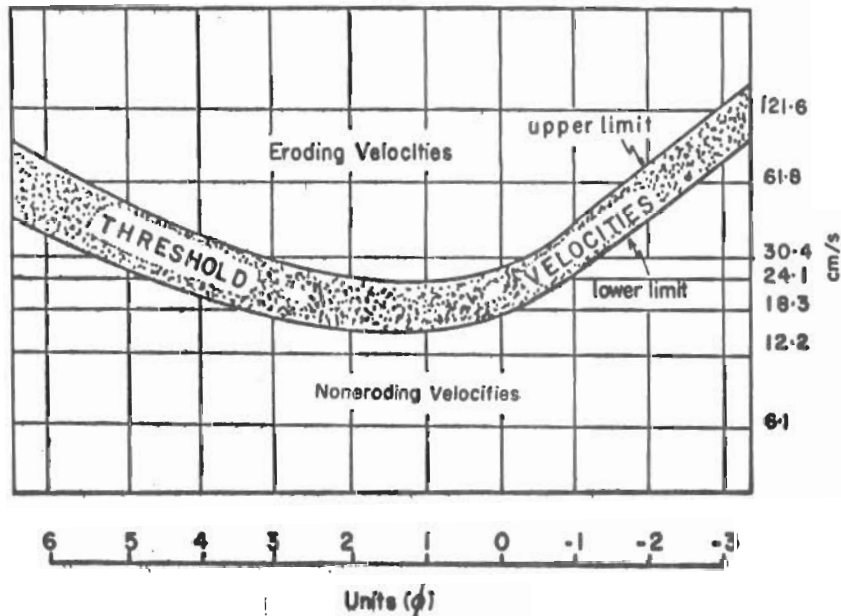

Figure 11. Mean velocities required to erode sand (U.S. Army, Corps of Engineers, Coastal Engineering Research Center, 1966).

sediment sizes is between -0.5 and 1.9 phi, so that for velocities less than 15 centimeters per second little or no entrainment will take place; for the size of particles, velocities greater than 24 centimeters per second are necessary for erosion to take place. Figure 12 reveals how infrequently these velocities were attained.

IV. SUMMER BEACH MORPHOLOGY

1. Introduction.

Changes in beach morphology within the study area between 2 July and 12 August can be divided into two major periods of activity. The initial or preweld period covers the time before and up to the welding of a large ridge on 12 July. Although smaller ridges were migrating shoreward in other parts of the study area, a large ridge and runnel system extending from profile PL-3 to a point 350 meters south of profile PL-0 was the site of the most dynamic changes in beach morphology within the study area (Fig. 13). Between 13 July and 12 August, accretion was due to numerous ridges of different sizes and locations migrating landward across the low tide terrace, eventually welding on the backshore. The changes in beach morphology during this period comprise what may be considered a postweld period. Hayes and Boothroyd (1969) discussed low tide beach morphology relative to the occurrence of northeasterly storms, and defined the following stages of beach morphology that are broadly applicable to this study.

a. Early poststorm; the profile is flat to concave and beach surface is generally smooth and uniformly medium grained.

b. Early accretion; small berms, beach cusps, and ridge and runnel systems form rapidly.

c. Late accretion or maturity; landward-migrating ridges weld onto the backshore to form broad, convex berms.

Characteristic preweld profiles PL-0 and PL-5 for 2 July are shown in Figures 14 and 15. Profile PL-0 approximates the conditions at PL-1, PL-2, and PL-3, or the southern end of the study area. A typical profile of the southern end consists of a large ridge (average height 80 centimeters) which migrates landward during high tide. The large berm at PL-0 with a steep high tide beach face and a slope varying between 9° and 10°, is more characteristic of a later stage of maturity of a poststorm beach profile than the berm at profile PL-5. Although ridge and runnel systems are at both profile locations, the large berm and nearly welded ridge at PL-0 are indicative of a nearly welded beach profile. Other profiles (PL-5 through PL-8) which do not have a broad berm exist contemporaneously with profiles such as PL-0. The ridge has not migrated as far landward on these profiles, resulting in a wider runnel and low tide terrace; the beach-face slope varies between 6° and 8°. Profiles PL-5 and PL-11 are shown in Figure 15, with PL-11 representing the northern end of the study
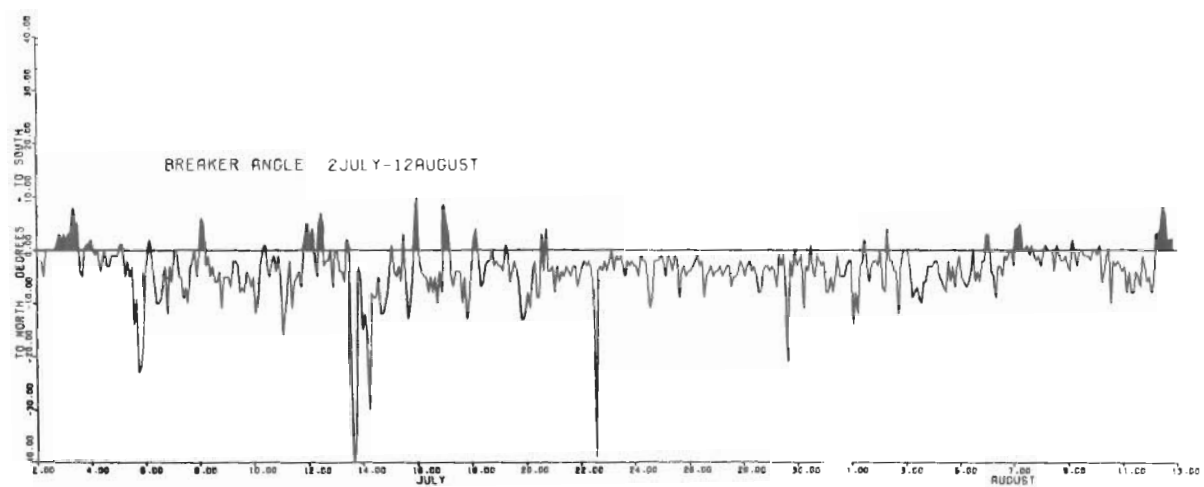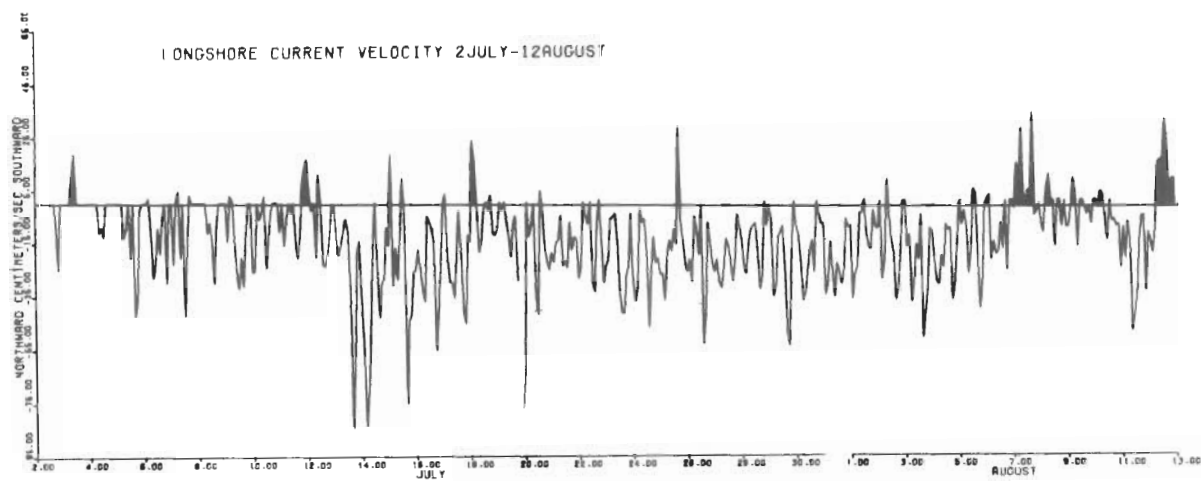
Figure 12.   Longshore current velocity and breaker-angle measurements,
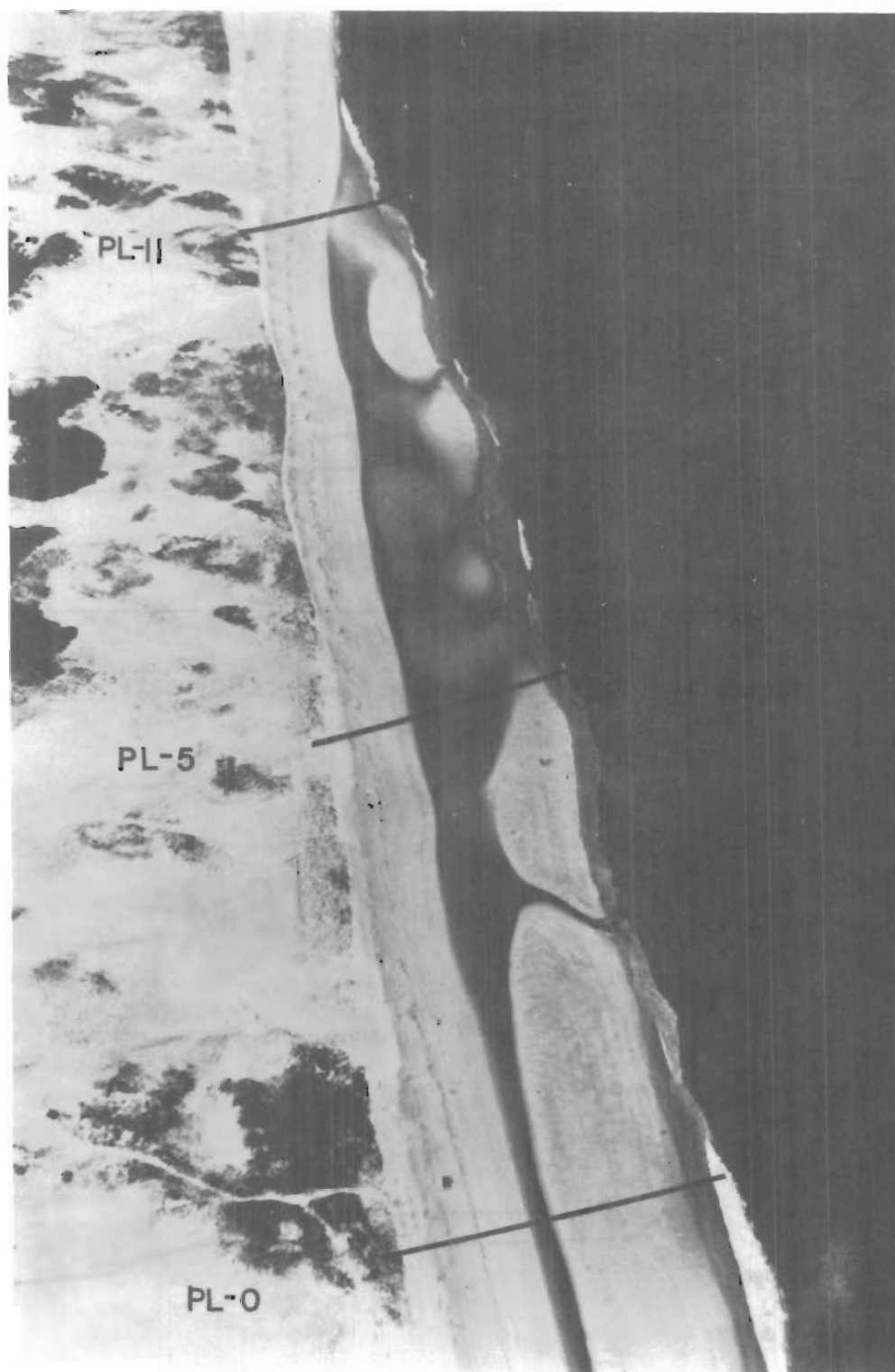   July-August 1971.

Figure 13. Aerial view of study area on 28 June 1971 showing profiles PL-0, PL-5, and PL-11. Area is 660 meters long.
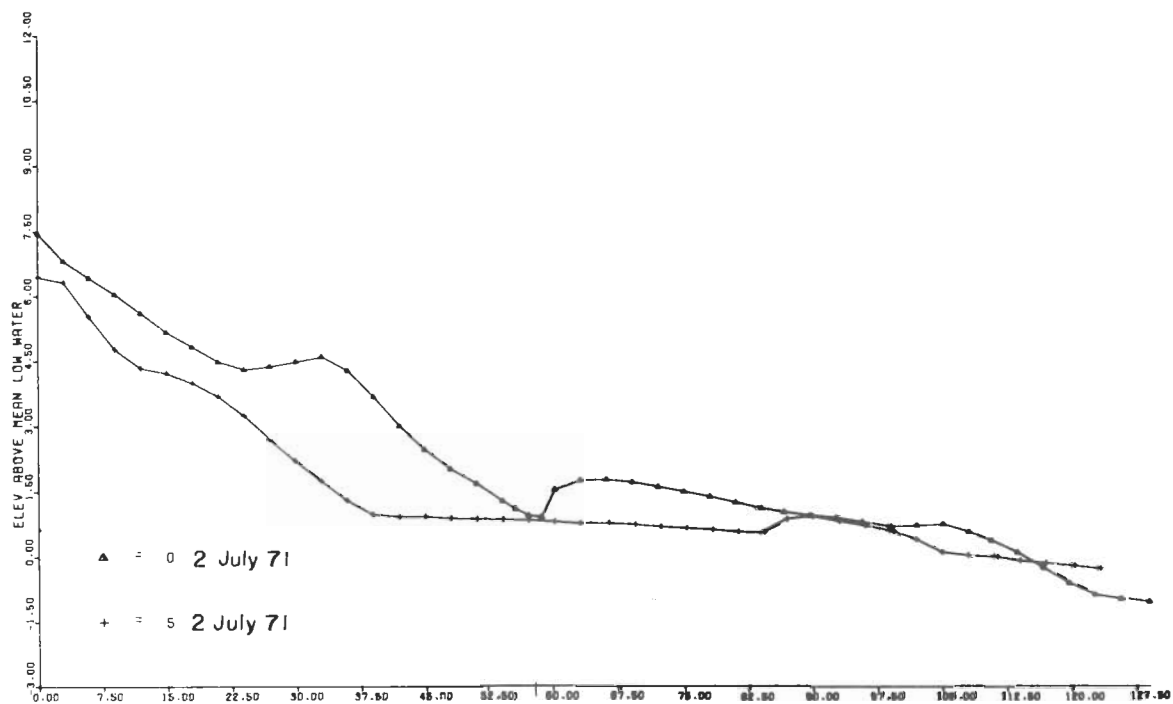
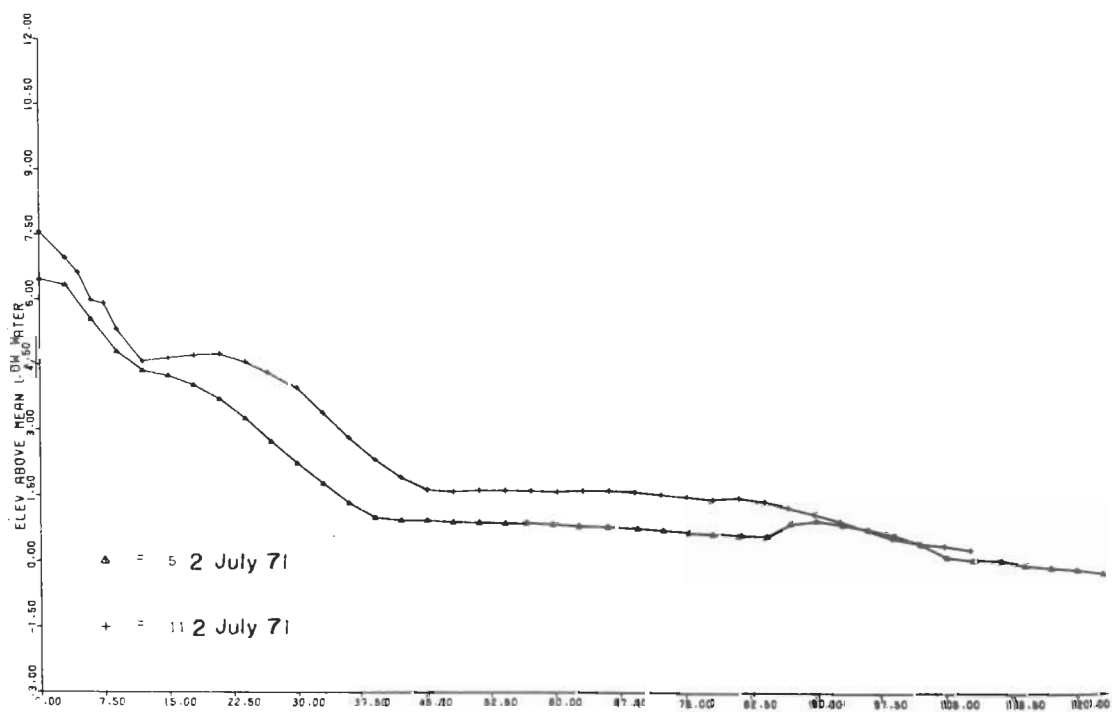Figure 14. Profiles PL-0 and PL-5, 2 July 1971.

Figure 15. Profiles PL-5 and PL-11, 2 July 1971.

area (PL-9, PL-10, and PL-11). By comparing these profiles with the profiles in Figure 14, it is apparent that PL-11 is intermediate in development, less mature than PL-0, but more mature than PL-5. Figure 16 gives ridge slip-face migration rates for profiles PL-4, PL-9, and PL-10, representing the central and northern end of the study area. The figure shows that migration rates are approximately equal for these locations. Although migration rates are similar for these locations, a greater volume of sand was transported shoreward on profiles PL-9 and PL-10 than on PL-4. The greater amounts of sand transported at PL-9 and PL-10 is a result of the distance of the nearshore bar from the beach at the different profile locations (Fig. 17), the closest bar between PL-9 and PL-11.

Typical accretionary profiles between 13 July and 12 August are shown in Figures 18 and 19. In Figure 19, profile PL-0 has assumed a "late mature" profile, characterized by a broad berm, a relatively steep beach face, and a lack of any large-sized ridge and runnel systems. On profile PL-6, the position of the last high tide swash was located approximately 41 meters landward of the same last high tide swash on PL-0 (on 1 and 2 August). The last high tide swash on PL-11 was about 14 meters seaward of the last high tide swash on the beach face of PL-6. The southern profiles remained most mature, with the northern profiles less mature, and the central profiles at a lesser stage. The relative maturity of a given profile depends primarily on how quickly sediment is moved landward after a storm. During a storm, the backshore and foredune ridges at the northern and southern ends of the study area are less likely to erode than the same features between profiles PL-4 and PL-8 because of the shielding effect of the large berm.

2. Preweld Period.

The preweld period of beach morphology (before 12 July) is shown in Figures 20 and 21. The figures show a typical early accretional beach with a large ridge, a wide runnel (16 meters), and an active beach face shoreward of the ridge. The ripples in the runnel were formed by subcritical flow at or near high tide. The ridge migrated shoreward as the ridge surface became flooded before high tide. Sediment was transported across the ridge surface, primarily under upper flow regime conditions, and deposited on the ridge slip face as flow separation took place. In Figure 22, the first swash has partially overlapped the ridge surface. Sediment is transported across the ridge surface either in a sheetlike manner or in the form of small ridges. Figure 23 shows flow separation occurring over the slip face of the ridge. Flow conditions are not always uniform over the slip face as shown by the current eddys in the figure.

As the ridge moves shoreward toward the backshore, the ridge gradient (measured from the ridge crest seaward) undergoes a progressive steepening (Fig. 24). On 2 July, the ridge gradient at PL-6 was 0.035 centimeter per centimeter, while the high tide beach-face gradient for the same
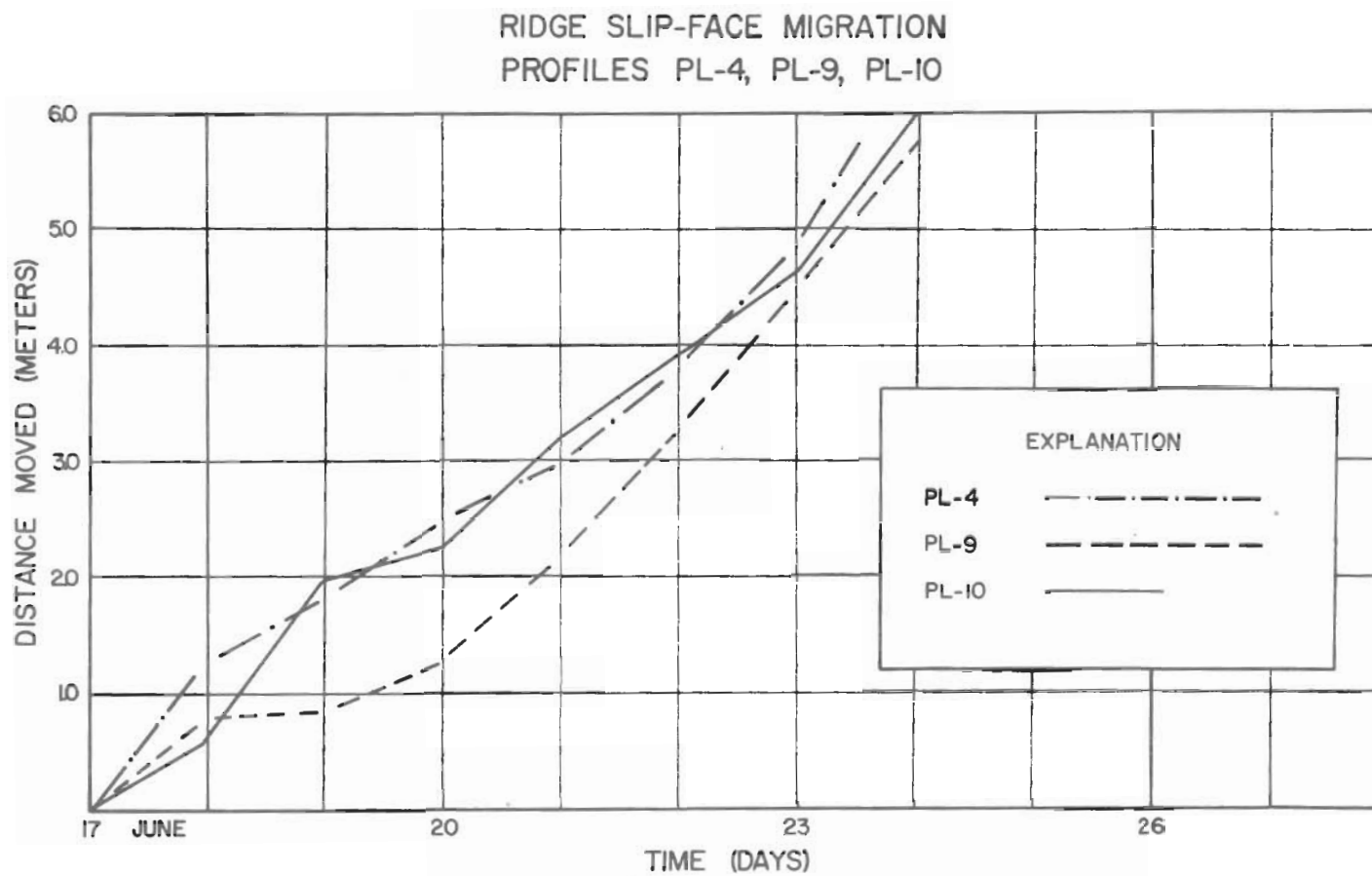
RIDGE SLIP-FACE MIGRATION
PROFILES PL-4, PL-9, PL-10

Figure 16. Ridge slip-face migration data for profiles PL-4, PL-9, and PL-10 between
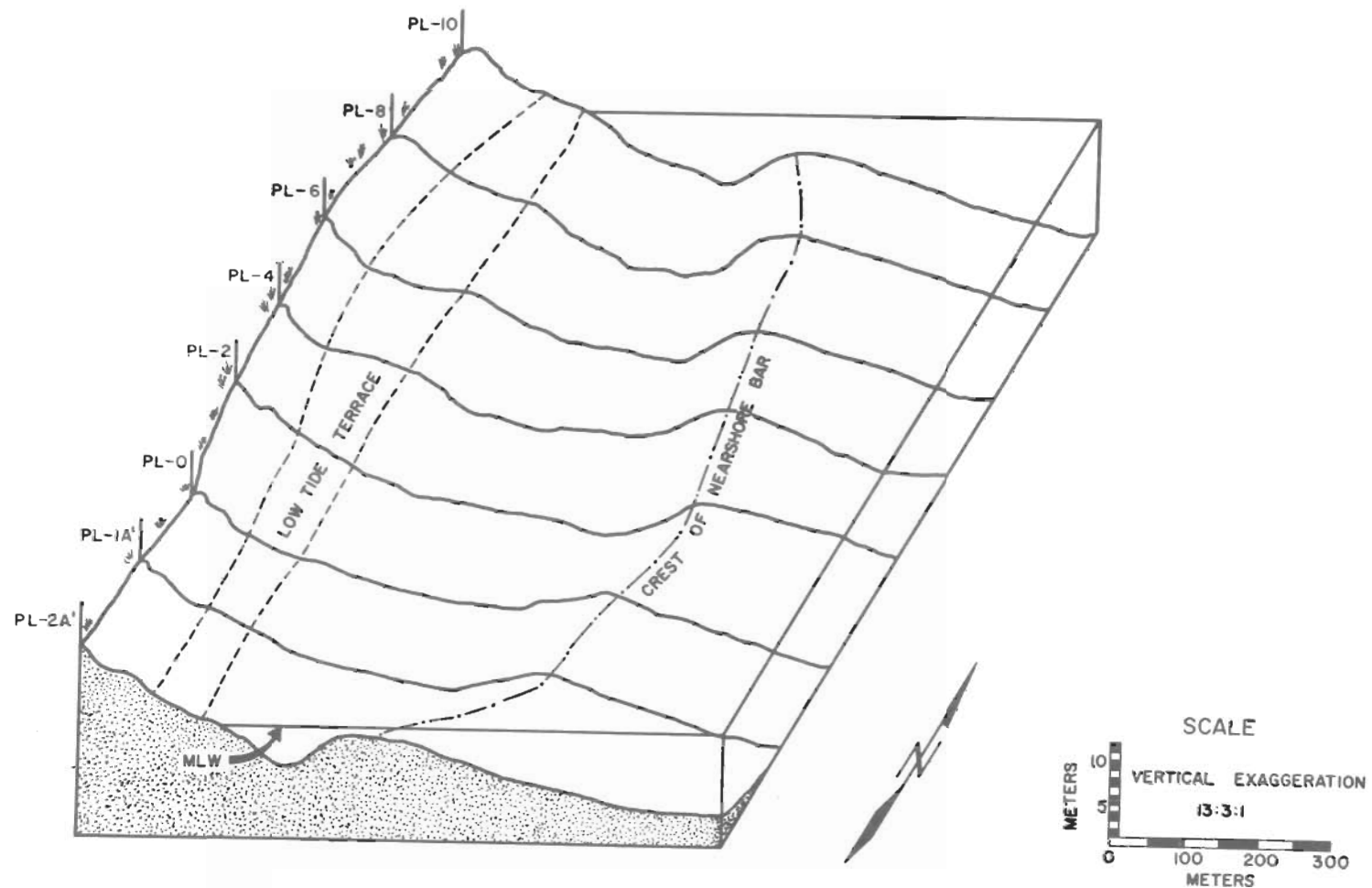17 and 24 June 1971.

Figure 17. Block diagram of study area, 28 July 1971. Note the varying distance between the nearshore bar and the low tide terrace.
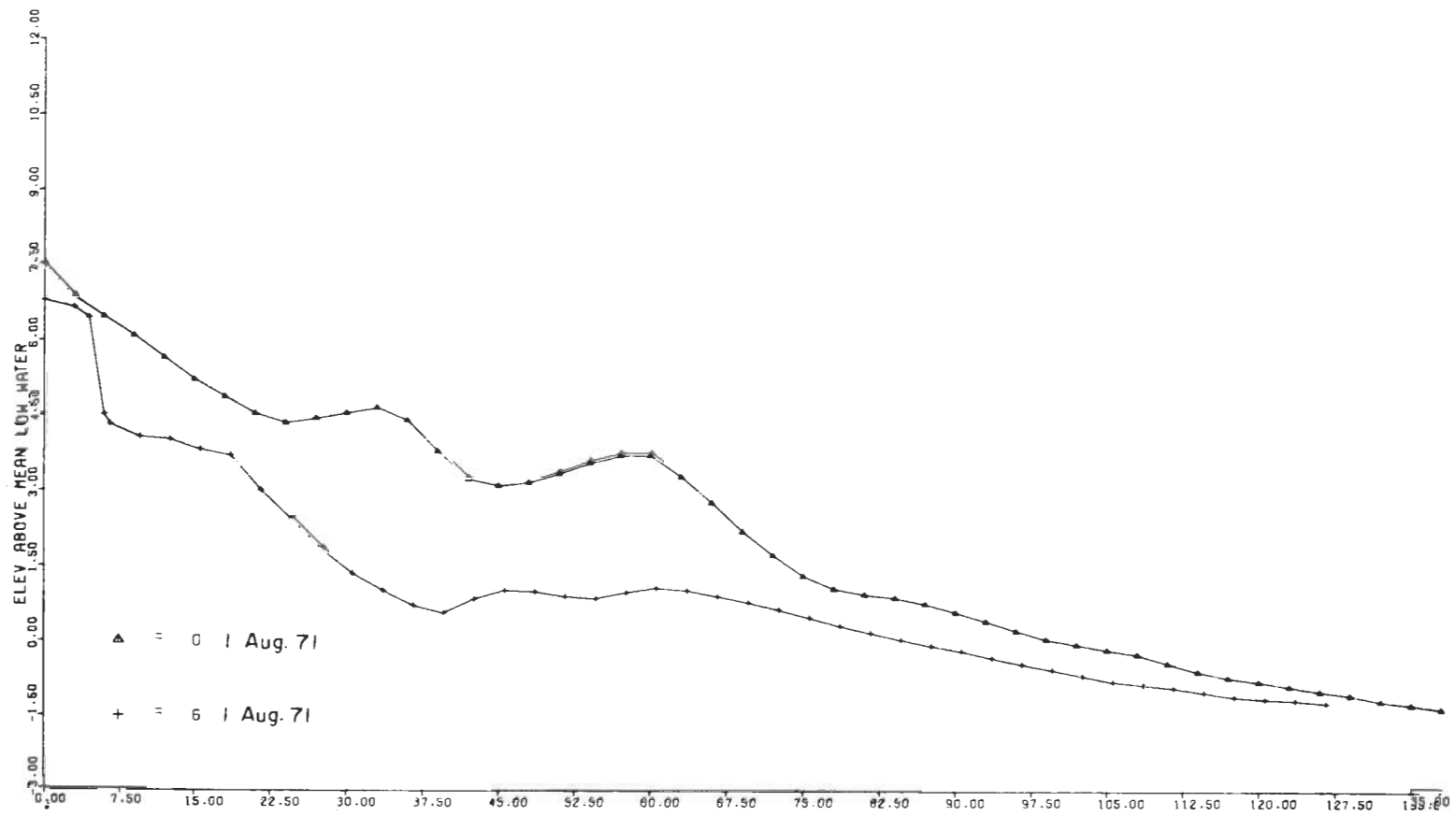
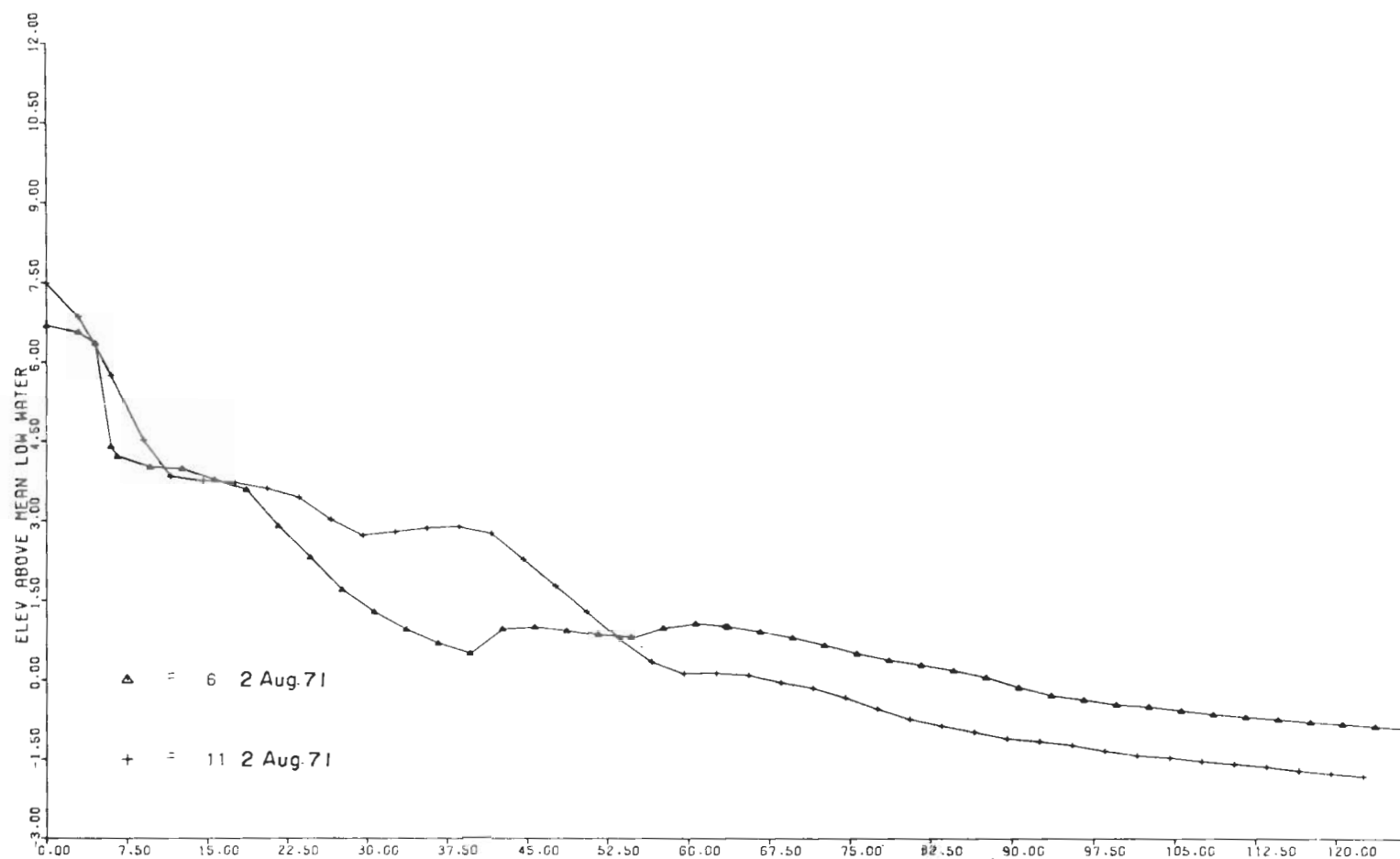Figure 18.   Profiles PL-0 and PL-6, 1 August 1971.

Figure 19.   Profiles PL-6 and PL-11, 2 August 1971.

Figure 20. View looking south at profile PL-0, 20 June 1971.

Figure 21. Upper flow regime conditions in a runoff channel, which has dissected the ridge surface near PL-0.

Figure 22. Initial swash overtopping ridge. Note small ridges. Scale is 3 meters.

Figure 23. Flow separation occurring over the ridge slip face. Scale is 30 centimeters.
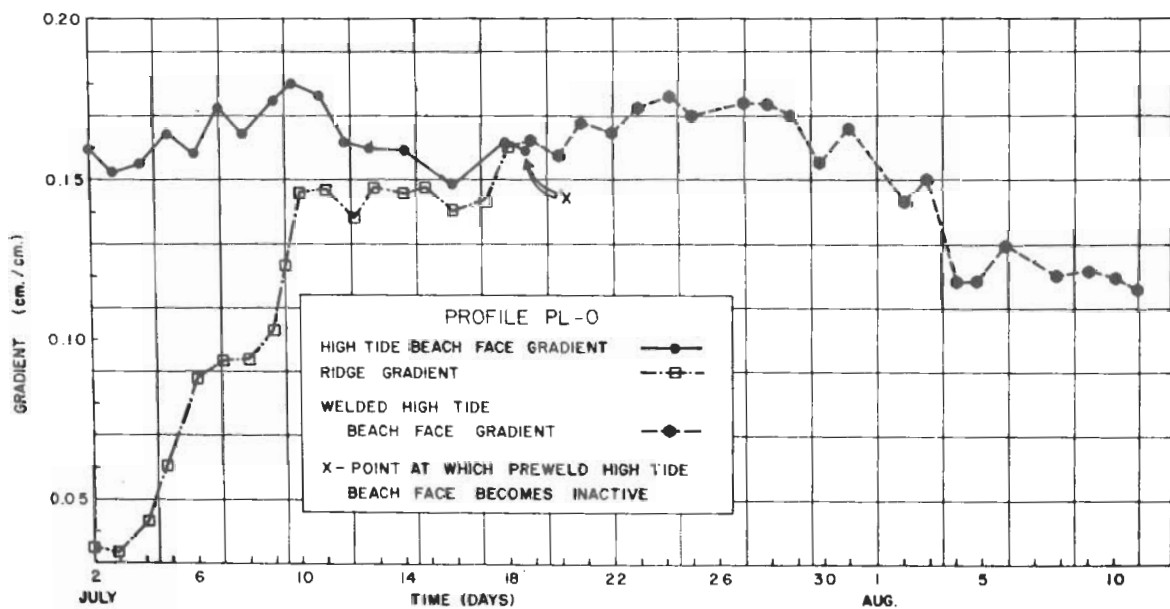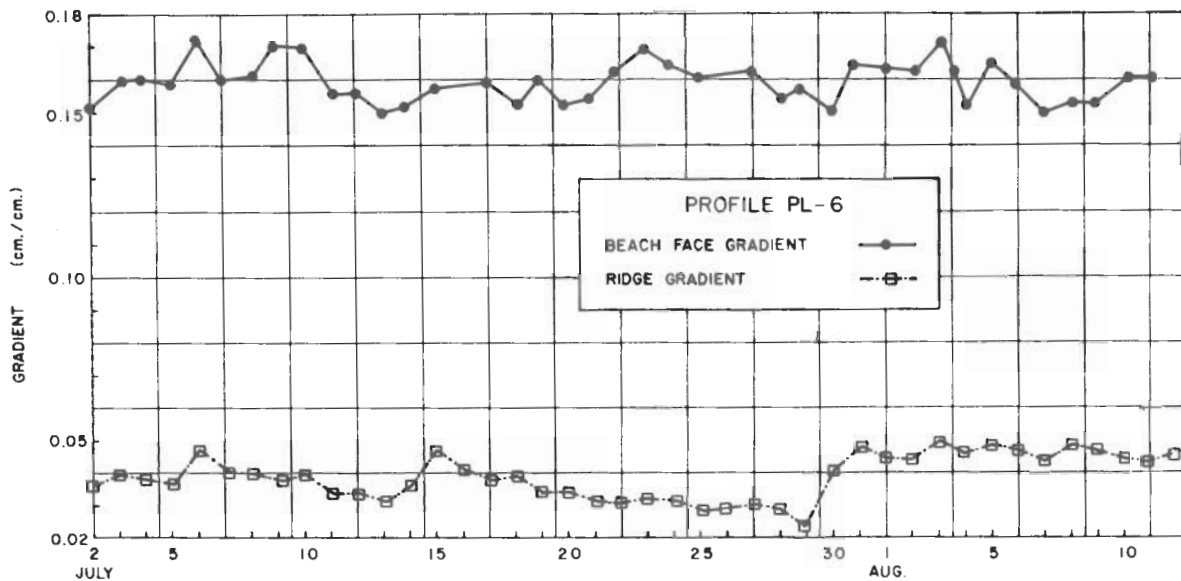
Figure 24. High tide beach face and ridge gradients at PL-0 and
PL-6, measured July-August 1971.

profile was 0.16 centimeter per centimeter. Since the beginning of gradient measurements on 2 July, the ridge grew three-dimensionally, thereby offering more surface area or resistance to wave action as time progressed. The result of a greater resistance to wave action was a gradual steepening of the ridge gradient (Fig. 25). Calculations of breaker power for this period revealed an increase between 7 and 9 July, which also steepened the ridge gradient (Fig. 24).

Other processes acting concurrently with the landward migration of the ridge may also reshape or alter ridge and backshore morphology. The aerial photo in Figure 13 shows a large runoff channel north of PL-10. A closeup photo of the channel (Fig. 21) reveals that upper flow regime conditions often exist in these channels. The antidunes in this photo have an amplitude of 8 to 10 centimeters and result in a noticeable "calving" of the ridge with the returning flow of water from the runnel. Scarps up to 30 centimeters high along the edges of runoff channels were present throughout the study period. Returning flow from runnels may also cause noticeable erosion at the base of the beach face (Fig. 26). Runnel currents strong enough to erode the beach face are usually a result of difference in elevation on an elevated runnel caused by a nonsimultaneous welding of a ridge along the backshore.

Although the changes in morphology in the large ridge area between PL-0 and PL-3 were more rapid than changes at other parts of the study area, distinct morphological changes associated with less mature stages of beach morphology were noticeable between PL-4 and PL-10. The migration and subsequent welding of small ridges (amplitude <40 centimeters) occurred on PL-9, PL-10, and PL-11 between 2 and 9 July (Fig. 27). Profiles PL-4 through PL-8 were sites of less active accretion during the preweld phase. Beach face and ridge gradient changes at PL-6, a typical early accretionary profile, revealed no steepening of the ridge gradient as at PL-0 for the same time period (Fig. 24). The area between PL-4 and PL-8 remained the least mature part of the study area throughout the summer period. Profiles PL-9 through PL-11, initially at a less mature stage of development than the area between PL-0 and PL-4, developed a broad convex berm after a large ridge had welded onto the backshore.

The transition between the early preweld period and the postweld period at PL-0 is shown in Figures 28 and 29. In Figure 28, evidence of the upper flow regime conditions on the ridge surface can be seen in the form of plane beds with grain lineations. Previous high tide upper flow regime plane beds are evident in the area of the slip face exposed below the ridge surface. The numerous lobes of sediment extending into the runnel are the result of late-stage erosion of the ridge surface as the water level dropped below the crest of the ridge. The small lobe in the center of Figure 28 is the area of the first weld within the study area on 11 July (Fig. 29). As the time of complete welding of the ridge approached, the active slip face diminished in amplitude, and on 12 July, the ridge completely welded to the backshore. At times the relict form of the former runnel may remain for a period of several days after

Figure 25. Wave steepening of ridge gradient.

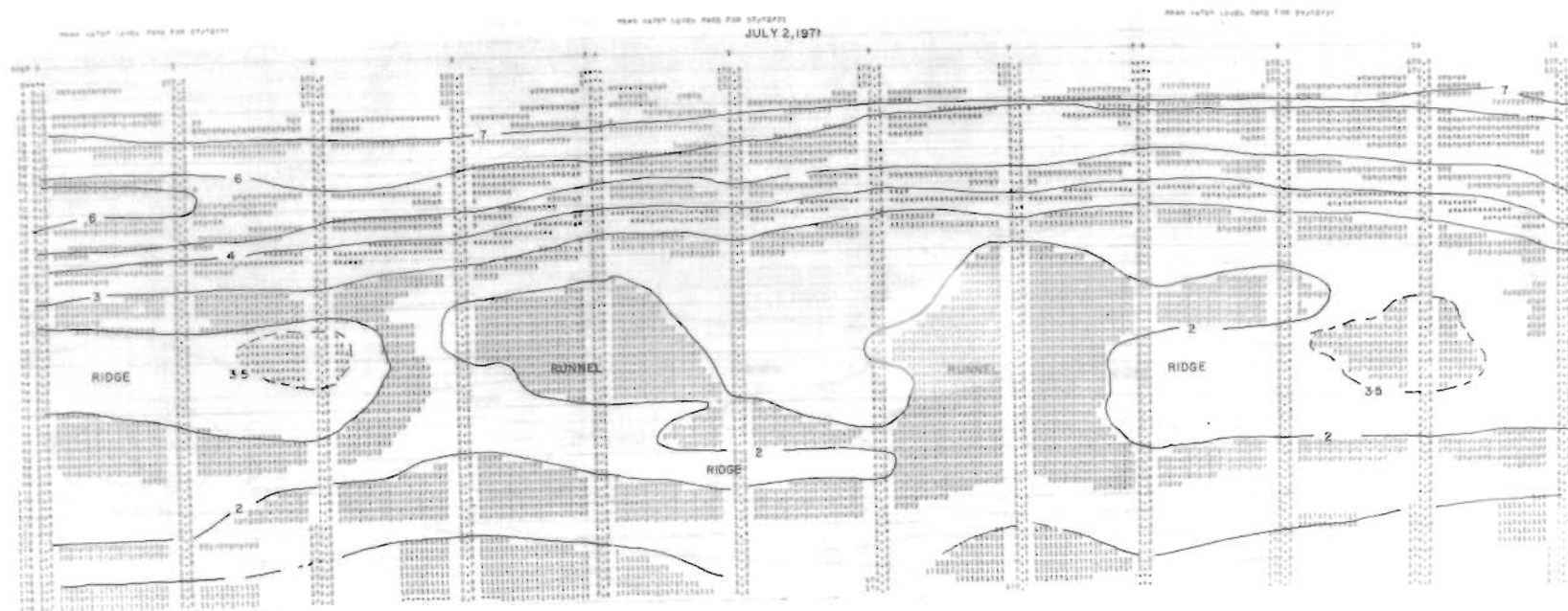Figure 26. Erosion on backshore caused by runnel currents on
berm surface.

44

Figure 27. Maps of beach topography for 2 and 9 July 1971. Note ridge accretion of PL-1, PL-2, and PL-8 between 2 and 9 July. The ridges between PL-0, PL-2, PL-8, and PL-10 migrated landward and increased vertically in size during this period.

JULY 9,1971

RIDGE   5   4-5

RIDGE

2.5

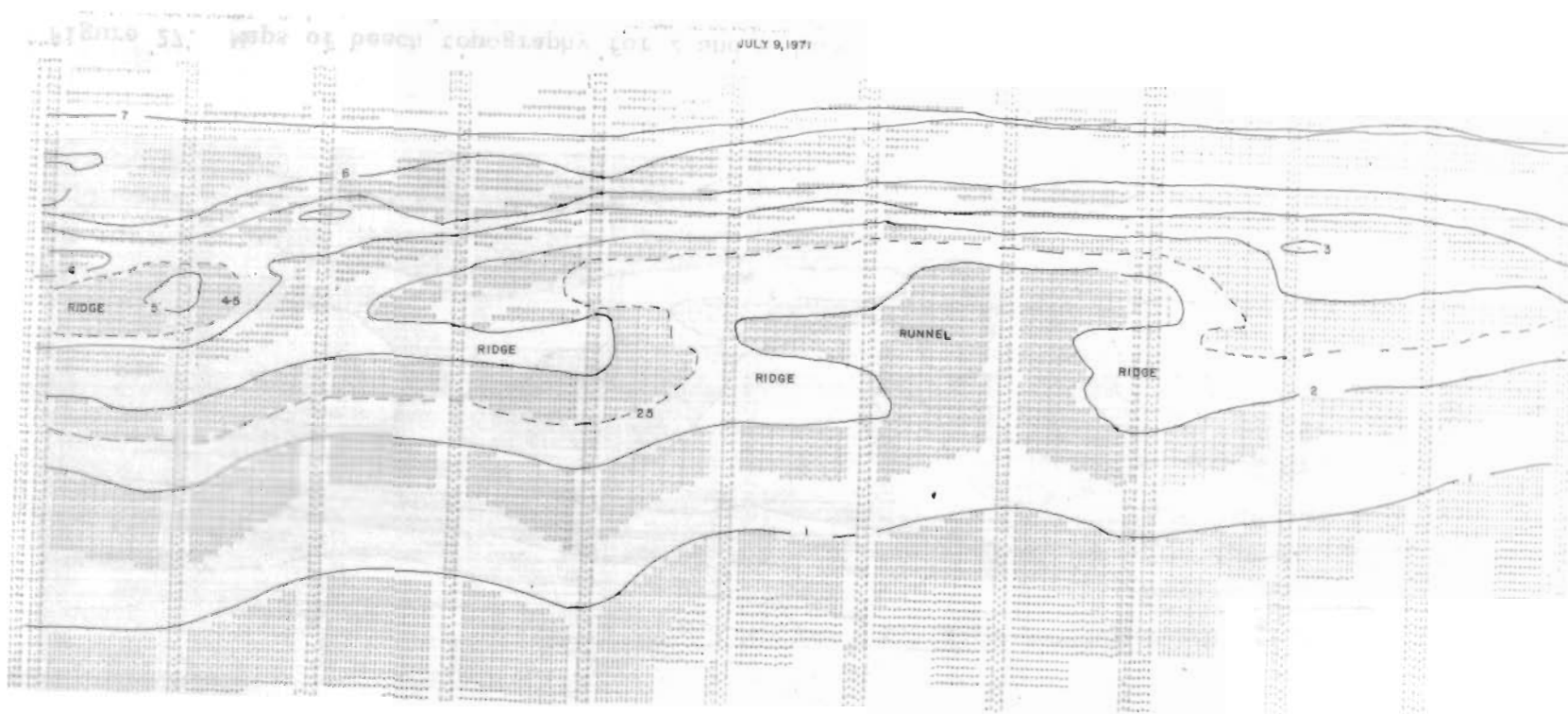RIDGE

RUNNEL

RIDGE

RIDGE

Figure 27.   Maps of beach topography for 2 and 9 July 1971.--Continued
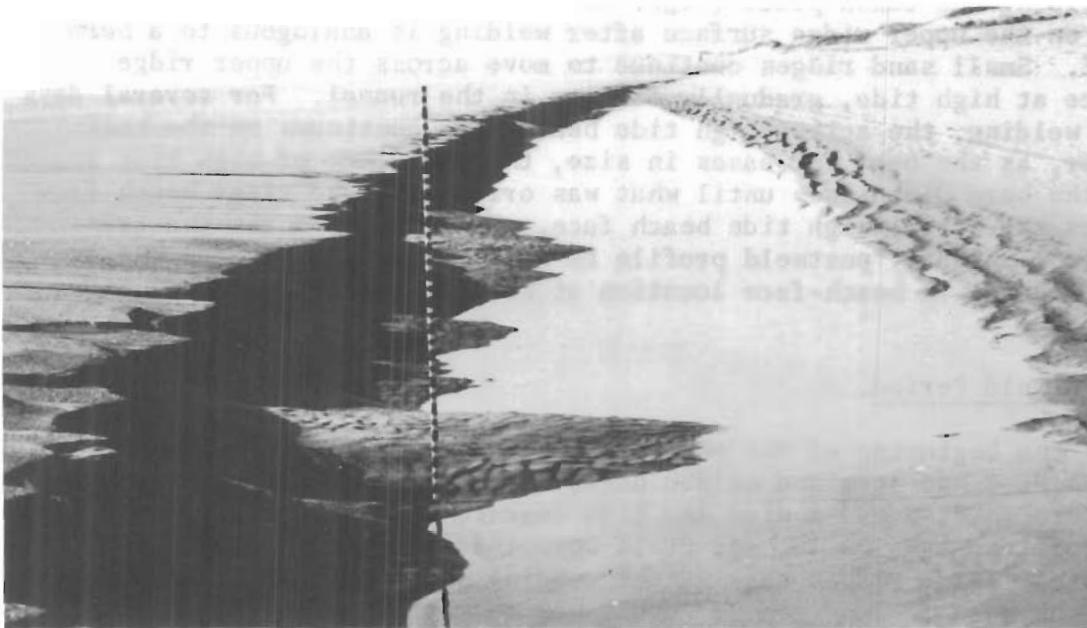
Figure 28.   Ridge and runnel system at PL-0, 10 July 1971 (looking
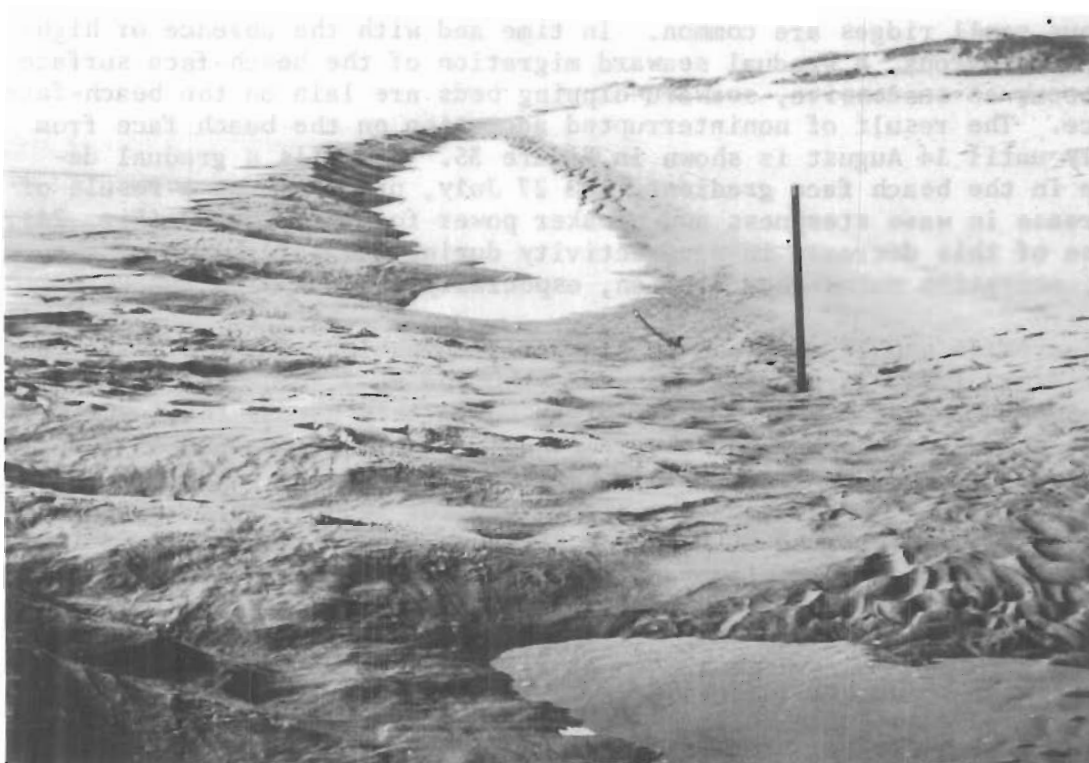   north).   Scale is 170 centimeters.

Figure 29.   Initial stage of ridge welding onto the backshore at
             PL-0, 11 July 1971 (looking north).

47

the welding has taken place (Figs. 30 and 31). The relict runnel which forms on the upper ridge surface after welding is analogous to a *berm runnel*. Small sand ridges continue to move across the upper ridge surface at high tide, gradually filling in the runnel. For several days after welding, the active high tide beach face continues on the backshore; however, as the berm increases in size, the frequency of high tide swashes over the berm diminishes until what was originally the ridge beach face becomes the active high tide beach face. This change marks the transition from an early postweld profile to a late postweld stage. The time of the change in beach-face location at PL-0 is marked by an X in Figure 24.

3. Postweld Period.

At the beginning of the postweld period on 13 July, profiles PL-0 through PL-3 had attained welded berms with steep beach faces; profiles PL-4 through PL-8 had a wide low tide terrace with scattered small ridges; and profiles PL-9, PL-10, and PL-11 were intermediate in development, with moderately large ridges nearing the welding stage (Figs. 32 and 33). The period between 13 July and 12 August was characterized by relatively low-energy conditions. A typical late postweld beach profile at PL-0 is shown in Figures 34 and 35. A large welded ridge where the mean high water mark is below the surface of the berm is a characteristic of the late postweld profile. A wide low tide terrace may also exist where numerous small ridges are common. In time and with the absence of high-energy conditions, a gradual seaward migration of the beach-face surface will occur as successive, seaward-dipping beds are lain on the beach-face surface. The result of noninterrupted accretion on the beach face from 22 July until 14 August is shown in Figure 35. There is a gradual decrease in the beach face gradient from 27 July, primarily as a result of a decrease in wave steepness and breaker power for this period (Fig. 24). Because of this decrease in wave activity during the later part of the study, accretion outweighed erosion, especially between P1-4 and PL-10.

Figures 36 and 37 show changes in beach morphology immediately after the welding of the large ridge between PL-0 and PL-3. The small ridges at PL-5, PL-6, and PL-7 on 13 July migrated quickly across the low tide terrace and welded before 20 July (Fig. 33). The northern end of the study area assumed a mature profile after the welding of the ridge at PL-8 by 20 July. The erosion-deposition map for 20 July (Fig. 36) shows that welding has occurred at PL-4 and PL-8, as indicated by the vertical accretion of 50 to 100 centimeters of sediment. The accretion at profile PL-6 is due to the formation of deltalike lobes of sediment on the runnel surface (Figs. 38, 39, and 40). This sediment lobe is probably caused by profiles PL-6 and PL-7 which are lower than the adjoining profiles; therefore, greater scour will occur as water empties from the runnel resulting in a deepened runoff channel. As the tide begins to flood, sediment is carried through the runoff channel and is deposited. Later, as the higher parts of the ridge adjacent to the runoff channel are flooded, residual currents keep the migrating ridge from assimulating the sediment lobe. Eventually, the lobe is overlapped by a ridge (Figs. 41 and 42).

Figure 30. Profile PL-0 on 12 July 1971, looking south. Note berm runnel. Scale is 300 centimeters.
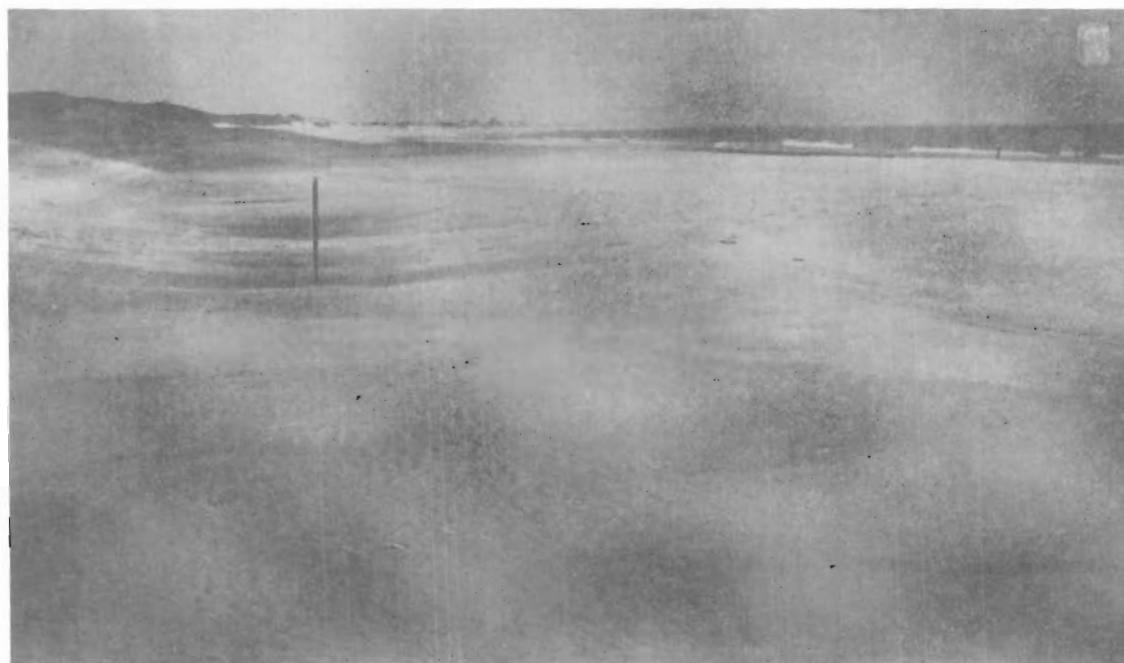

Figure 31. Profile PL-0 on 14 July 1971, looking north. Back surface of ridge is still active. Note small ridges on berm surface.
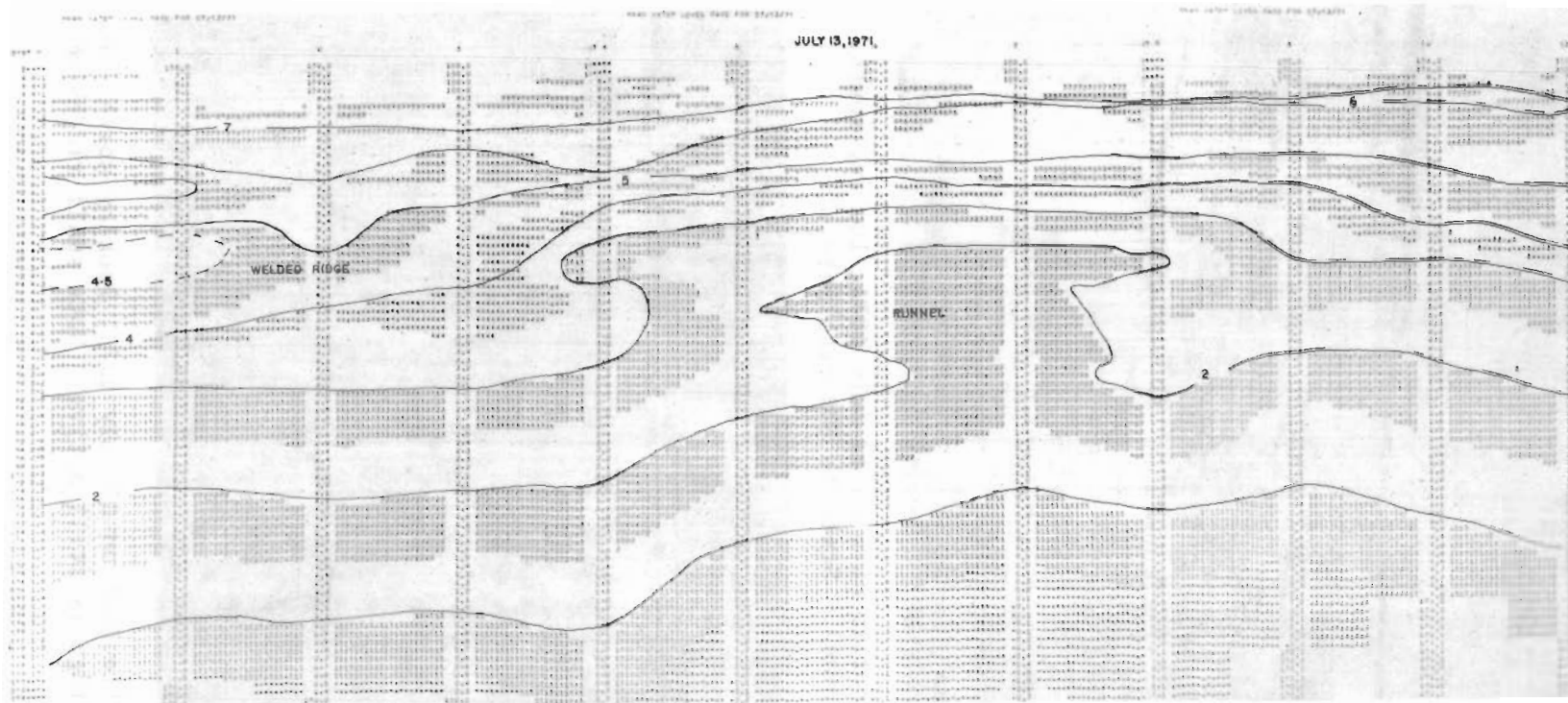
JULY 13, 1971.

Figure 32. Beach map for 13 July 1971. Ridge welding has occurred between profiles PL-0 and PL-2 and between profiles PL-9 and PL-11.
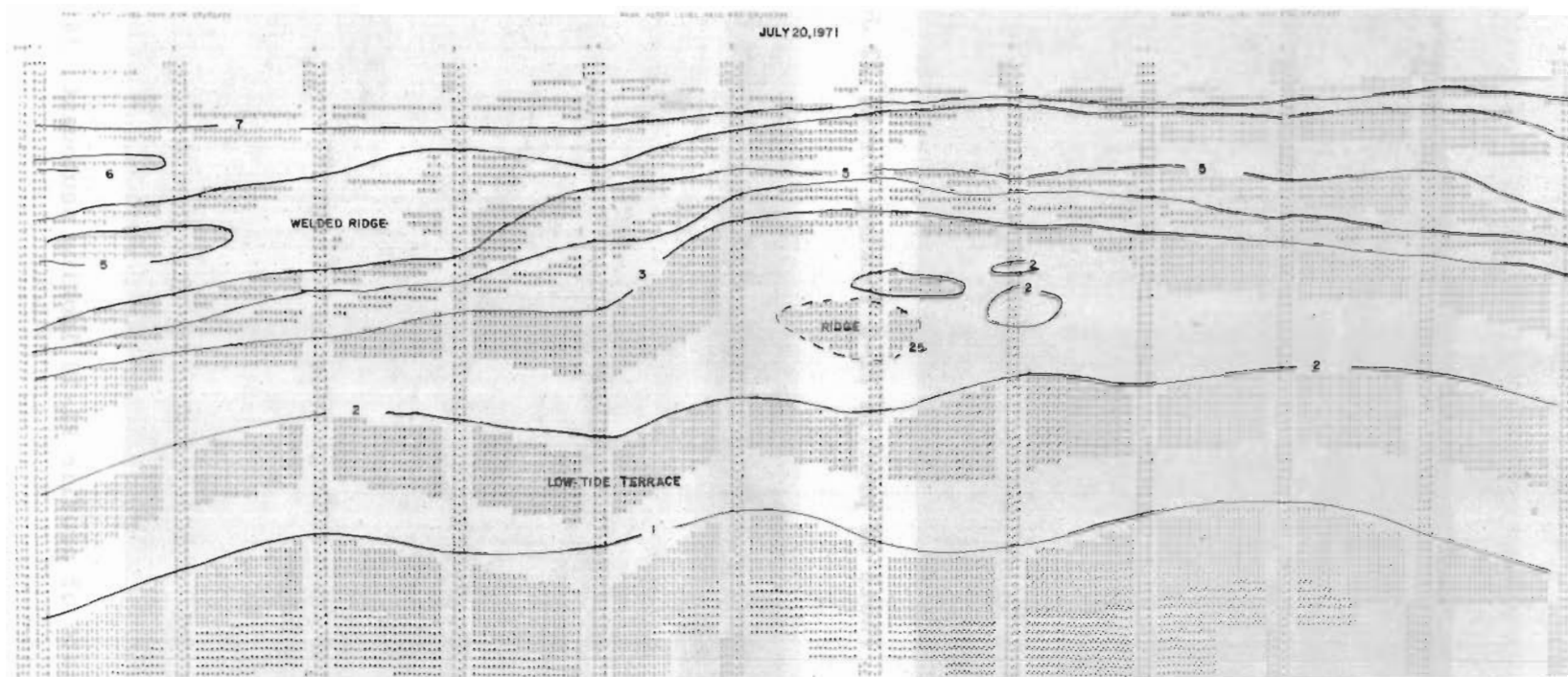
JULY 20,1971

WELDED RIDGE

RIDGE

LOW TIDE TERRACE

Figure 33. Beach map for 20 July 1971. Ridge welding has occurred at all profile locations except PL-5 to PL-7.
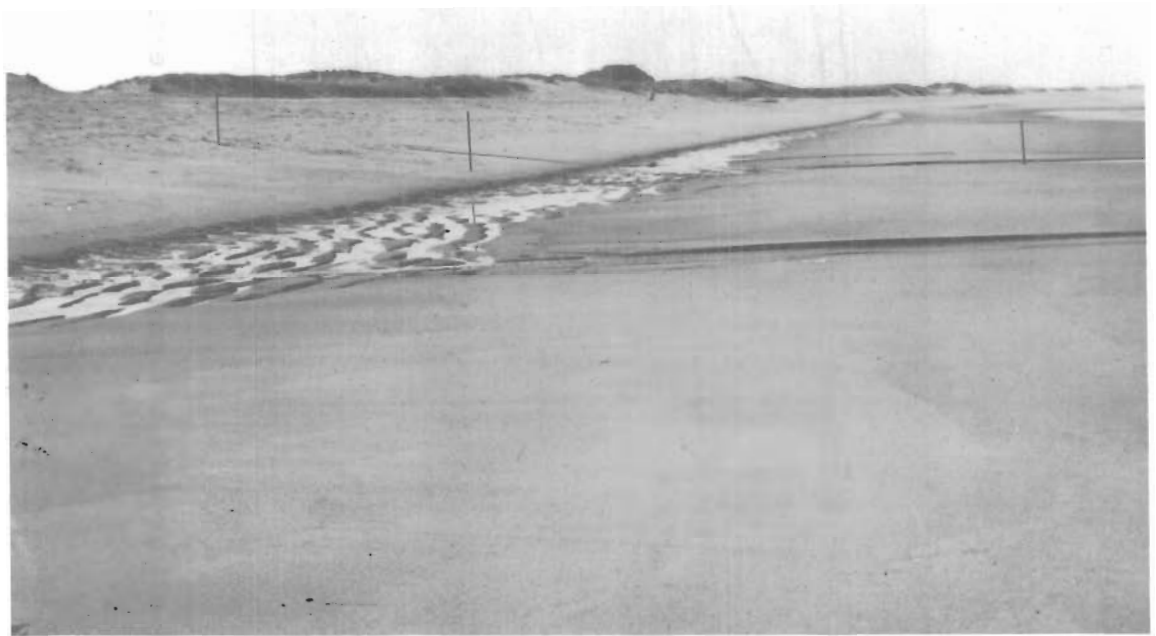
Figure 34. Photo of profile PL-0 looking north, 22 July 1971.

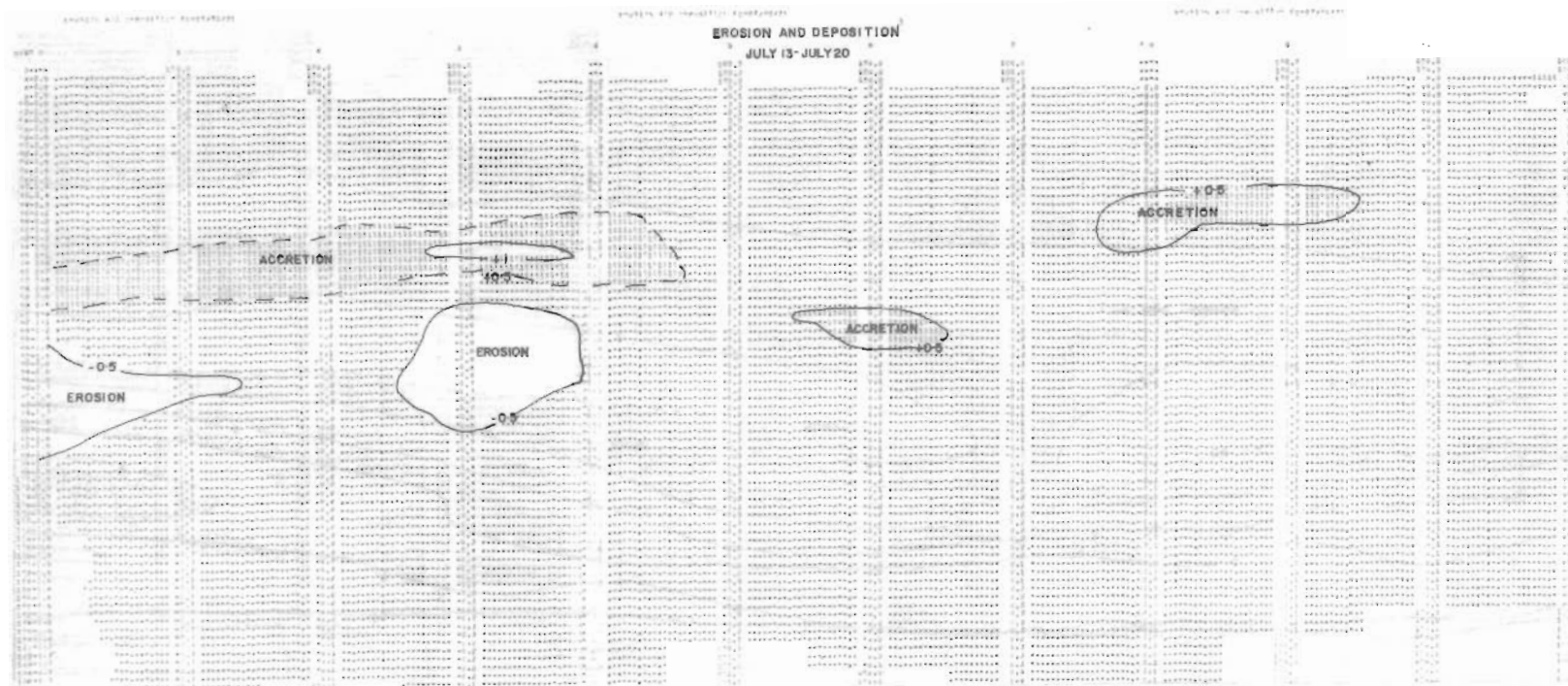Figure 35. Photo of profile PL-10 looking southeast, 14 August 1971.

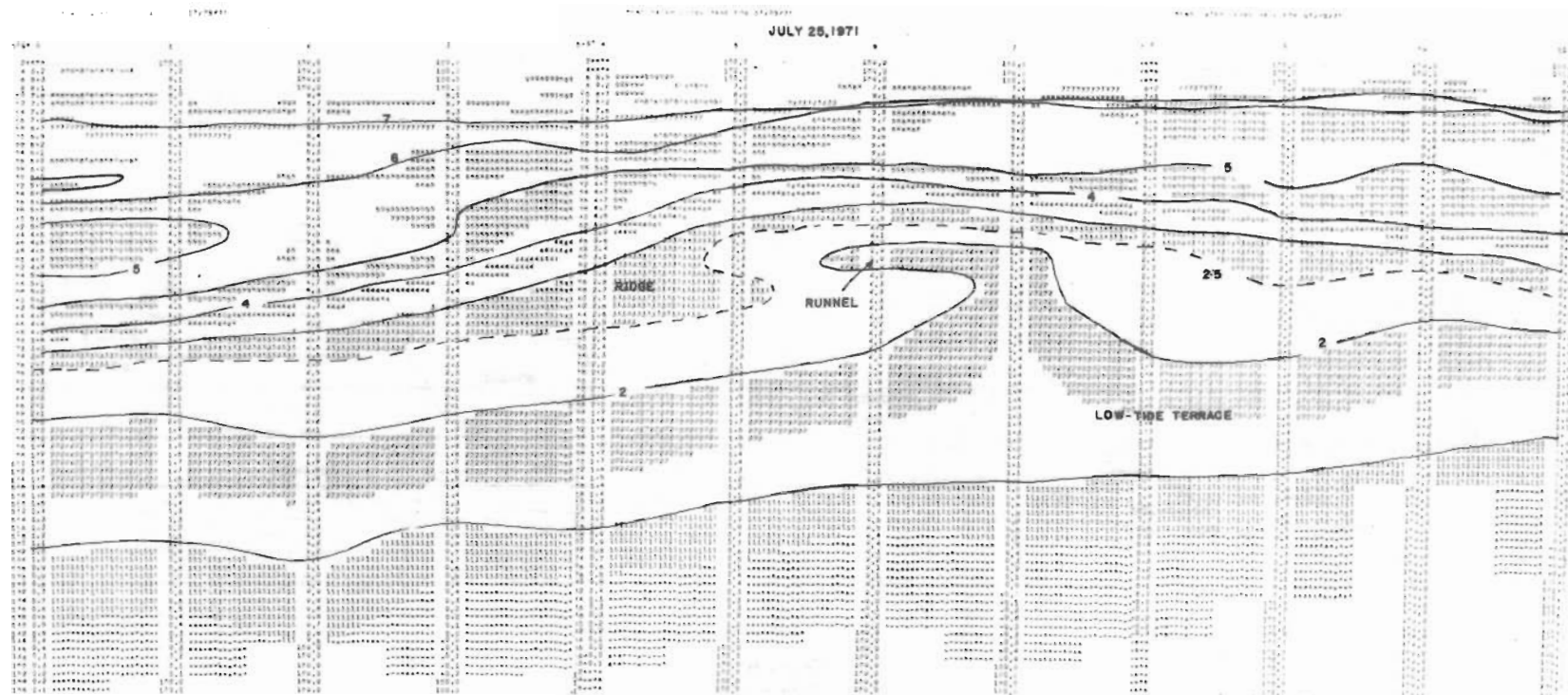Figure 36. Erosion-accretion map for the period 13 to 20 July 1971.

Figure 37. Beach map for 25 July 1971. Welded ridges are at all profile localities except PL-5, PL-6, and PL-7.
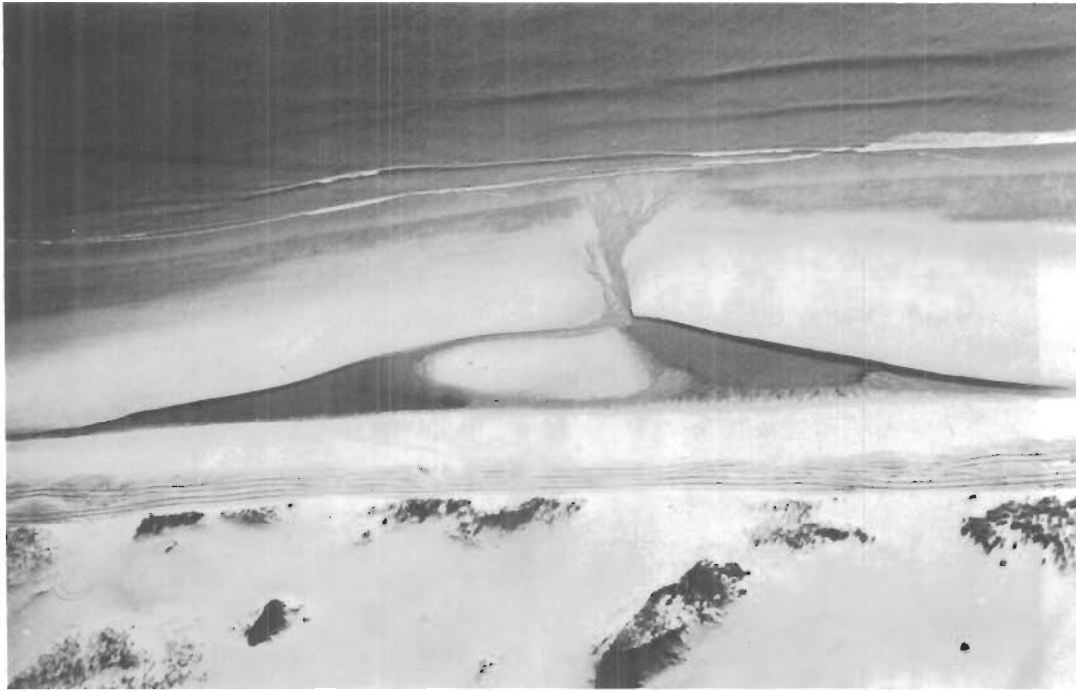
Figure 38.   Aerial photo of profiles PL-6 through PL-8 (toward left) 25 July 1971.   Profile PL-7 passes immediately to the right of the runoff channel.
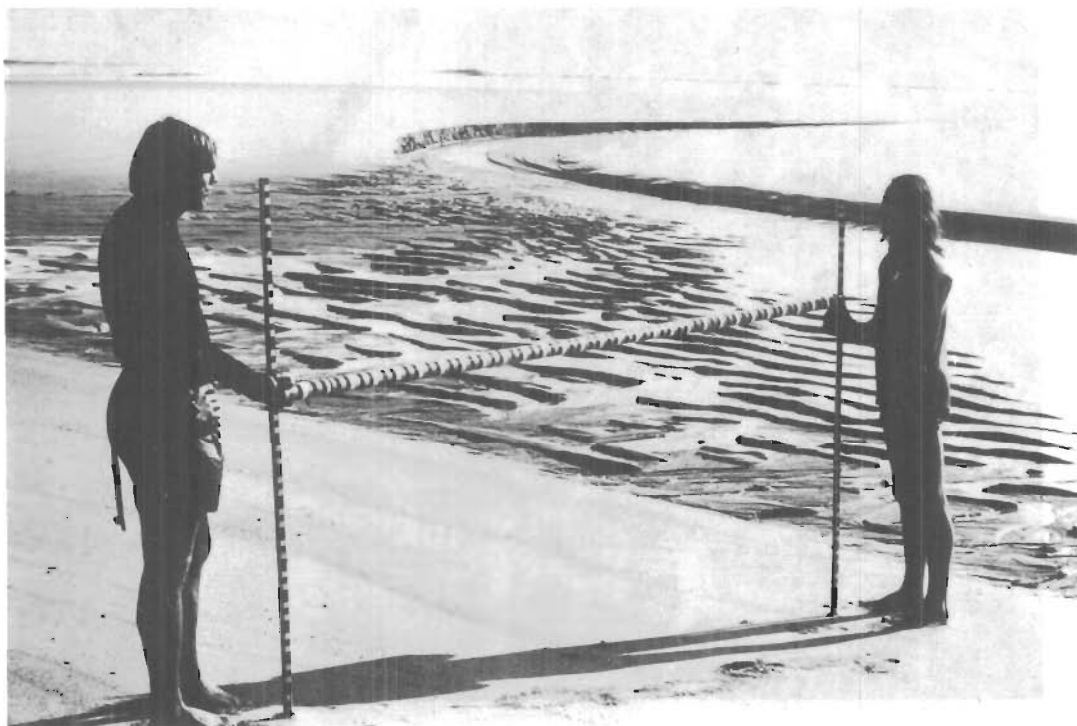

Figure 39.   Profiling across low tide terrace, 7 August 1971 (PL-7).

Figure 40. Aerial view of northern half of study area,
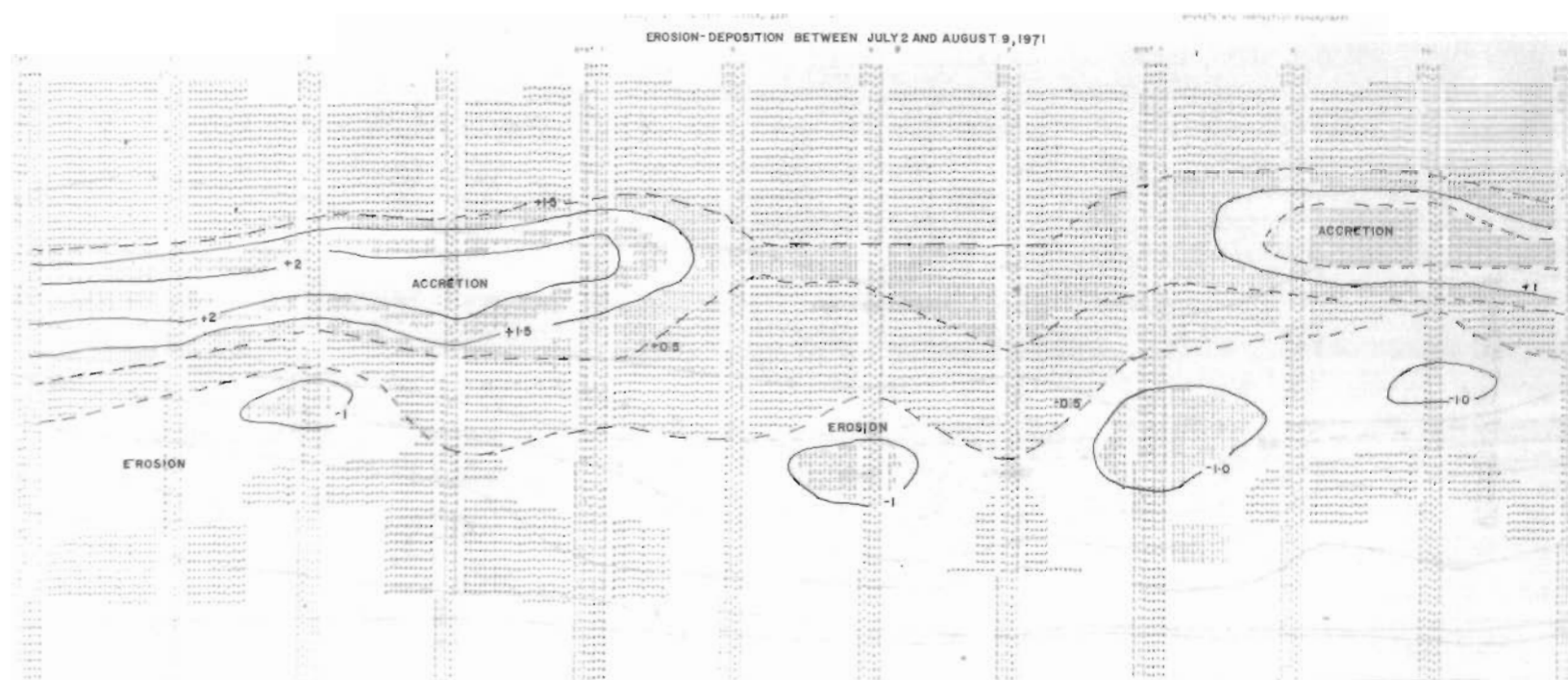25 July 1971 (profile PL-7).

Figure 41. Erosion-deposition map for 2 July to 9 August 1971. Maximum accretion (PL-0, PL-4, PL-9, and PL-11) occurs in areas where ridges have migrated across the low tide terrace and welded onto the backshore. The zones of maximum accretion are in those areas in which the nearshore bar is closest to the beach zone (see Fig. 17).
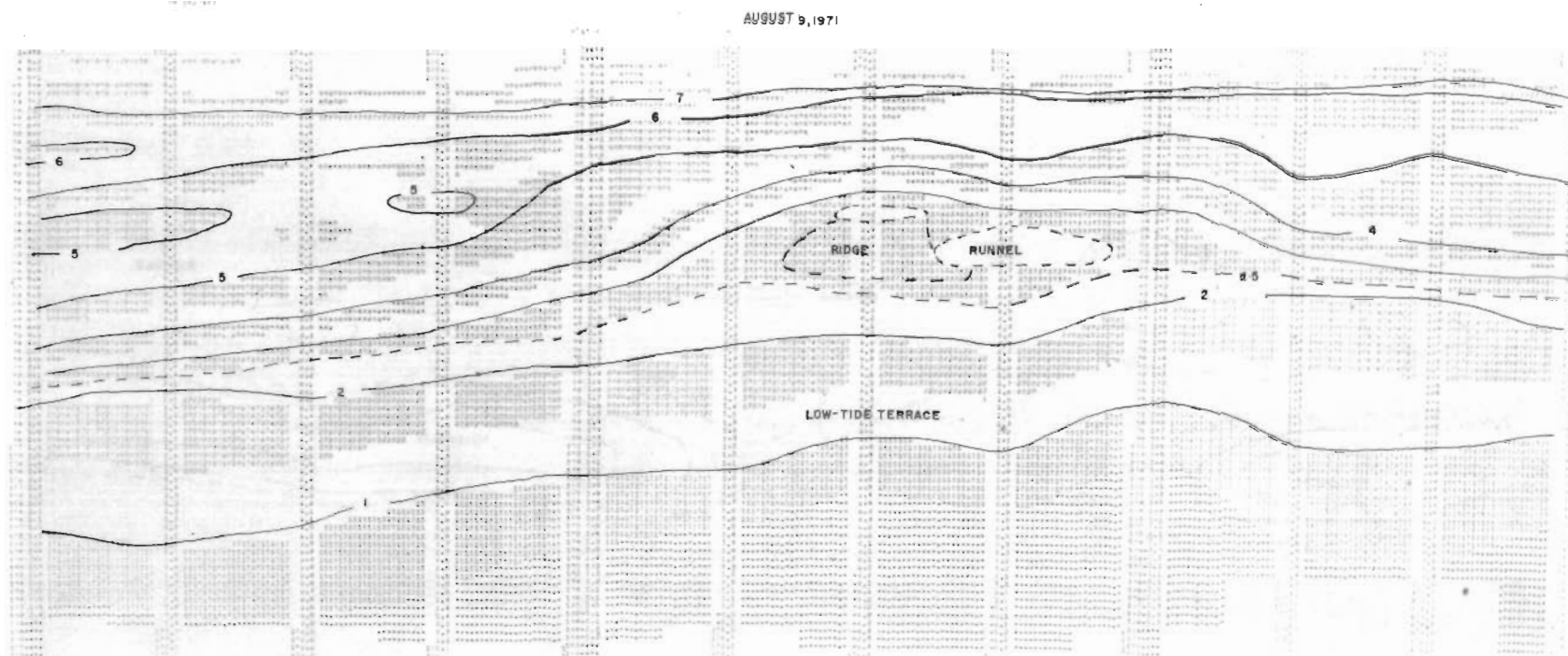
AUGUST 9, 1971

Figure 42. Beach map for 9 August 1971. Ridges have nearly welded in the area between PL-5 and PL-7.

The area between profiles PL-5 and PL-7 neared a welded beach profile (Fig. 42) at the conclusion of the study period. Ridges of sediment gradually filled in the runnel, and on 9 August the last remaining ridges had nearly welded (Fig. 43). A principal reason for the late welding of the central profiles was the strong runnel currents created by the lower elevation of this area. As sediment was transported across the ridge surface and over the slip face, it was caught by the currents in the runnel and transported seaward.

The net erosion and deposition for the study period are shown in Figure 41 which compares profiles on 2 July with those of 9 August. The northern and southern ends of the study area had the greatest accretion, while the central profiles had considerably less net accretion. The areas of greatest net erosion (PL-2, PL-6, PL-8, and PL-10) are due to ridges which were present on 2 July and had migrated landward before 9 August.

The adjacent zones of mature and early accretionary profiles resemble the *rhythmic topography* of Hom-ma and Sonu (1962) and Sonu and Russell (1966). According to Sonu and Russell (1966), sand wave phenomena along a shoreline may cause profiles "resembling the accepted *summer* and *winter* types to be encountered barely several hundred feet apart on the same stretch of beach." This explanation appears to be true in a general sense; however, the coexistence of adjacent profiles at different stages of maturity is directly related to the proximity of the nearshore bar and the availability of sediment to be moved onshore. The fact that during periods of uninterrupted accretion, mature profiles will develop at all profile locations, differs from Sonu's (1968) model of zones of net erosion on the shore in the lee of the sand wave or shoal (Fig. 44).

V. WINTER BEACH PROCESS MEASUREMENTS

Measurements were taken in the winter study period on all the beach process variables studied during the summer period, except for ground water elevation. Higher energy conditions were encountered more often during the winter than during the summer. These higher energy periods were associated with storms (5 January 1972 and 19 February 1972), and with the passage of high-pressure systems through the area and the strong northwesterly winds accompanying the highs.

1. Meteorological Measurements.

Barometric pressure, windspeed, and wind direction measurements for the winter period are shown in Figure 45. The relationship between barometric pressure, windspeed, and wind velocity is more direct for the winter study than for the summer study. As the area comes under the influence of a polar high-pressure system, the winds shift to the west or northwest as the barometric pressure is rising. The change in wind direction occurs 8 to 12 hours before the extreme high pressure is reached and will usually shift to the south or southwest as the center

Figure 43. Photo of central profile area, 9 August 1971; looking northeast.

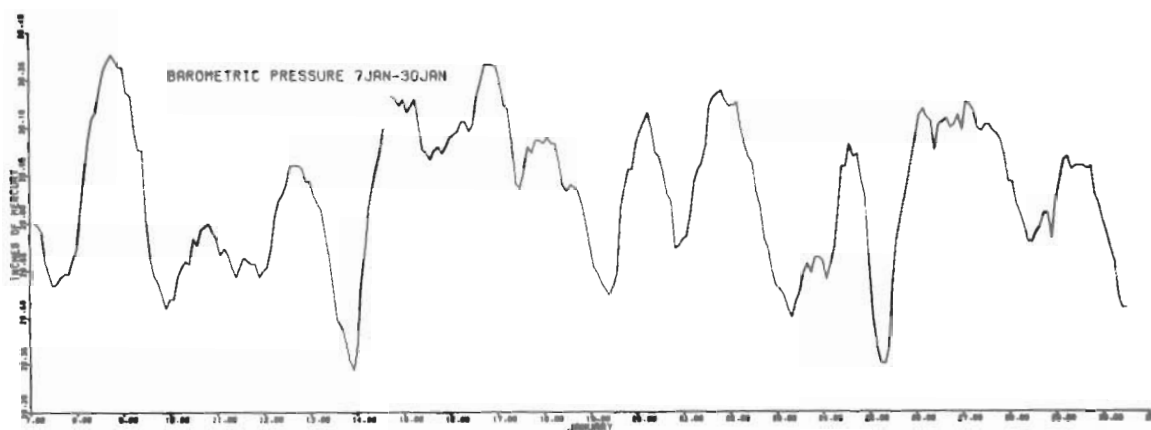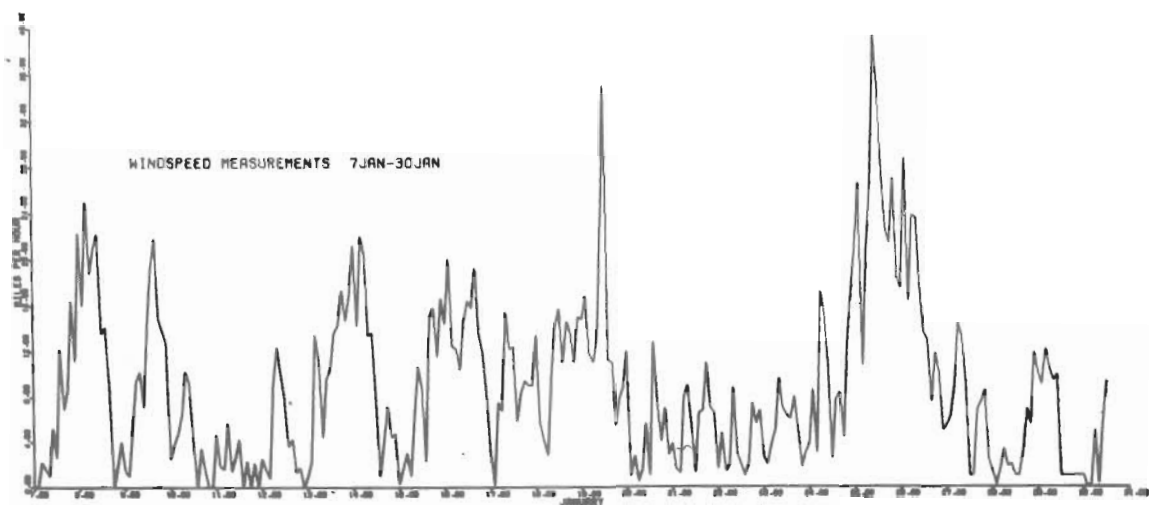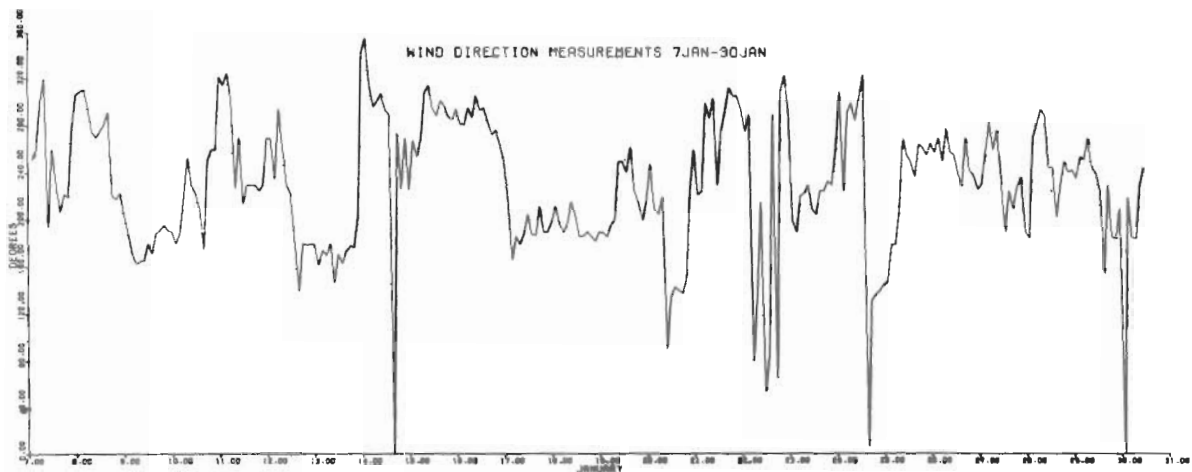Figure 44. Aerial photo of study area, 9 August 1971; looking north.

Figure 45.   Wind direction, windspeed, and barometric pressure
measurements, January 1972.

of the high-pressure system is over the area. Windspeed also increases with rising barometric pressure and usually reaches maximum velocity before the high-pressure system is centered over the area (Fig. 45, 19 and 25 January). The relationship between barometric pressure and along-shore wind components is shown in Figure 46. As a low-pressure system begins to move into the area (e.g., 13 January), the counterclockwise wind patterns associated with the low result in an increased negative or northerly alongshore wind component. After the low has passed, counter-clockwise winds around the low-pressure center blow onshore creating a positive or southerly alongshore wind component. The mean alongshore wind component for the period was -1.2 miles per hour, with a northerly (positive) maximum of 8.1 miles per hour and a southerly (negative) high of 24.6 miles per hour. The stronger winds associated with polar high-pressure systems result in higher alongshore wind components during the winter than in the summer. Windspeed with onshore-offshore wind components is compared in Figure 47. As a high-pressure system begins to influence the Plum Island area, the winds shift to the west or northwest. The higher wind velocity associated with rising pressure gives rise to higher offshore wind components.

Air and water temperatures were more clearly related than any of the variables studied during the winter period (Fig. 48) and were important beach process variables in terms of their influence on beach morphology. The warm temperatures between 9 and 14 January resulted in a lowering of the frost table in the back dune area making a greater thickness of sedi-ment susceptible to eolian erosion. The extremely low temperatures on 9, 17, and 26 January caused parts of the beach to become frozen which resulted in lessened erosion on the berm crest and beach face than during warmer periods having similar wave energy. The effects of temperature on beach morphology are discussed in Section VI.

2. Wave Measurements.

Wave parameters such as wave period, breaker power, wave height, and breaker depth are determined by local wind conditions to a greater degree during winter than during the summer. The relationship between wind-speed, breaker height, and breaker power is shown in Figure 49. The highest windspeeds measured during the winter period were offshore winds. Breaker-height measurements for 14, 19, and 25 January show an abrupt decrease from previous readings due to strong offshore wind velocities, with gusts measured in excess of 55 miles per hour. Maximum wind veloc-ity measurements were made during the periods immediately preceding the decrease in wave height. Breaker-power calculations for the same dates also show a marked decrease. The effect of these strong offshore winds is considered later.

Figure 50 shows the relationship between barometric pressure, along-shore wind components, and longshore drift. For example, on the night of 24 January, the barometric pressure began to drop as a low-pressure system moved into the area. The wind circulation on the leading edge
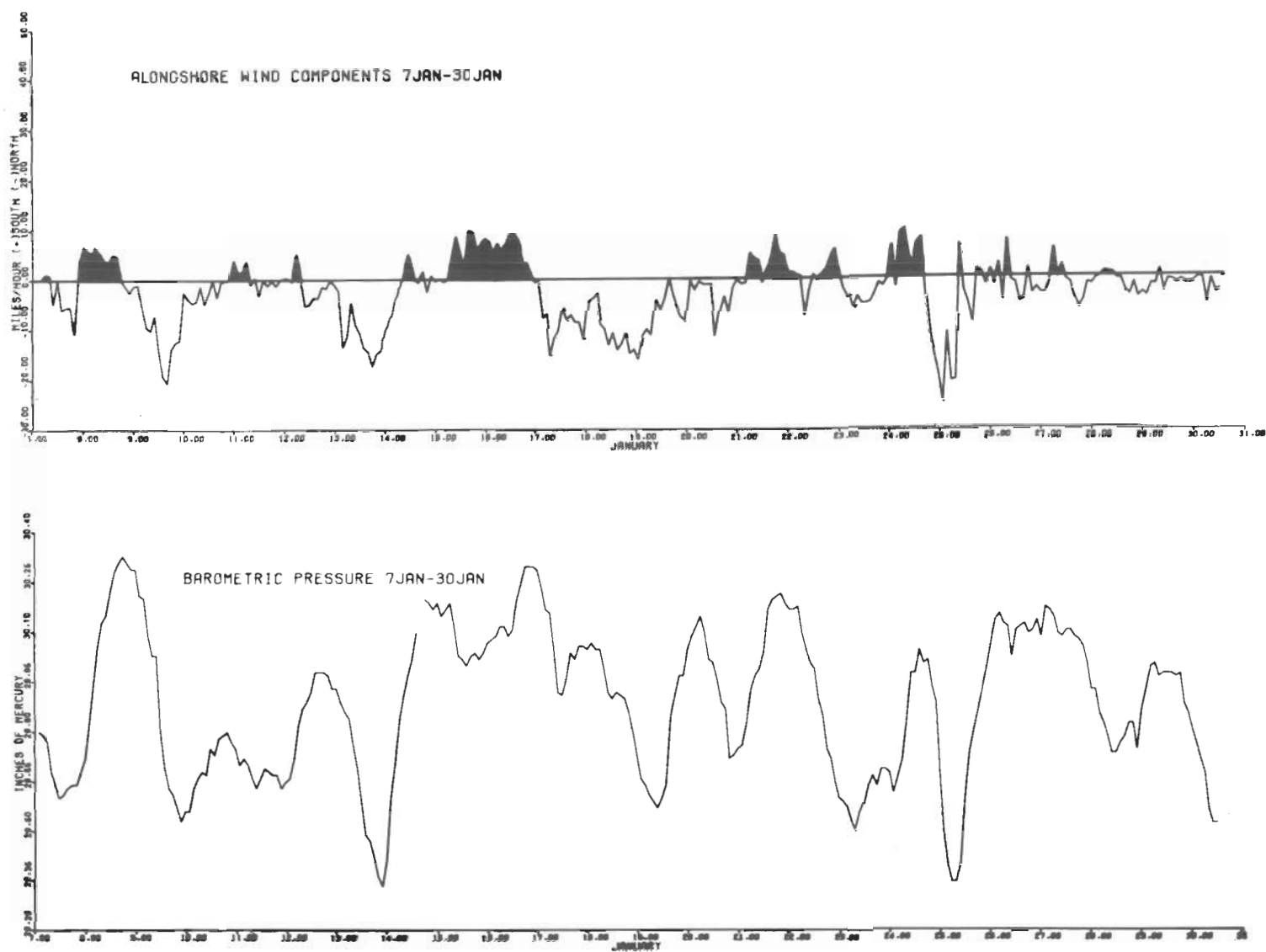
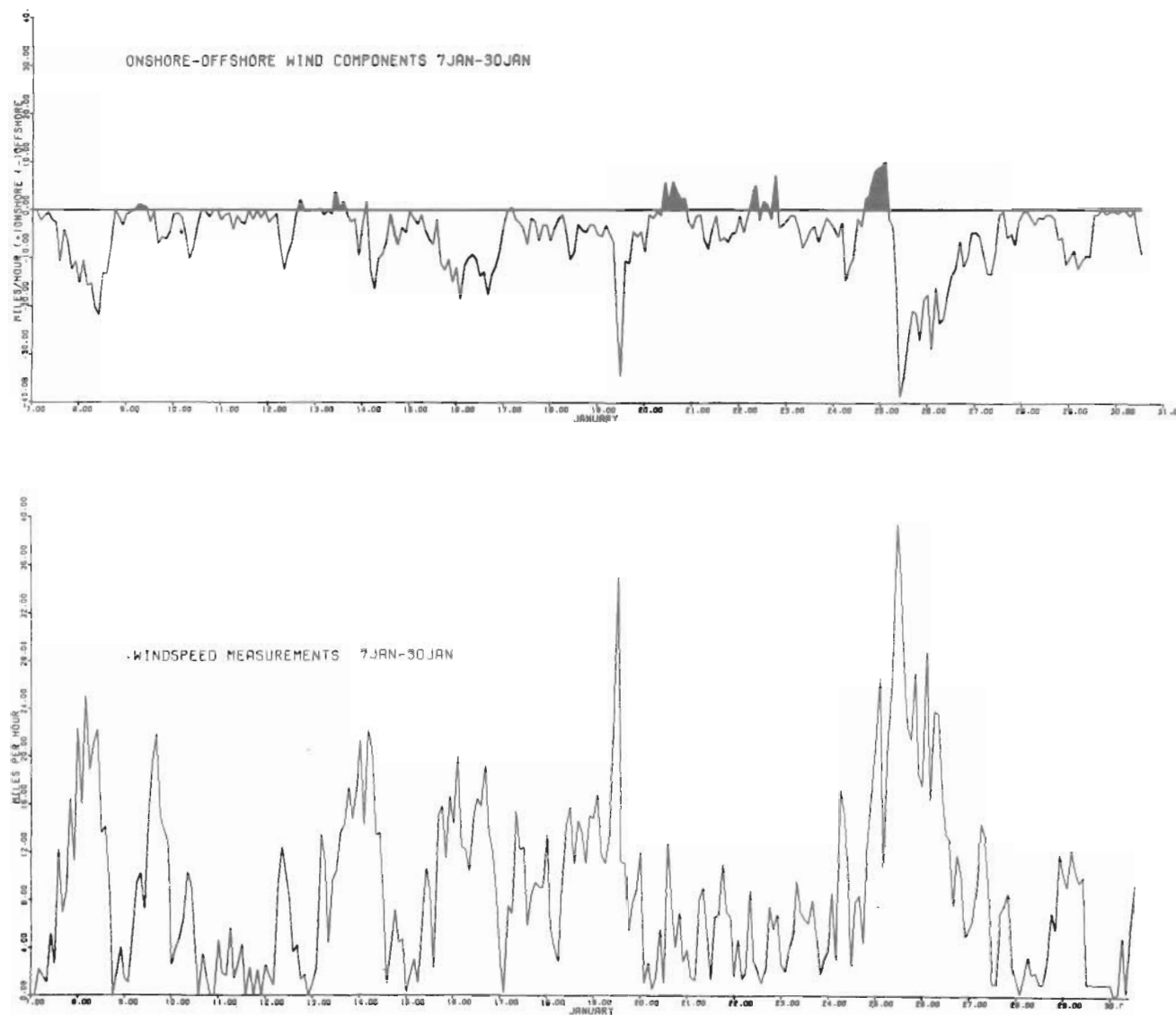Figure 46.   Alongshore wind components and barometric pressure, January 1972.

63

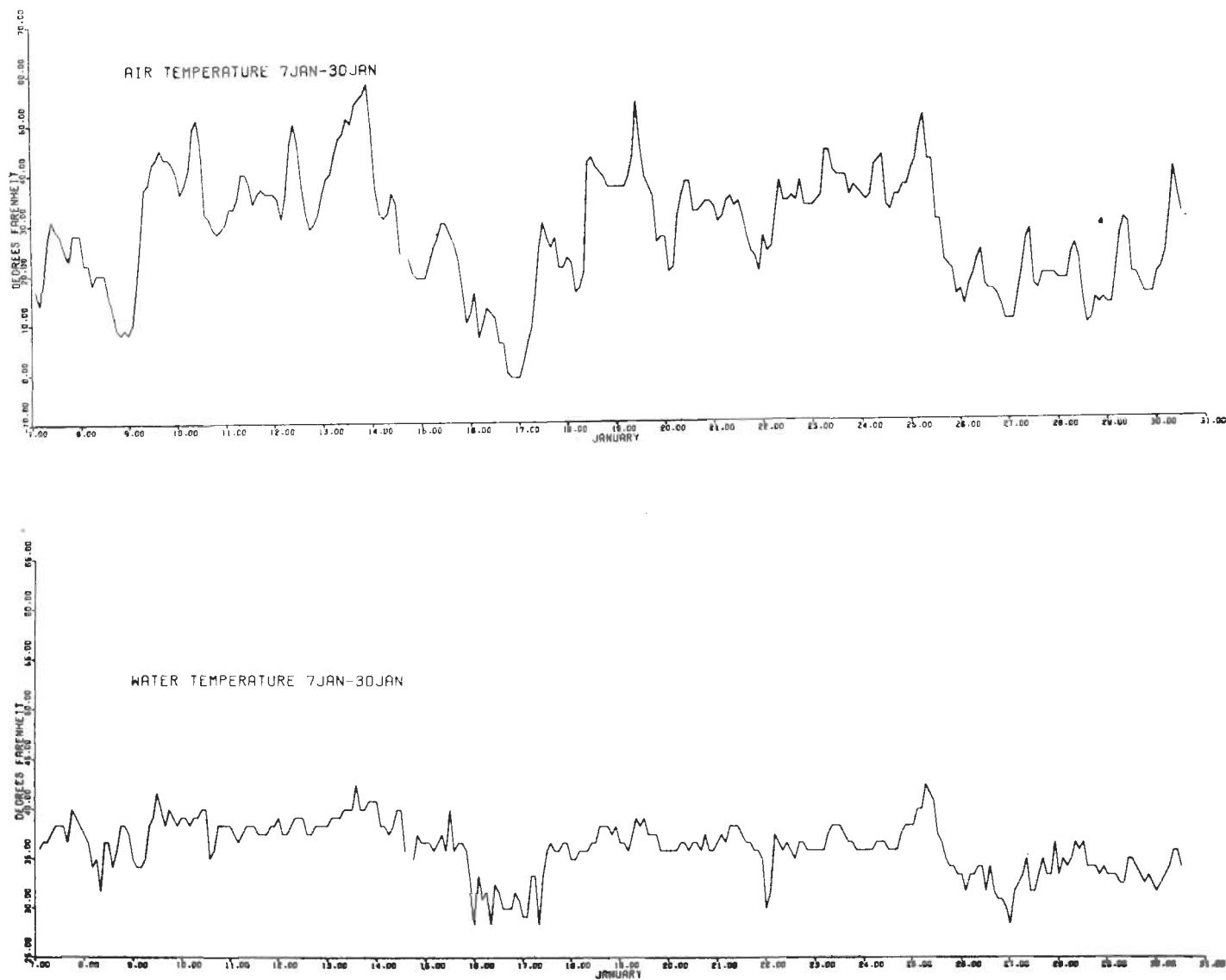Figure 47. Onshore-offshore wind components and windspeed, January 1972.

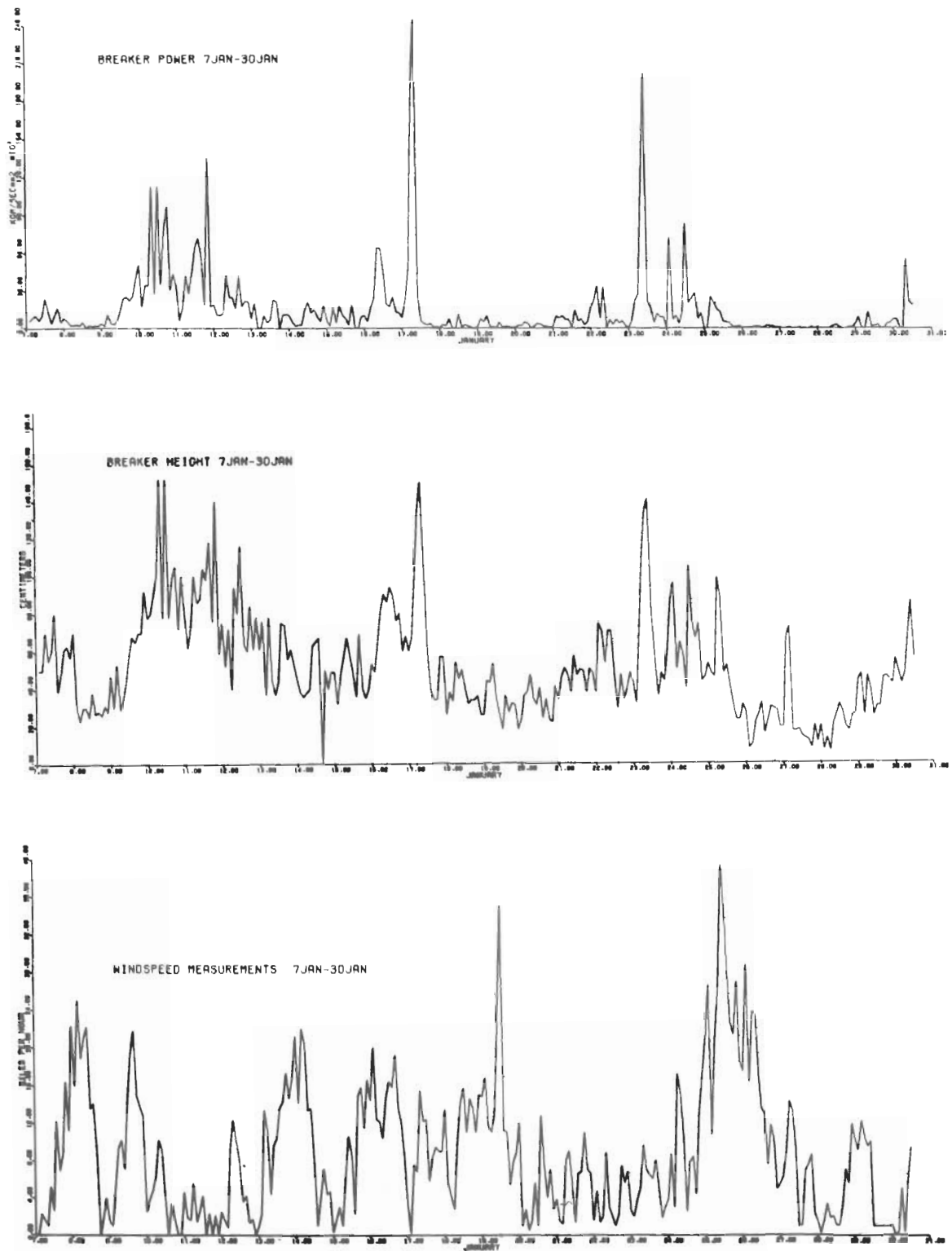Figure 48. Air and water temperatures, January 1972.

Figure 49. Breaker power, breaker height, and windspeed measurements, January 1972. Note the decrease in breaker power with strong offshore winds (e.g., 26 January).
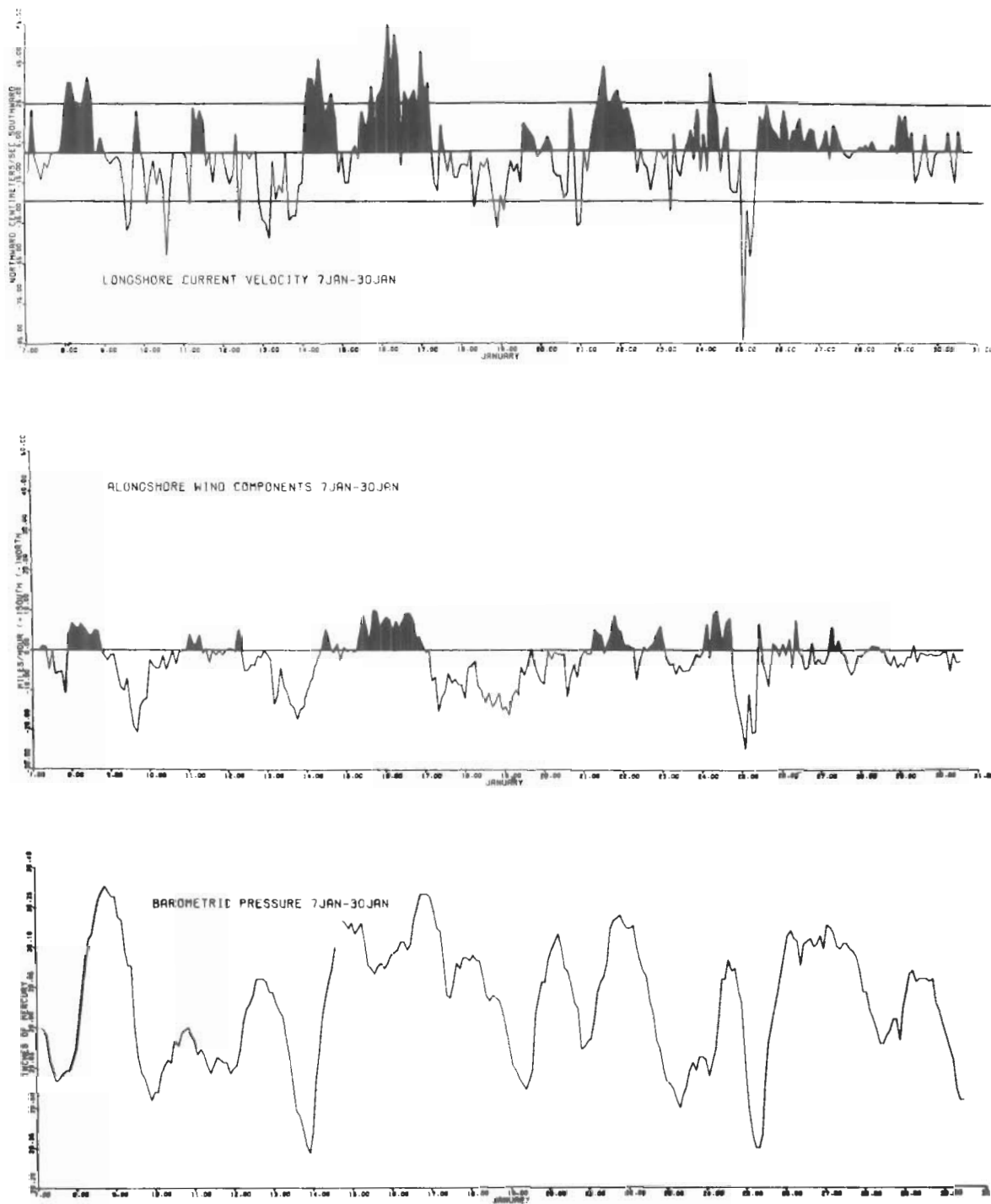
66

Figure 50. Longshore current velocity, alongshore wind components, and barometric pressure, January 1972. The solid line in the longshore drift diagram represents a velocity of 24 centimeters per second, the minimum velocity required to erode the sediment sizes in the study area (U.S. Army, Corps of Engineers, Coastal Engineering Research Center, 1966).

of the low resulted in southerly and southwesterly winds. Winds blowing
from the south or southwest (negative alongshore components) resulted in
negative longshore currents flowing toward the north. As the low-pressure
system moved offshore, the wind shifted to the north, and positive along-
shore wind components and positive longshore current velocities were
produced.

Sudden changes in wind direction will sometimes generate short-period
waves. These short-period waves break on the beach at greater angles
than longer period waves and cause strong longshore currents. Waves
measured on 8, 15, and 21 January show an inverse relationship between
breaker angle and wave period (Fig. 51).

Breaker type and breaker depth are shown in Figure 52. Breaker types
between 4 and 6 are either surging, surging-plunging, or surging-spilling.
Surging waves and breaker depths less than 50 centimeters characterize
wave conditions on the high tide beach face for 1 to 2 hours on either
side of the high tide. The semidiurnal tides at Plum Island are evident
in Figure 52, especially between 20 and 24 January. On these days, two
daily periods of surging breakers along with breaker depths less than 50
centimeters occurred at high tide conditions. Under higher energy condi-
tions, plunging waves will break on the beach face and this relationship
is invalid.

Several process variable relationships discussed under summer beach
process variables were similar for both summer and winter study periods.

VI. WINTER BEACH MORPHOLOGY

During the winter study period, strong offshore winds and subfreezing
temperatures resulted in changes in beach morphology that were more rapid
and pronounced than during the summer period.

A small northeaster on 5 January resulted in a poststorm beach pro-
file at all profile locations. The poststorm profile is characterized
by a flat, concave, upward profile caused by wave energy acting upon a
wider beach zone than during nonstorm periods. Heavy minerals are con-
centrated at the upper swash limit of the waves, usually at the base of
the dune scarp. The gradient of the high tide beach face after a storm
has passed is between 5^0 and 6^0 (Fig. 53). The high tide beach-face
gradient increases after a storm until a stable condition is reached or
until another storm occurs. The reason for the pronounced change in
gradient was because a neap berm formed 3 days after the storm. As the
neap berm grew, the gradient of the beach face steepened until 15 January,
after which time the gradient changes were due more to changes in wave
energy than to the effect of an enlarging neap berm. Changes in profile
PL-0 between 8 and 18 January are shown in Figure 54. The upper profile
shows the beach morphology 4 and 5 days after a storm. A neap berm
began to form on 7 January and by 10 January was large enough to con-
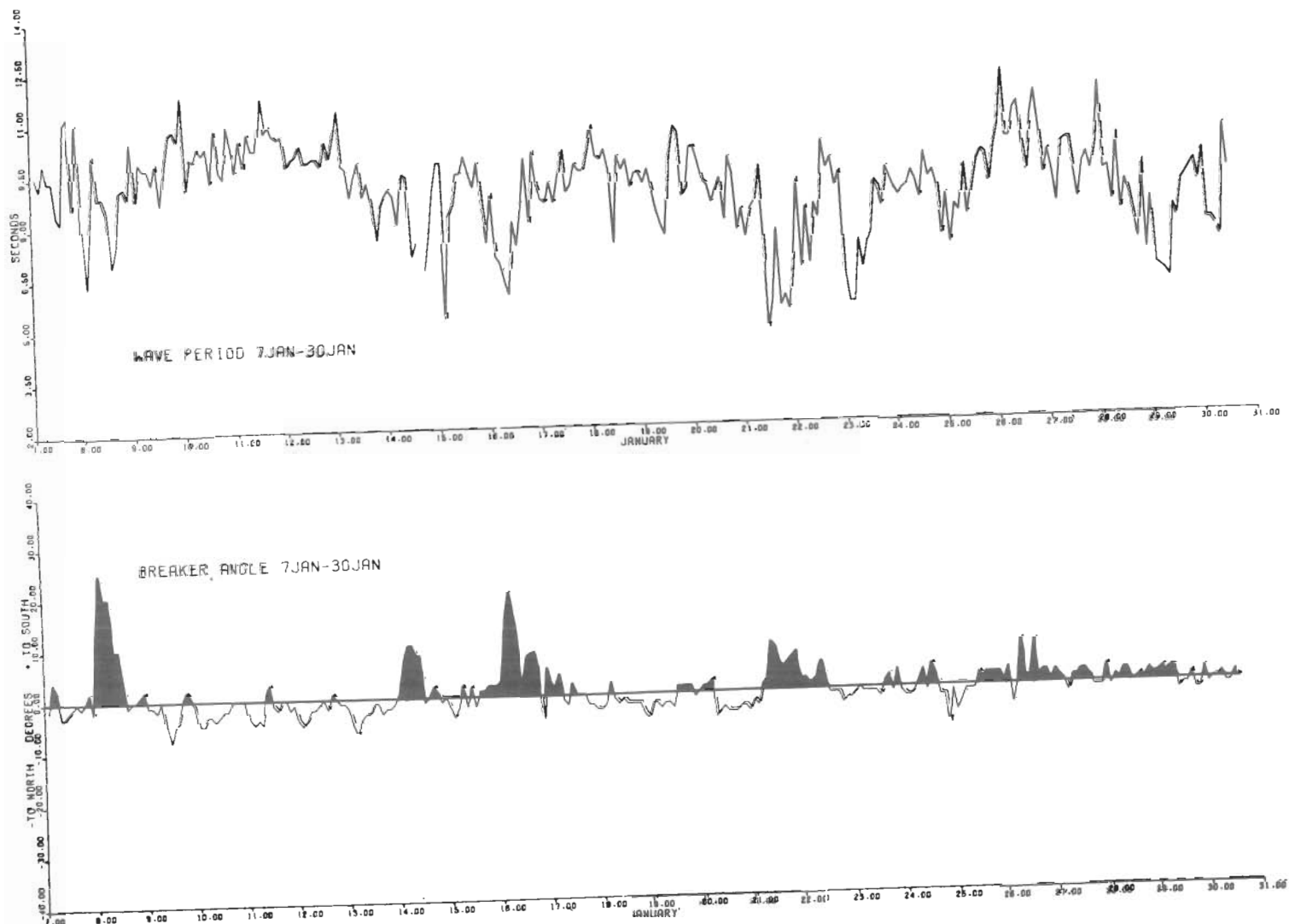siderably affect the beach face gradient (Figs. 55 and 56). Sediment

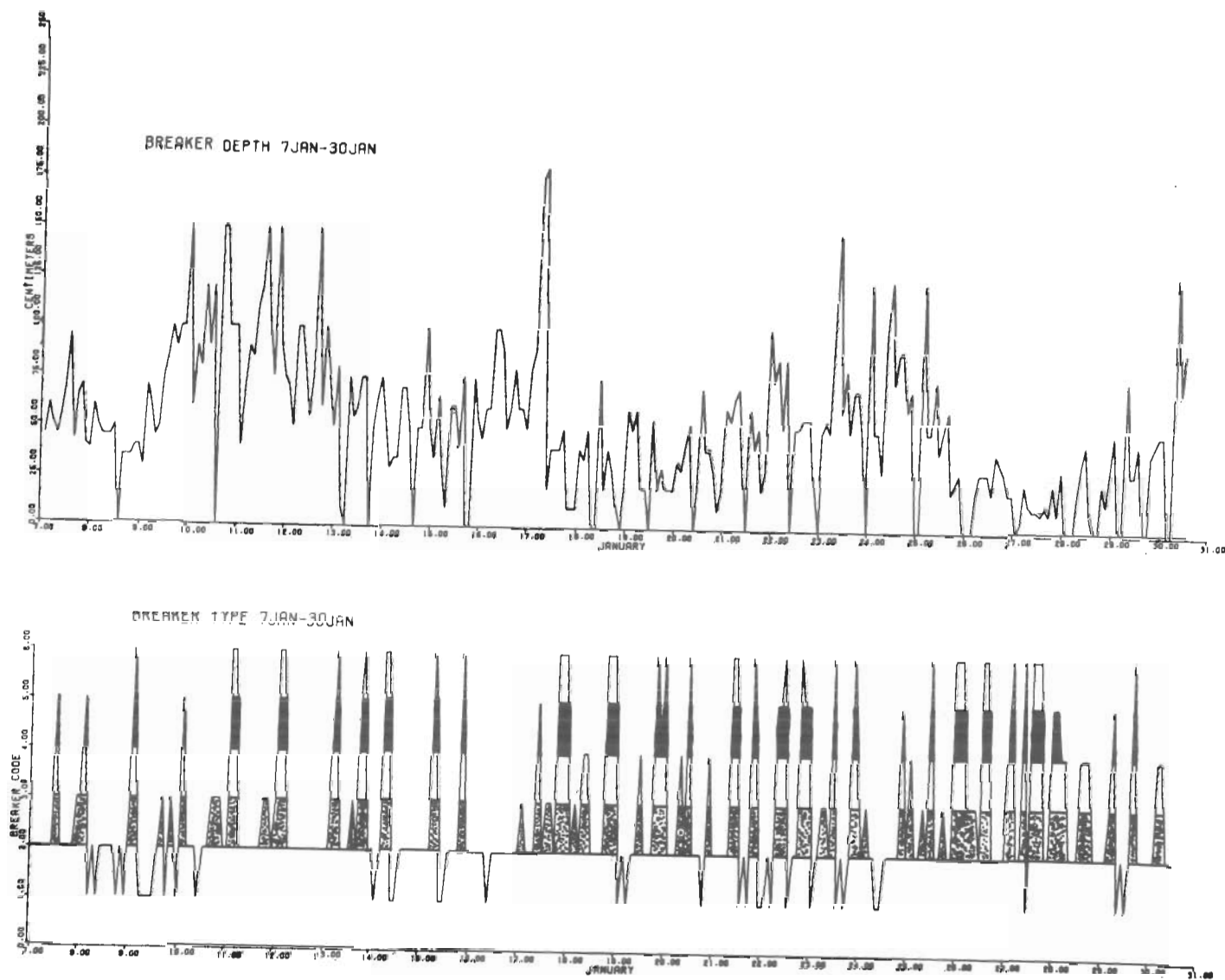Figure 51. Wave period and breaker angle, January 1972.

69

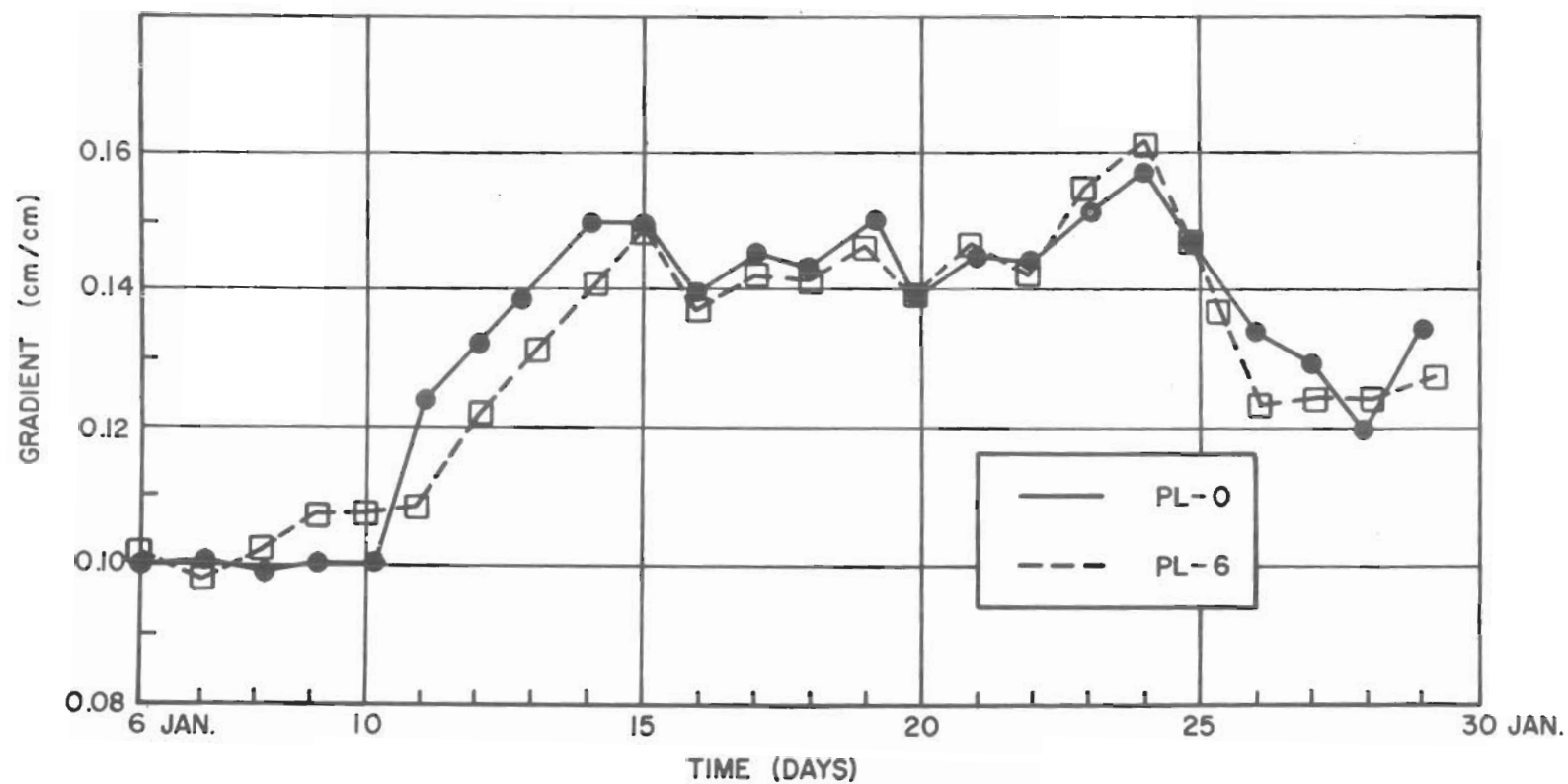Figure 52. Breaker depth and breaker type, January 1972.

Figure 53. Beach gradient change, January 1972. Note rapid accretion after storm of 5 January 1972.
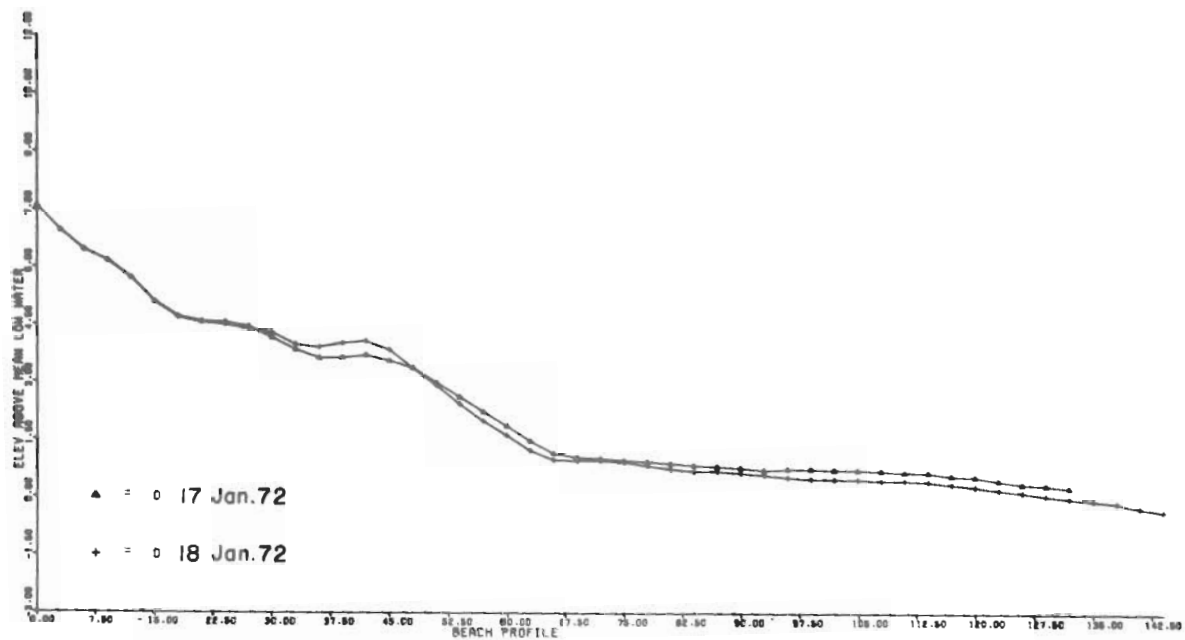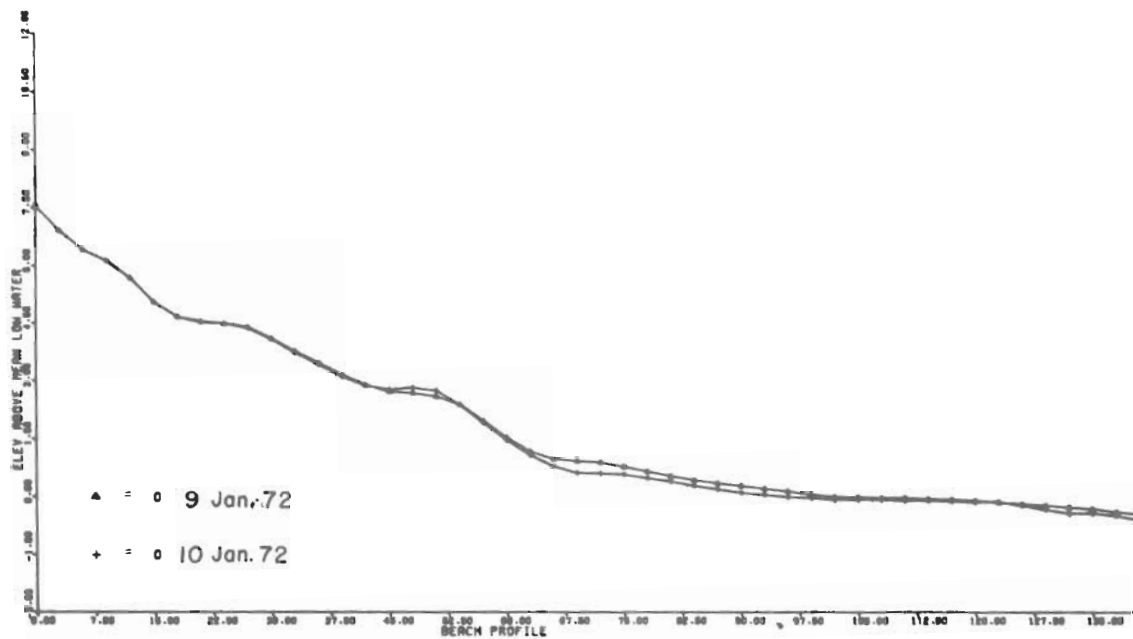
Figure 54. Beach profiles at PL-0 measured on 9, 10, 17, and
18 January 1972. Note neap berm accretion.

Figure 55. Poststorm beach, profile PL-0; looking north, 7 January 1972.

Figure 56. Poststorm beach, profile PL-0. Note eolian ripples in back dune area. View toward southwest.

accretion on the neap berm is caused by erosion of sediment at the base of the beach face which is then deposited at the distal end of the neap high tide swash. As tides move from neap conditions toward spring conditions, the neap berm moves up the beach face (lower diagram, Fig. 54).

Accretion on the neap berm also occurs in the form of sediment moved from the back dune region onto the beach by westerly and northwesterly winds. Immediate poststorm conditions on 7 January are shown in Figure 55. A small neap berm had begun to form; however, the profile was generally featureless. As the low-pressure system moves out of the area and the winds shift to the west, considerable sediment is moved onto the beach by eolian transport. Coarse-grained eolian wind ripples migrating across the back dune area are shown in Figure 56. Similar eolian ripples are common on the backshore during the winter (Fig. 57). While sediment from the dunes was deposited on the beach, small ridges were forming offshore and migrating landward. During the study period these ridges were of low amplitude, and were rarely as long and continuous as the ridges during the summer. Although actual measurement of ridge migration rates was difficult (to qualitatively locate a ridge slip face from one low tide to the next), ridges moved more quickly across the low tide terrace during early poststorm conditions than during later stages in beach development (Fig. 58).

Temperature extremes in winter caused changes in beach morphology not experienced during the summer. Relatively higher winter temperature for the first part of the study (in the lower fifties) caused a lowering of the frost table in the back dune area. The level of the frost table marks the limit to which sediment is eroded from the dune area by the wind. The result of the lowered frost table was that more sediment moved onto the beach from the dunes than would have been eroded had the frost table been closer to the surface. A comparison of profiles from 25 and 26 January, after offshore winds averaged 40 miles per hour on 25 January (Fig. 59), reveals up to 30 centimeters of deposition on the low tide terrace. The sand deposited on the low tide terrace was delivered to the surf zone by the wind. The waves depositing the sand were flattened out by the offshore wind which was strong enough to maintain a constant tidal elevation for 3 hours preceding high tide on 26 January.

Extreme cold which causes parts of the beach to become frozen is important to erosion of the beach face and berm. Most of the water that ponds on the berm at high tide percolates into the sand and when the temperature is below the freezing point of saltwater it will freeze the berm and sometimes the beach face. At the next flood stage of the tide the frozen part of the beach face inhibits erosion. However, after a break occurs in the frozen surface, the beach surface is vulnerable to erosion. Erosion at the berm crest near high tide is shown in Figures 60 and 61. The effects of this process are generally greatest along the edges of bays between beach cusps, although similar effects have been noted on the high tide beach face where a frozen high tide swash may also inhibit erosion.

Figure 57. Strong offshore winds blowing sediment onto the beach.
Note blowing of tops off waves. Looking southeast.

Figure 58. Typical small poststorm ridge migrating landward; stakes
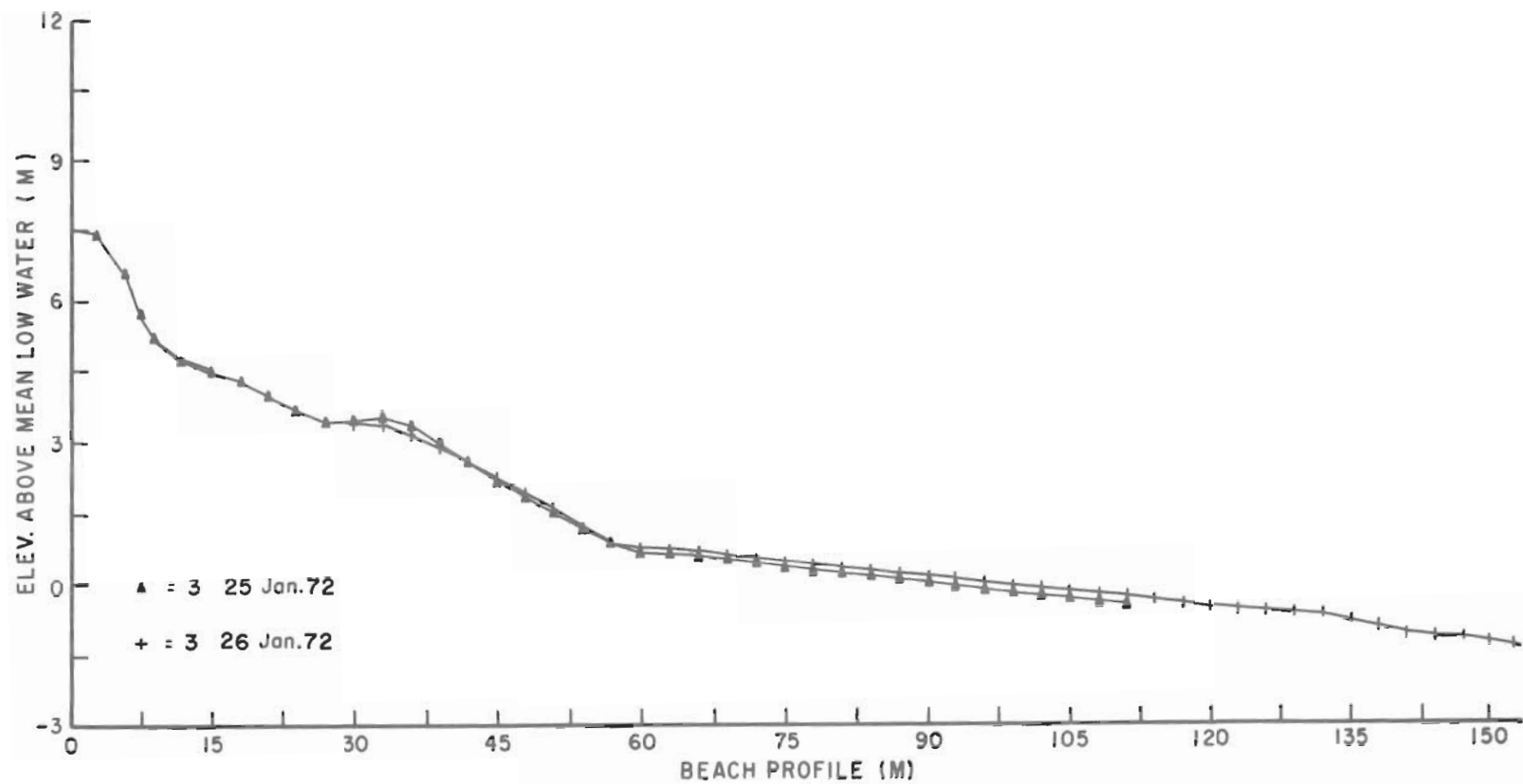in background are at profile PL-0.

Figure 59. Profile PL-3, 25 and 26 January 1972. Note net deposition during this period by eolian sedimentation.

Figure 60.   Frozen berm crest and beach face at high tide.

Figure 61.   Frozen berm crest and beach face at high tide. Greater
current velocities in cusp bays may erode through the
ice cover.

77

In contrast to the summer study period when beach morphology was characterized by large ridge and runnel systems, welded ridges, and wide low tide terraces, beach morphology for the winter study period consisted of typical early preweld and late preweld profiles characterized by neap berms, beach cusps, and small ridge and runnel systems. Poststorm profiles at PL-0, PL-5, PL-6, and PL-11 are shown in Figures 62 and 63. A similar situation on profile PL-0 existed during the summer period. Profile PL-0 responded more quickly after the storm than other profiles characteristic of the central and northern parts of the study area. The incipient berm was not removed on PL-0 during the storm of 7 January as on the other profiles. Profiles PL-6 and PL-11 (Fig. 62) representing the central and northern parts of the area do not exhibit different stages of beach maturity as exist between PL-0 and PL-5.

Continued neap berm accretion between 10 and 17 January resulted in the profile changes on PL-6 (Fig. 64). The change in slope of the beach face was due to the highest breaker-power measurements of the study period on 17 January before the measurement of the beach profiles. Profile PL-11 on 10 and 17 January was run through a bay between beach cusps, explaining why a well-developed neap berm was not present.

Beach cusps which commonly develop during the initial stages of early accretionary beach morphology were ubiquitous throughout the study period. The spacing of the cusps varied between 25 and 30 meters (Figs. 65 and 66).

Detailed mapping of the cusps between PL-0 and PL-4 did not reveal any significant migration under varying energy conditions. Beach cusps have been observed to have a controlling influence on the direction and intensity of longshore drift under certain conditions. Field observations in January 1972 show that at or near high tide, rip currents, caused by the beach cusps, tend to keep beach face velocities within a certain range, regardless of the angle of wave approach. Lower velocities of rip currents associated with low breaker angles (5° to 10°) are "accelerated" as they enter the rip system, and higher velocities associated with greater breaker angles are "decelerated" as they enter the system, i.e., the velocities within the rip system appear to be relatively constant unless the breaker angle or wave conditions are such that a cusp and its associated rip system are completely bypassed.

The first stages of an early accretional beach profile were present at the conclusion of the study period--a wide low tide terrace, a relatively steep neap berm, and numerous beach cusps. Figure 67 shows the similar stages of beach profile development at PL-7 and PL-11 near the termination of the study. The neap berm grew seaward from 25 January until the end of the study because of a marked decrease in breaker power during this time period.
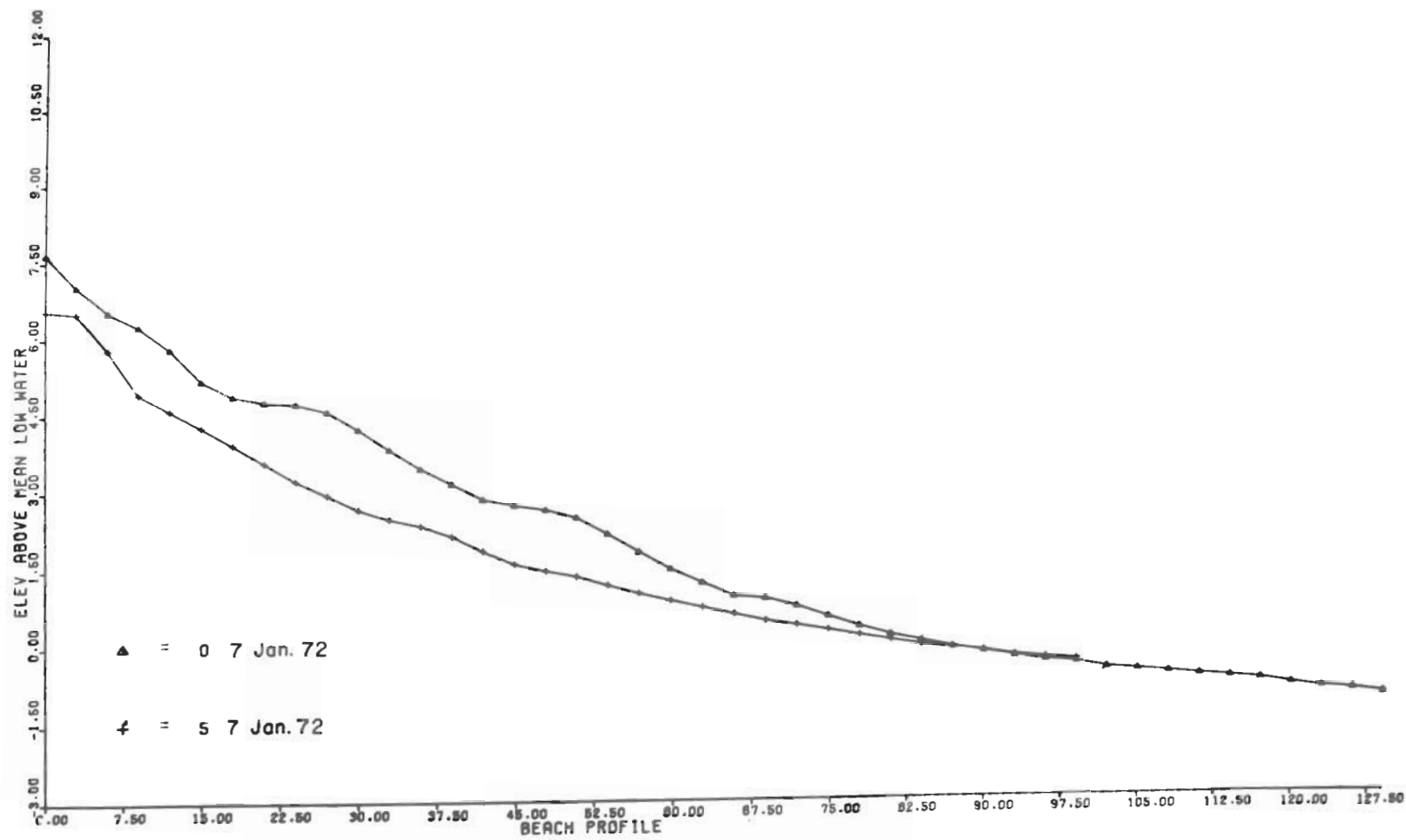
78

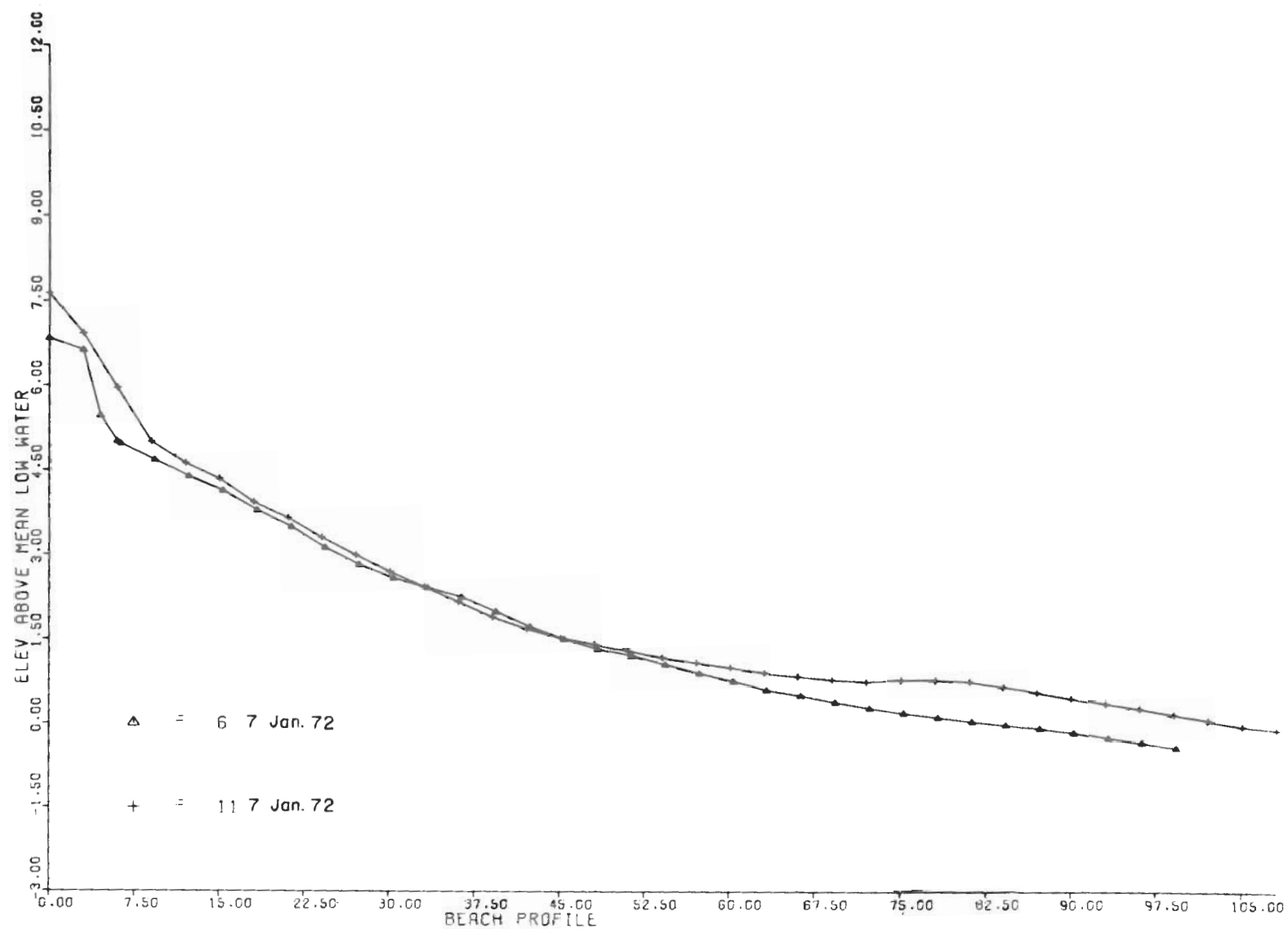Figure 62. Profiles PL-0 and PL-5, 7 January 1972.

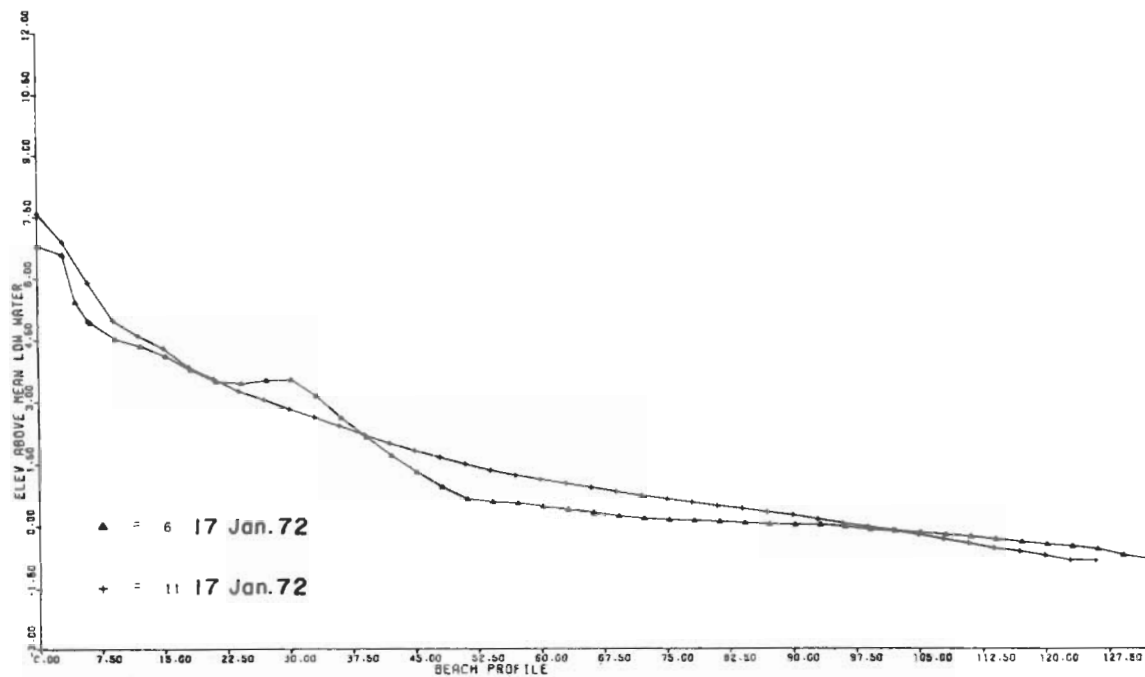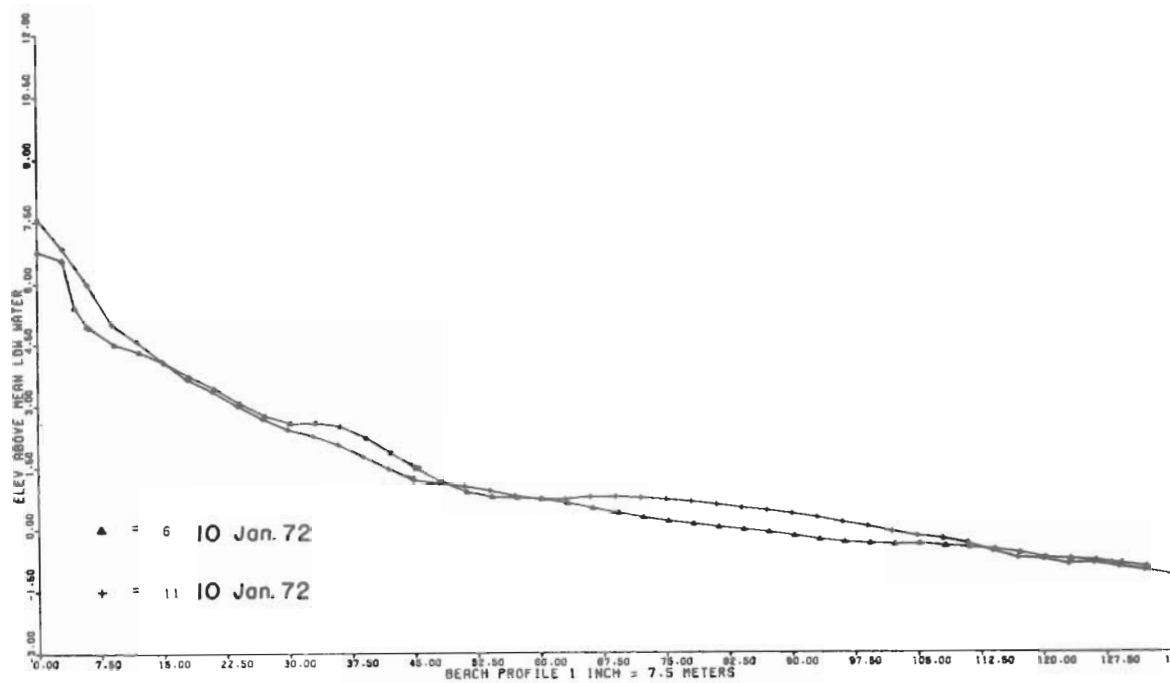Figure 63.   Profiles PL-6 and PL-11, 7 January 1972.

Figure 64. Profiles PL-6 and PL-11 on 10 and 17 January 1972. Note development of neap berm on PL-6 during this period. Profile PL-11 on 17 January runs through a bay between two cusps.

Figure 65.   Beach cusps at profile PL-0.   Note extensive ponding on
the berm surface.

Figure 66.   Beach cusps looking northward from profile PL-0.   The
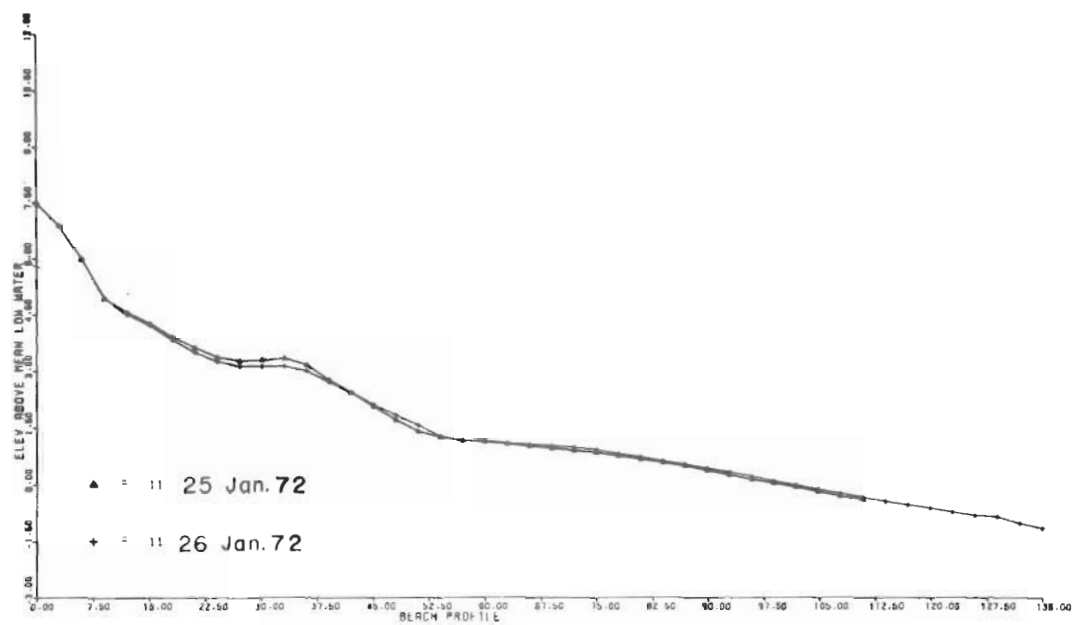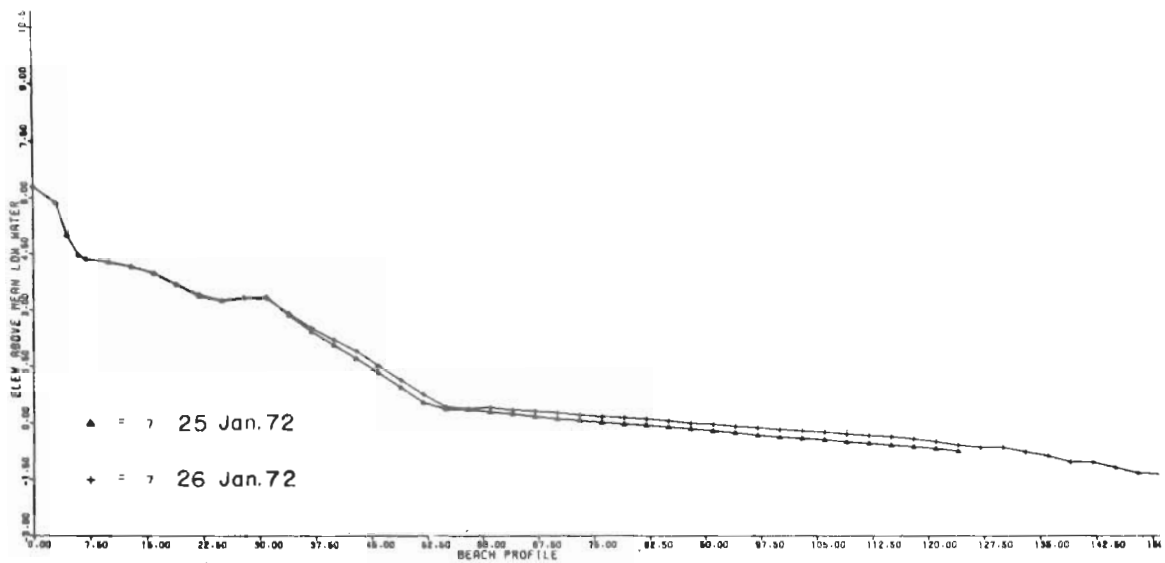spacing between cusps is approximately 20 meters.

Figure 67. Profiles PL-7 and PL-11, 25 and 26 January 1972.

83

VII. BEACH PROFILE CLASSIFICATION AND CHARACTERISTICS

Based on the original classification of beach profiles by Hayes and Boothroyd (1969), and detailed observations of beach morphology between June and August 1971 and during January and February 1972, a modified scheme is proposed for the classification of beach profiles.

1. Early Preweld or Poststorm Profile (duration dependent upon severity of storm).

A flat, concave, upward beach profile with heavy mineral concentration (garnet, hornblende, and magnetite) near the distal end of the storm swash is commonly at the base of the dune scarp. The grain size is uniformly medium sand (Hayes and Boothroyd, 1969). Small ridges (amplitude <20 centimeters) appear in 1 day to 1 week after the storm passes and move quickly across the low tide terrace. A beach step is rarely present. The gradient of the high tide beach face varies between 4° and 6° (Fig. 68).

2. Late Preweld Accretional Profile (up to 6 weeks after storm).

Late preweld beach profiles characteristically have small neap berms with beach cusps. A wide low tide terrace is present where ridge and runnel systems migrate (Fig. 69). The sand is generally uniformly fine on the low tide terrace (1.5 to 1.9 phi), with a coarse zone (often bimodal, -0.4 to +0.8 phi) at the beach step. Mean grain-size measurements for the high tide beach face vary between 0.5 and 1.0 phi, with a zone of coarser sediment at the berm crest and finer sediment on the neap berm (1.1 to 1.6 phi). Coarse eolian ripples formed by strong offshore winds may exist on the berm and the beach face. Zones of coarse sediment may also occur in other areas of higher swash energy such as at the base of cusp bays. Large runoff channels between the ridge and runnel systems are also prevalent. As the landward-migrating ridges weld onto the backshore and form wide berms, the early postweld stage is reached.

3. Early Postweld (2 to 3 days to several weeks after welding).

After the large berm has formed by ridge migration and welding of the ridges to the backshore, there is a period during which the active high tide beach face is landward of the berm (Fig. 70). Small ridges may still migrate across the berm surface and weld onto the backshore. The gradient during the early postweld period is steeper on the high tide beach face than on the seaward side of the berm ridge.

4. Late Postweld.

Late postweld takes place after the active high tide beach face is no longer landward of the berm, but exists on a former ridge beach face. High tide swash does not overtop the berm crest during late maturity (Fig. 71).

Figure 68.   Typical poststorm or early preweld profile.

Figure 69.   Preweld profile; note dune northwest-southeast orientation
and multiple ridges on the low tide terrace.

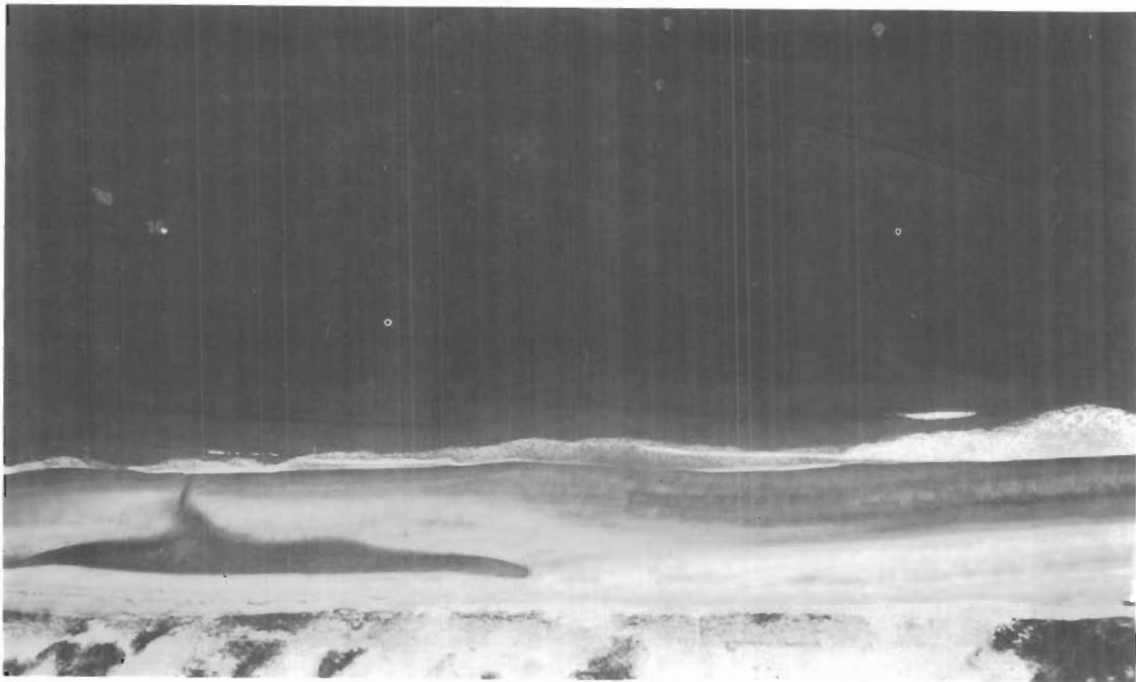Figure 70. Late preweld profile, 6 July 1971.

Figure 71. Contemporaneous preweld and postweld profiles
PL-0 through PL-7, 7 August 1971.

All of these beach profile types may be found in any season of the year. The maturity of a beach profile is a direct consequence of the frequency and strength of northeasterly storms.

VIII.   STORM PROCESS MEASUREMENTS AND PROFILE CHANGES, 19 TO 26 FEBRUARY 1972

A large northeaster passed over Plum Island on 19 February 1972 and caused considerable erosion of the backshore and foredune ridges in the study area. Although continuous bihourly measurements were not taken, closely spaced beach processes were measured by a small field crew and these reflect the major changes in beach process variables.

The beach process variables measured during and after the storm (Fig. 72) included barometric pressure, windspeed and direction, wave period, breaker height, longshore current velocity, and breaker angle. At the beginning of process measurements at 11:00 p.m. on 18 February, the low was centered off Cape Hatteras, North Carolina. As the low moved northward, barometric pressure steadily decreased over the study area. With the decrease in pressure, wind velocity increased from the northeast, wave period decreased, and breaker height increased (Figs. 72 and 73). The wind shift to the northeast resulted in breaker angles shifting from negative to positive readings and longshore current velocity increasing in a southerly (positive) direction. As the pressure continued to drop, windspeed increased to a peak of 39.4 miles per hour at noon on 19 February. This strong onshore wind moved a large amount of sediment by eolian transport and deposited this material in the back dune area. The maximum wave height and lowest wave period occurred about 2 hours after the highest wind measurement; however, this could be a function of the time between readings. The short-period waves generated by the strong onshore winds increased in height to an average of 330 centimeters. After a change in wind direction from near 90° to near 45°, the breaker angle increased from +2° to a maximum of +6°. Although the breaker angle did not greatly increase, longshore current velocities increased considerably. Strong longshore currents moved large dock sections, picnic tables, and telephone poles down the beach. High tide occurred at 3:00 p.m. on 19 February near the peak in energy conditions and resulted in abnormally high tides. Logs were carried by the swash and deposited near the PL-0 backup stake, 9.1 meters above MLW.

Late in the day on 19 February, as the low-pressure system began to move farther offshore, the barometric pressure began to rise. With the rise in barometric pressure, a decrease in the onshore winds led to a lower breaker height and an increase in the wave period. Longshore current velocity and the breaker angle also decreased as the pressure rose. As the low moved farther north (Fig. 74) the winds changed to the northwest and began blowing offshore. For several hours, wave height increased due to the strong offshore winds; however, with time the tops of the waves were blown off and the breaker height decreased. Wave period increased as high pressure moved into the area.
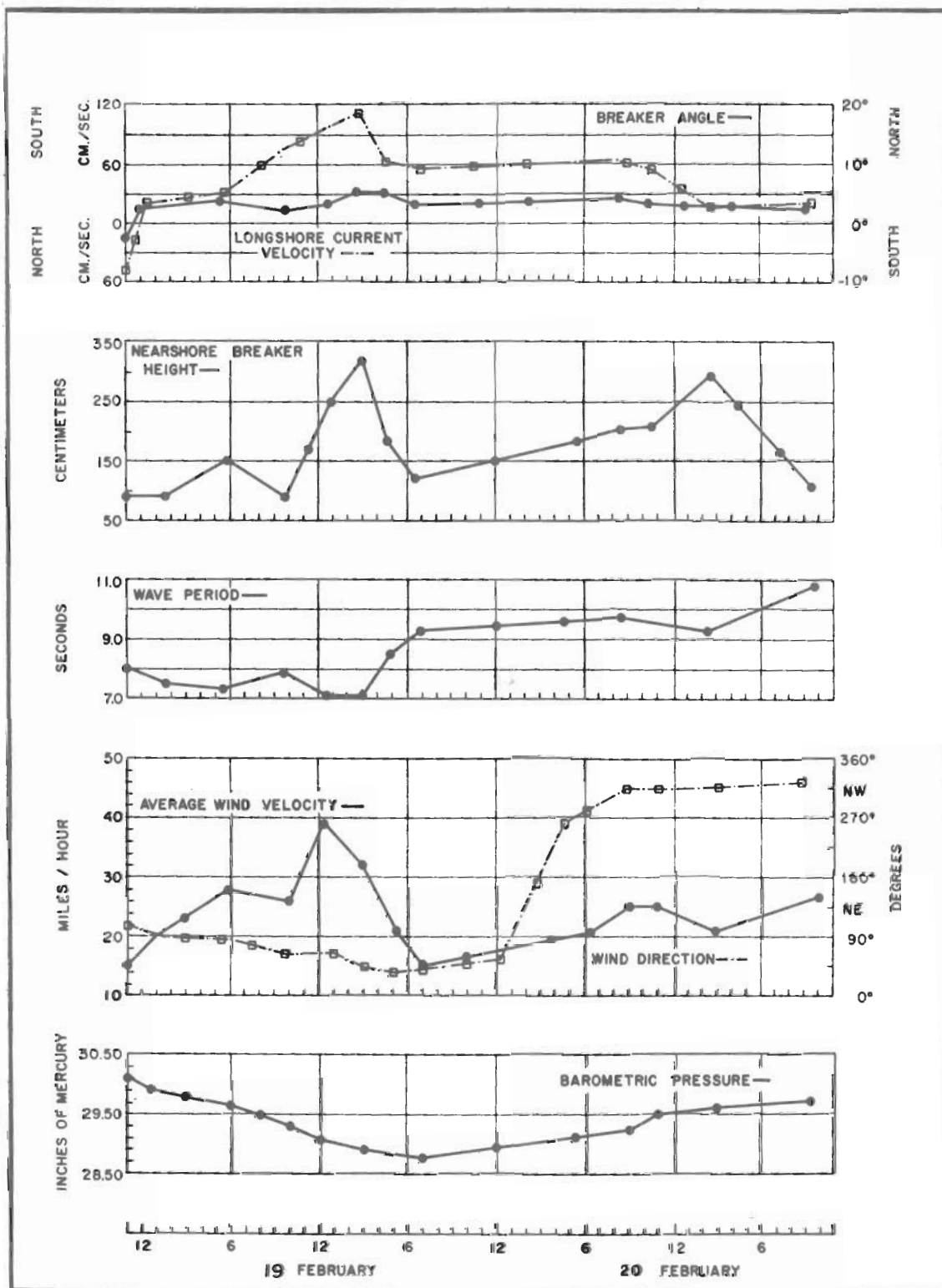
87

Figure 72. Beach process variable measurements, 18 to 20 February 1972.
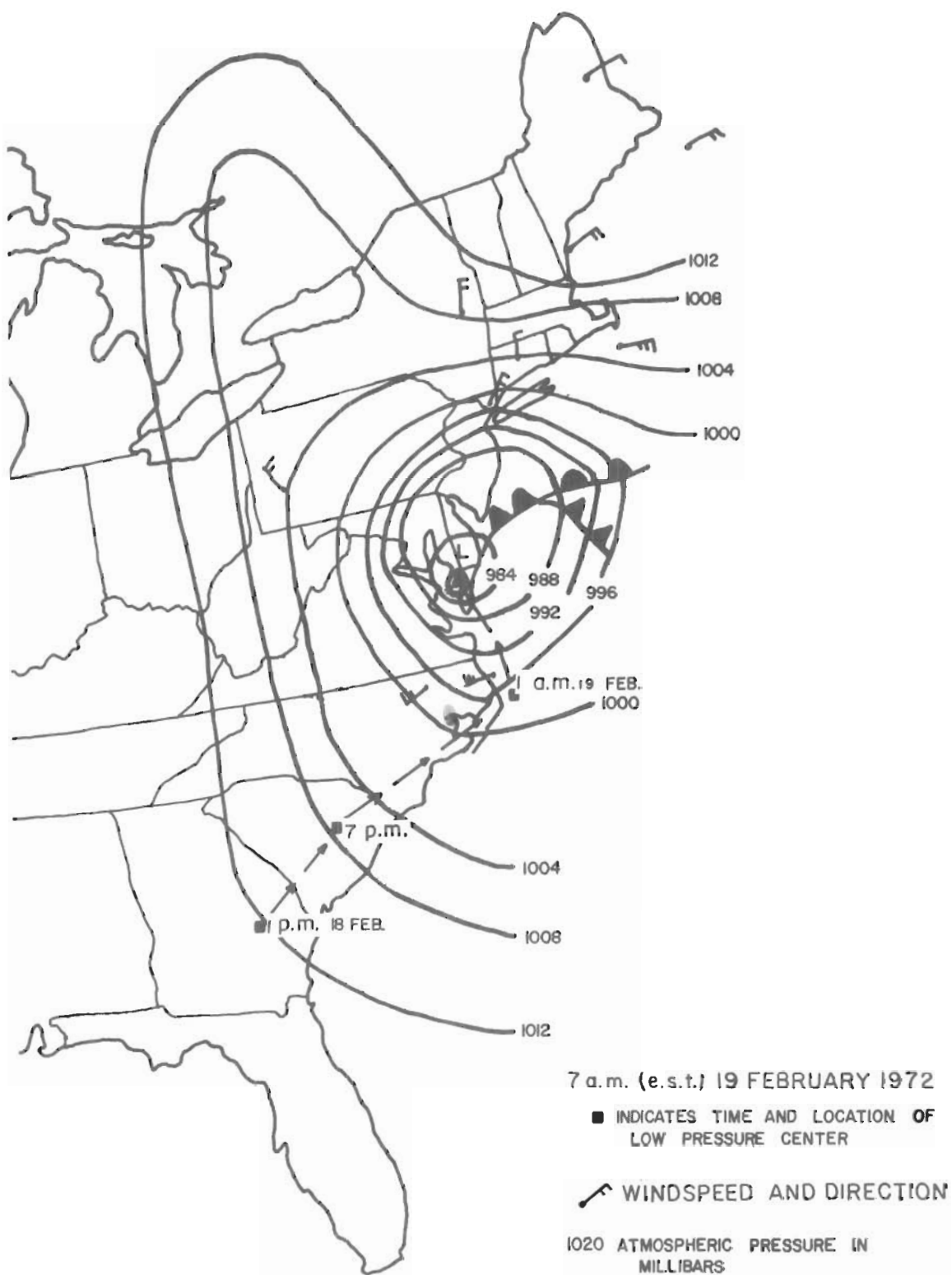
Figure 73. Surface weather map, 19 February 1972 (National Oceanic and Atmospheric Administration, 1972).
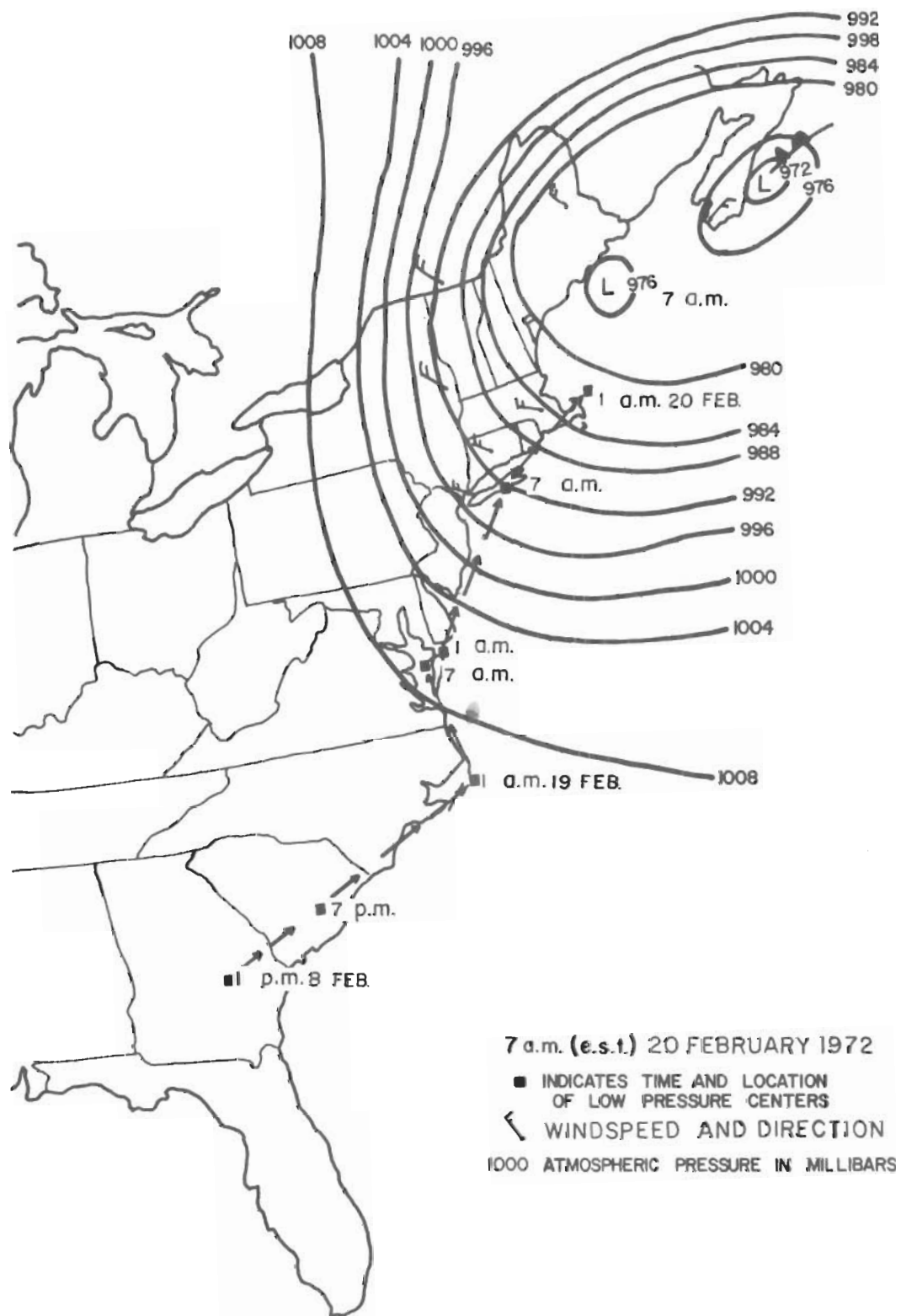
89

Figure 74. Surface weather map, 20 February 1972 (National Oceanic and Atmospheric Administration, 1972).

Figures 73 and 74 emphasize the importance of the location of the low-pressure system in relation to Plum Island in terms of storm intensity. The peak wind and wave energy conditions occurred between 2:00 p.m. and 6:00 p.m. on 19 February while the center of the low was near Long Island. The predominant wind pattern is onshore (Fig. 73) when the low is south of Plum Island. As the low-pressure system moves northward, the intensity of the storm diminishes on Plum Island and the winds associated with the low become dominantly offshore.

Poststorm Conditions.

The large volume of sediment removed by the northeaster of 19 February is shown in Figures 75 and 76. The erosion at PL-0 was concentrated in the area between the low tide terrace and the foredune ridge with little erosion on the low tide terrace (Fig. 76). The same concentrated zone of erosion is shown in Figure 75; however, there is a steep dune scarp at PL-6 but not at PL-0. This tendency toward greater erosion in the central part of the study area may be related to the character of the offshore bar which is farther offshore and deeper in the central area.

Photos in Figures 77 and 78 show conditions near the study area immediately after the storm; Figure 77 was taken from PL-2 looking south toward PL-0 and PL-1, and shows a small washover in the foreground of the photo. Larger washovers on other parts of Plum Island breached the entire width of the island. The amount of landward erosion is noted by the two stakes (not visible before the storm) in the center of the photo (Fig. 78). Stumps exposed by the storm are also shown in the figure. Damage to Plum Island was most extensive to the north of the study area (Figs. 79 and 80). Heavy mineral concentrations at the base of the dune scarp are visible in the top photo in Figure 79 along with evidence of offshore winds in the form of snow and newly deposited sediment on the beach face. The height of the swash reached on the foredune ridge is shown in the lower photo (Fig. 79). In areas of such concentrated erosion, slumping continued for several days after the storm had passed. The physical damage to dwellings at the northern end of Plum Island is shown in Figure 80.

Two days after the storm, small ridges appeared on the low tide terrace indicating the beginning of poststorm accretion (Fig. 81). The continued presence of offshore winds for several days after the storm is shown by the breakers with blown tops in Figure 81. An aerial view of the study area 3 days after the storm shows semicontinuous ridge and runnel systems migrating landward. Erosive effects of the storm are shown along the dune scarp and in the blowout in the extreme right of the photo in Figure 82.

Poststorm beach-face gradient changes were slower after this storm than after the northeaster of 5 January 1972 (Fig. 83). The reason for this slower change in gradient is directly related to the amount of sediment removed after each storm. During the small northeaster in
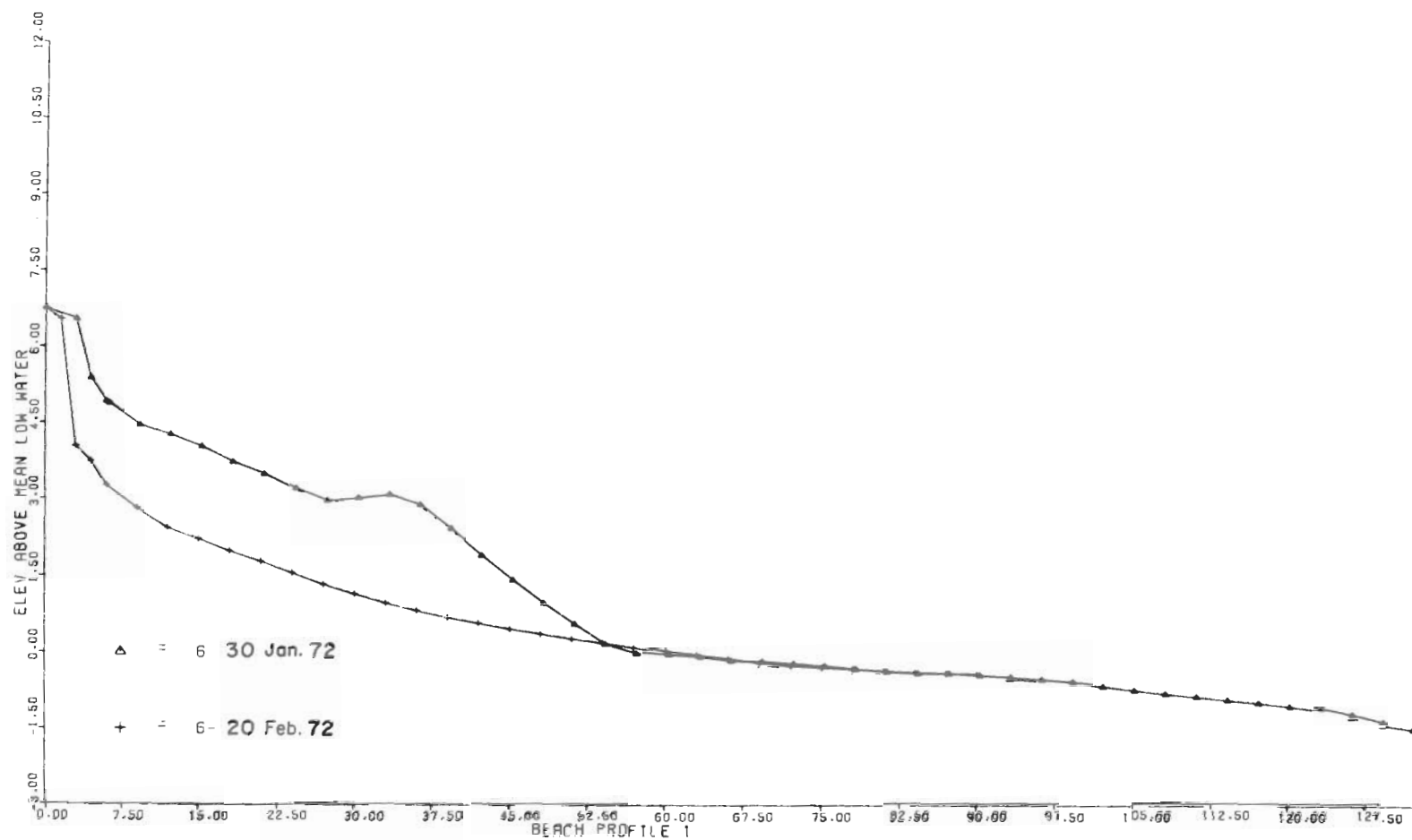
Figure 75. Profile PL-6, 30 January to 20 February 1972.
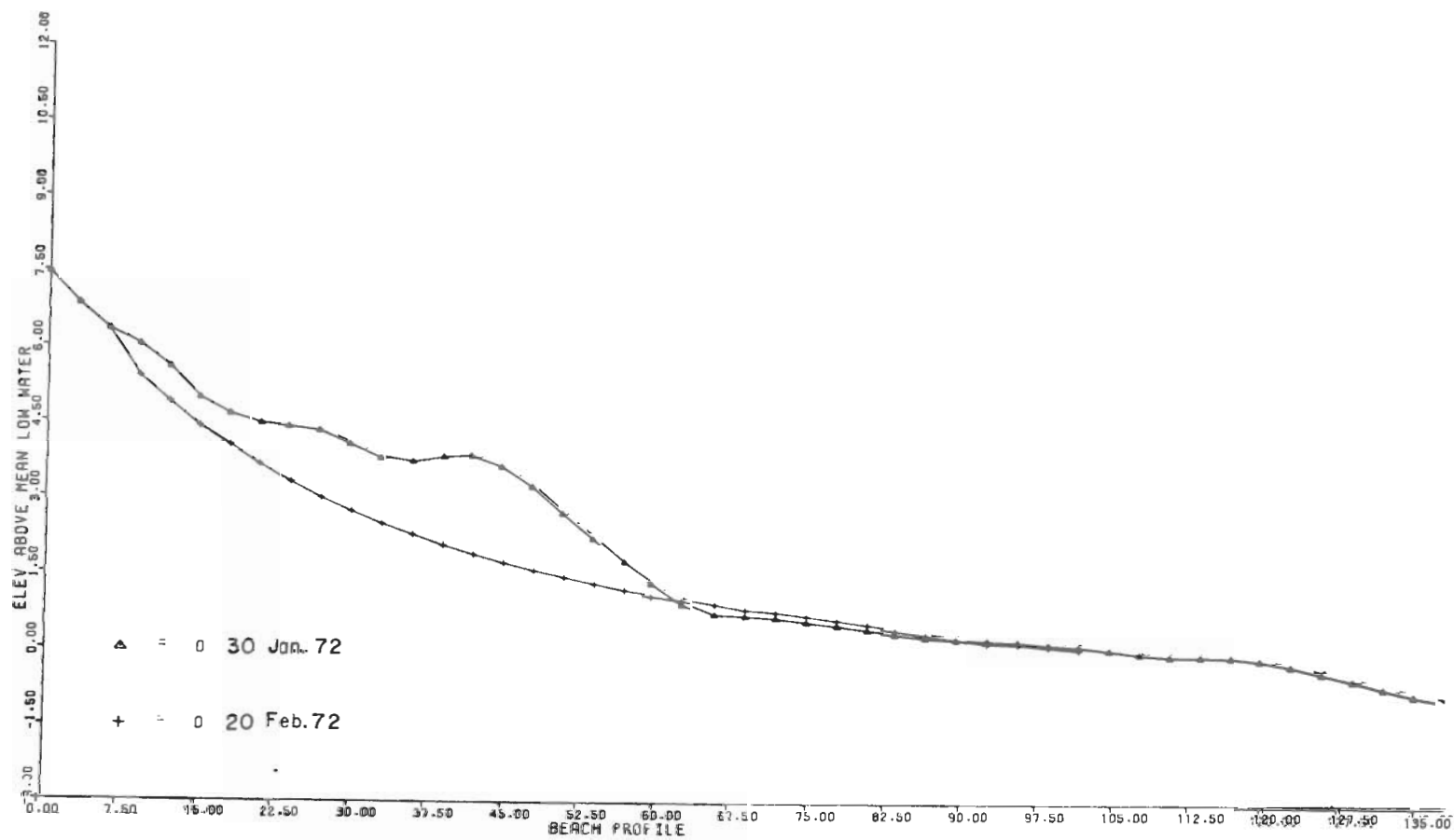
Figure 76. Profile PL-0, 30 January to 20 February 1972.

Figure 77. View of storm damage to the south of PL-0. Note small washover in foreground.

Figure 78. View of storm damage to the north of PL-0. Amount of landward erosion is noted by the two stakes in center background.

94

Figure 79. Photos showing erosion of the dune scarp north of the study area.

Figure 80. Storm-damaged cottages at the northern end of Plum Island, February 1972.

Figure 81. Photo showing first ridge to appear after storm of 22 February 1972.

Figure 82. Aerial view of study area 3 days after the storm.
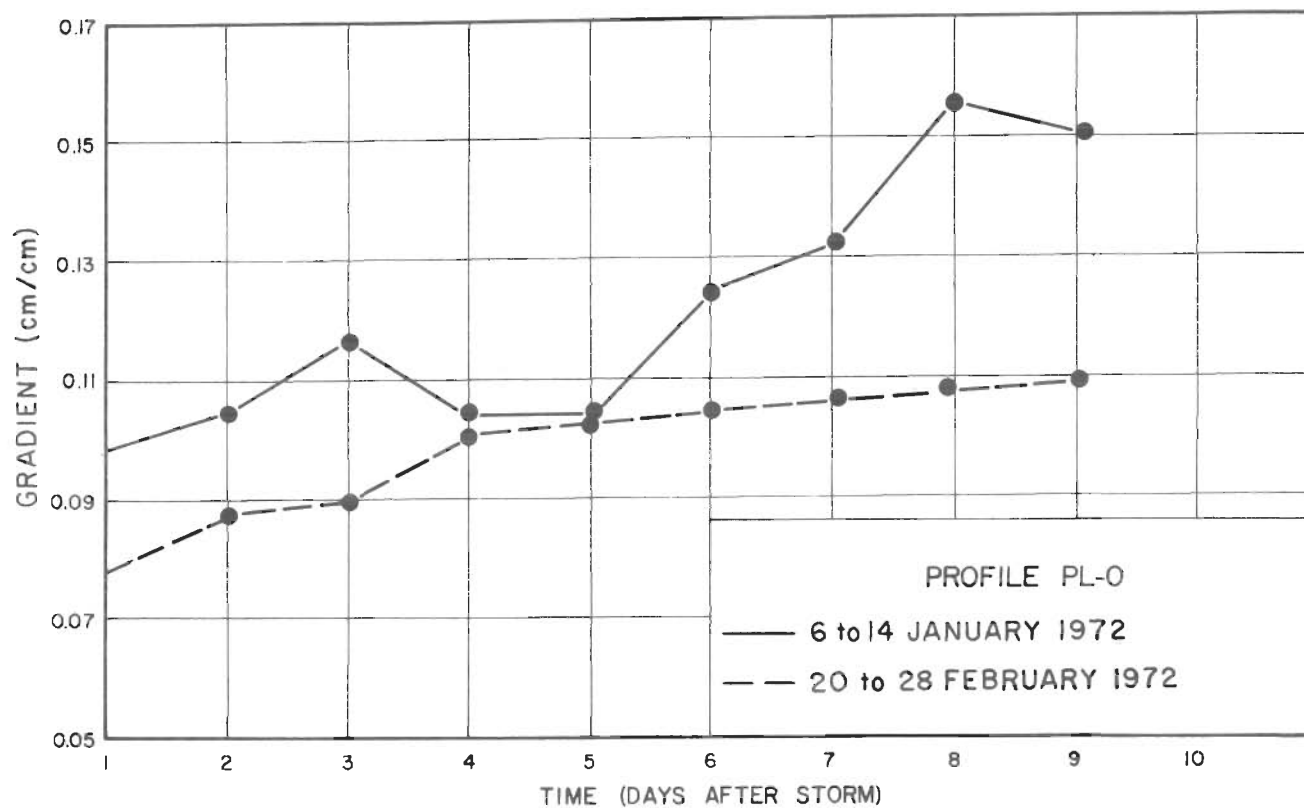
Figure 83. Poststorm beach-face gradient changes, January and February 1972.

January, sediment was not moved far offshore and neap berms appeared several days after the storm; however, during the February storm, sediment moved far enough offshore to preclude neap berm formation. Immediate poststorm accretion in this instance is accomplished by small-scale ridge and runnel systems migrating landward.

IX. CONCLUSIONS

An analysis of summer and winter process measurements and changes in beach morphology during both investigations reveals the following similarities and differences between the two periods.

1. Detailed beach profiling for summer and winter periods shows no typical summer or winter beach profile at Plum Island. Beach morphology differs from summer to winter; however, the difference is due to the stage of development of the beach profile in relation to storm effects.

2. Adjacent profiles at different stages of development are thought to reflect the proximity of the nearshore bar (Fig. 17). The closer the bar is to shore, the faster the sediment is returned to the beach zone after a storm; hence, a profile can quickly develop.

3. The passage of high- and low-pressure systems through the area during either season produces identical results in wind direction, wave conditions, and longshore current directions.

4. High-pressure systems during the winter months are of greater intensity than those in the summer months. This results in a stronger offshore wind component during the winter which moves larger amounts of sediment from land toward the sea.

5. A beach process unique to the winter periods is the limiting effect of ice on erosion.

6. Local winds control most beach process variables in the summer and winter, except for offshore disturbances which generate the long-period swell measured on several occasions.

7. Changes in breaker power and wave steepness result in rapid changes in the high tide beach-face gradient, often within several hours.

8. Changes in breaker height and tidal stage result in changes in ground water elevation. These changes in ground water elevation lag 1 to 3 hours behind other process variable changes.

9. Poststorm beach recovery is rapid even after a severe northeaster. The intensity of a storm apparently dictates the accretional processes which rebuild the beach. A small storm will be followed by beach accretion through neap berms; however, after a severe storm, landward ridge and runnel migration is the immediate accretional response.

99

LITERATURE CITED

ALLEN, R.H., "A Glossary of Coastal Engineering Terms," MP 2-72, U.S. Army, Corps of Engineers, Coastal Engineering Research Center, Washington, D.C., Apr. 1972.

ANAN, F.S., "Provenance and Statistical Parameters of Sediments of the Merrimack Embayment, Gulf of Maine," unpublished Ph.D. Dissertation, University of Massachusetts, Amherst, Mass., 1971.

COASTAL RESEARCH GROUP, "Coastal Environments: N.E. Massachusetts and New Hampshire," Cont. No. 1-CRG, Department of Geology Publication Series, University of Massachusetts, Amherst, Mass., 1969.

DaBOLL, J.M., "Holocene Sediments of the Parker River Estuary, Massachusetts," Cont. No. 3-CRG, Coastal Research Group, Department of Geology Publication Series, University of Massachusetts, Amherst, Mass., 1969.

DAVIS, R.A., Jr., and FOX, W.T., "Beach and Nearshore Dynamics in Eastern Lake Michigan," Technical Report No. 4, Western Michigan University, Kalamazoo, Mich., 1971.

DOLAN, R., FERM, J.C., and McARTHUR, D.S., "Measurements of Beach Process Variables, Outer Banks, North Carolina," Technical Report No. 64, Coastal Studies Institute, Louisiana State University, New Orleans, La., 1968.

DUNCAN, J.R., Jr., "The Effects of Water Table and Tide Cycle on Swash-Backwash Sediment Distribution and Beach Profile Development," *Marine Geology*, Vol. 2, 1964, pp. 186-197.

EMERY, K.O., "A Simple Method of Measuring Beach Profiles," *Limnology and Oceanography*, Vol. 6, No. 1, Jan. 1961, pp. 90-93.

FOX, W.T., and DAVIS, R.A., Jr., "Fourier Analysis of Weather and Wave Data from Lake Michigan," Technical Report No. 1, Williams College, Williamstown, Mass., 1970.

FOX, W.T., and DAVIS, R.A., Jr., "Fourier Analysis of Weather and Wave Data from Holland, Michigan, July 1970," Technical Report No. 3, Williams College, Williamstown, Mass., 1971.

HARRISON, W., and KRUMBEIN, W.C., "Interactions of the Beach-Ocean-Atmosphere System at Virginia Beach, Virginia," TM-7, U.S. Army, Corps of Engineers, Coastal Engineering Research Center, Washington, D.C., Dec. 1964.

HARRISON, W., et al., "A Time Series from the Beach Environment," Contribution No. 12, Land and Sea Interaction Laboratory, Environmental Science Services Administration, Norfolk, Va., 1968.

HARTWELL, A.D., "Hydrography and Holocene Sedimentation of the Merrimack River Estuary, Massachusetts," Cont. No. 5-CRG, Coastal Research Group, Department of Geology Publication Series, University of Massachusetts, Amherst, Mass., 1970.

HAYES, M.O., and BOOTHROYD, J.C., "Storms as Modifying Agents in the Coastal Environment," Coastal Environments: N.E. Massachusetts and New Hampshire, Cont. No. 1-CRG, Coastal Research Group, Department of Geology Publication Series, University of Massachusetts, Amherst, Mass., 1969, pp. 245-265.

HOMA-MA, M., and SONU, C.J., "Rhythmic Patterns of Longshore Bars Related to Sediment Characteristics," Proceedings of the Eighth Conference on Coastal Engineering, 1963, pp. 1-29.

IPPEN, A.T., ed., Estuary and Coastline Hydrodynamics, McGraw-Hill, New York, 1966.

McCORMICK, C.L., "Holocene Stratigraphy of the Marshes at Plum Island, Massachusetts," unpublished Ph.D. Dissertation, University of Massachusetts, Amherst, Mass., 1968.

NATIONAL OCEANIC AND ATMOSPHERIC ADMINISTRATION, "Surface Weather Maps," National Weather Service, Eastern Region, Long Island, N.Y., Feb. 1972.

SONU, C.J., McCLOY, J.M., and McARTHUR, D.S., "Longshore Current and Nearshore Topographies," Proceedings of the 10th Conference on Coastal Engineering, 1966, pp. 525-549.

SONU, C.J. and RUSSELL, R.J., "Topographic Changes in the Surf Zone Profile," Proceedings of the 10th Conference on Coastal Engineering, 1966, pp. 502-504.

SONU, C.J., "Collective Movement of Sediment in the Littoral Environment," Proceedings of the 11th Conference on Coastal Engineering, 1968, pp. 373-400.

U.S. ARMY, CORPS OF ENGINEERS, BEACH EROSION BOARD, "Shore Protection Planning and Design," TR-4, 1st ed., U.S. Government Printing Office, Washington, D.C., 1954.

U.S. ARMY, CORPS OF ENGINEERS, COASTAL ENGINEERING RESEARCH CENTER, "Shore Protection Planning and Design," TR-4, 3d ed., U.S. Government Printing Office, Washington, D.C., 1966.

VOLLBRECHT, K., "The Relationship Between Wind Records, Energy of Longshore Drift, and Energy Balance off the Coast of a Restricted Water Body, as Applied to the Baltic," Marine Geology, Vol. 4, 1966, pp. 119-148.

Abele, Ralph Warren
  Analysis of short-term variations in beach morphology (and con-
current dynamic processes) for summer and winter periods, 1971-72,
Plum Island, Massachusetts / by Ralph Warren Abele, Jr. — Fort
Belvoir, Va. : U.S. Coastal Engineering Research Center, 1977.
  101 p. : ill. (Miscellaneous report — U.S. Coastal Engineering
Research Center ; no. 77-5) (Contract — U.S. Coastal Engineering
Research Center ; DACW72-71-C-0023)
  Bibliography : p. 100.
  Report analyzes the relationship between wave and meteorological
variables and beach morphology during summer and winter periods,
1971-72, at Plum Island, Massachusetts. Variations in beach process
variable were directly related to storm systems in the area.
  1. Coastal morphology. 2. Beach profile. 3. Breakers. 4. Currents.
5. Waves. 6. Plum Island, Massachusetts. I. Title. II. Series:
U.S. Coastal Engineering Research Center. Miscellaneous report
no. 77-5. III. Series: U.S. Coastal Engineering Research Center.
Contract DACW72-71-C-0023.
TC203   .U581mr   no. 77-5   627